An AREVA and Siemens company

ANP-10300NP
Revision 0

AURORA-B: An Evaluation Model for Boiling Water Reactors; Application to Transient and Accident Scenarios

December 2009

AREVA

AURORA-B: An Evaluation Model for Boiling Water Reactors; Application to Transient and Accident Scenarios

Nature of Changes

Item	Page	Description and Justification
1.	All	This is a new document.

Contents

Tables

Figures

This document contains a total of 273 pages.

Abstract

AURORA-B is an evaluation model for predicting the dynamic response of boiling water reactors (BWRs) during transient, postulated accident, and beyond design-basis accident scenarios. The evaluation model contains a multi-physics code system based on three extensively validated computer codes, the S-RELAP5 thermal-hydraulic system code, a kinetics version of the MICROBURN-B2 core simulator, and the RODEX4 fuel thermal-mechanical code.

This Licensing Topical Report presents the general framework of the AURORA-B evaluation model and its qualification for BWR analyses. In addition, an application methodology is presented that is specifically focused on analysis of selected transient and accident scenarios. Deterministic analysis principles are used in the application methodology to demonstrate that plant operational and Technical Specification licensing requirements are satisfied through the use of conservative initial conditions, boundary conditions, and assumed equipment operational characteristics.

Nomenclature

Acronym	Definition
ABWR	Advanced Boiling Water Reactor
AOO	Anticipated Operational Occurrence
APRM	Average Power Range Monitor
ASME	American Society of Mechanical Engineers
AST	Alternate Source Term
ATWS	Anticipated Transient without Scram
ATWSP	ATWS Peak Pressure Event with Main Steam Isolation Valve Closure
BOHL	Beginning of Heated Length
BWR	Boiling Water Reactor
CCD	Component Calculational Device
CET	Component Effects Test
CFR	Code of Federal Regulations
CHF	Critical Heat Flux
CPR	Critical Power Ratio
CSAU	Code Scaling Applicability and Uncertainty
ECCS	Emergency Core Cooling System
EM	Evaluation Model
EMDAP	Evaluation Model Development and Assessment Process
EPRI	Electric Power Research Institute
EPU	Extended Power Uprate
FIST	Full Integral Simulation Test
FMA	Foundation Methodology Assessment
FoM	Figure of Merit
FWCF	Feedwater Controller Failure
GDC	General Design Criteria
HPCI	High Pressure Coolant Injection
HPCS	High Pressure Core Spray
IET	Integral Effects Test
ISP	International Standard Problem
LHGR	Linear Heat Generation Rate
LOCA	Loss of Coolant Accident
LPRM	Local Power Range Monitor
LRNB	Load Rejection No Bypass
LTR	Licensing Topical Report
LTSF	LOFT Test Support Facility
LWR	Light Water Reactor

MCPR	Minimum Critical Power Ratio
MELLLA	Maximum Extended Load Line Limit Analysis
MSIV	Main Steam Isolation Valve
MSIVF	Main Steam Isolation Valve Closure - High Flux Scram Event
PIRT	Phenomena Identification and Ranking Table
PRFO	Pressure Regulator Failed Open with no Scram
PTD	Plant Transient Data
PWR	Pressurized Water Reactor
RIP	Reactor Internal Pump
RLBLOCA	Realistic Large Break Loss of Coolant Accident
RPS	Reactor Protection System
RPT	Recirculation Pump Trip
SE	Safety Evaluation
SET	Separate Effects Test
SLCS	Standby Liquid Control System
SRP	Standard Review Plan
SRV	Safety/Relief Valve
TBV	Turbine Bypass Valve
TCV	Turbine Control Valve
TSV	Turbine Stop Valve
TTNB	Turbine Trip No Bypass
USNRC	US Nuclear Regulatory Commission
ΔCPR	Transient Change in CPR for a Fuel Assembly
ΔMCPR	Transient Change in MCPR

1.0 Introduction

AURORA-B is a comprehensive evaluation model developed by AREVA NP Inc.* for predicting the dynamic response of boiling water reactors (BWRs) during transient, postulated accident, and beyond design-basis accident scenarios. The evaluation model (EM) contains a multi-physics code system with flexibility to incorporate all the necessary elements for analysis of the full spectrum of BWR events that are postulated to affect the nuclear steam supply system of the BWR plant.

The AURORA-B EM is designed to be broadly applicable to many BWR events and calculational procedures (e.g. deterministic or statistical procedures). However, the relevant event characteristics differ depending on the event scenario and the criteria that are being evaluated. The differences in events, criteria, and calculational procedures are addressed by defining specific application methodologies. Compliance with all applicable regulations will be assured for the defined events and criteria when the AURORA-B EM is applied within the framework of a specific application methodology.

This Licensing Topical Report (LTR) presents the AURORA-B EM and qualification of the EM for analysis of BWR events. In addition, an application methodology is presented that is designed for analysis of transient and accident scenarios excluding loss of coolant accidents, instability events, control rod withdraw error, the BWR control rod drop scenario, and later stages of the anticipated transients without scram (ATWS) scenario. Deterministic analysis principles are applied to satisfy plant operational and Technical Specification requirements through the use of conservative initial conditions, boundary conditions, and assumed equipment operational characteristics.

* AREVA NP Inc. is an AREVA and Siemens Company

The application methodology is applied to demonstrate compliance of plant operations with the relevant General Design Criteria (GDC) stipulated in Appendix A of 10 CFR 50 (Reference 1). This is achieved by confirming or establishing operational constraints that ensure all relevant acceptance criteria delineated in the plant-specific licensing bases are satisfied during plant operations for the events analyzed with this methodology. The EM is applied over the full domain of operating conditions, from low power conditions at which power operations commence up to and including operation at extended power uprate (EPU) conditions with expanded flow windows. EPU conditions are typically defined in the US licensing environment as 120% of original licensed thermal power. Expanded flow windows may go as low as 80% of rated core flow when operating at EPU conditions.

The AURORA-B EM and the deterministic application methodology have been developed in compliance with the evaluation model development and assessment process (EMDAP) defined in Regulatory Guide 1.203 (Reference 2). Application of the EMDAP is facilitated for AURORA-B because the analysis requirements are well established through AREVA's extensive history with BWR analyses and the mature code systems upon which the EM is built.

The foundation of AURORA-B is built upon three extensively validated computer codes. Coupled together, these "component calculational devices" (CCDs) make up the multi-physics computational framework (code system) that provides the necessary systems, components, geometries, processes, etc. to assure adequate predictions of the relevant BWR event characteristics for its intended applications. The three codes making up the foundation of the code system are;

- S-RELAP5 – This CCD serves as the backbone of the methodology into which the other CCDs have been installed. S-RELAP5 provides the transient thermal-hydraulic, thermal conduction, control systems, and special process capabilities (i.e. valves, jet-pumps, steam separator, critical power correlations, etc.) necessary to simulate a BWR plant. The basis of the CCD to which extensions and improvements were made is the code version associated with the pressurized water reactor realistic large break loss of coolant accident methodology (Reference 3). A theoretical description of the models and correlations found in this code can be found in Reference 4.

- MB2-K – This CCD uses advanced nodal expansion methods to solve the three-dimensional, two-group, neutron kinetics equations. The MB2-K code is consistent with the MICROBURN-B2 steady state core simulator (Reference 5). MB2-K receives a significant portion of its input from the steady state core simulator via data transfer files. Because of this, MICROBURN-B2 is also considered a CCD of the EM. [

  ] A theoretical description of the models and correlations found in this code can be found in Reference 6.

- RODEX4 – A subset of routines from this CCD (Reference 7) are used to evaluate the transient thermal-mechanical fuel rod (including fuel/clad gap) properties as a function of temperature, rod internal pressure, etc. The fuel rod properties are used by S-RELAP5 when solving the transient thermal conduction equations in lieu of standard S-RELAP5 material property tables. The RODEX4 kernel incorporated within S-RELAP5 receives a significant portion of its input from the full RODEX4 steady state fuel performance code via data transfer files. [

  ] consistent with the S-RELAP5 heat structure conditions as a calculation evolves. A theoretical description of the models and correlations found in this code can be found in Reference 8.

This LTR defines the AURORA-B EM and the deterministic application methodology by establishing the requirements, developing the assessment base, developing the capabilities of the EM, and assessing the adequacy of the EM. Additional details for the deterministic application methodology are then presented, including the means by which operational constraints are confirmed or established that assure compliance with applicable regulations and how conservative initial conditions, boundary conditions, and assumed equipment operational characteristics are selected. Finally, the uses and application requirements for AURORA-B are established.

2.0 Application of the EMDAP

The EMDAP has been defined by the US Nuclear Regulatory Commission (USNRC) as an acceptable process for developing and assessing evaluation methodologies that may be used to analyze the behavior of a nuclear power plant. Methodology developers are encouraged to follow the EMDAP process as it streamlines the review cycle and regulatory interactions. Additional emphasis is placed on the EMDAP since Regulatory Guide 1.203 is designed to be complementary to the guidance provided to USNRC reviewers that is found in Chapter 15.0.2 of NUREG-0800, the Standard Review Plan (SRP) for the Review of Safety Analysis Reports for Nuclear Power Plants (Reference 9).

The S-RELAP5 computer code has been selected as the foundation on which to build AURORA-B because of AREVA's extensive history and experience with the code, including a number of USNRC approved methodologies. The S-RELAP5 computer code is USNRC approved for pressurized water reactor (PWR) large and small break loss of coolant accident (LOCA) analysis, and PWR non-LOCA transient analysis (References 3, 10, and 11). Particularly, the realistic large break LOCA (RLBLOCA) methodology is based on the Code Scaling Applicability and Uncertainty (CSAU) process (Reference 12) that is defined for best estimate LOCA applications, and is a predecessor to the EMDAP. Since the S-RELAP5 code and documentation have undergone extensive review and revision to ensure accuracy and clarity for the RLBLOCA methodology, application of the EMDAP in AURORA-B development is reduced in scope compared to development of an entirely new code system using EMDAP. Instead, the EMDAP is utilized to guide the refinement and extension of the existing tools for use in the new evaluation model and assure they are adequate for addressing the systems, components, phenomena, etc. associated with BWR events. A summary of the changes made to S-RELAP5 relative to the code and documentation supporting the RLBLOCA methodology is provided in Section 7.2.

The following sections define the process for completing the EMDAP by outlining how each step of EMDAP is addressed. Several of the steps require comprehensive and detailed discussion of the BWR plant that is general in nature and not specific to a particular EM. In such cases, the details are provided by reference to supporting documents. The reference material is provided in References 13, 14, and 15. The information contained in these supporting documents is summarized in this LTR, as appropriate.

3.0 Establish Requirements for Evaluation Model Capability (EMDAP Element 1)

The following subsections establish the application envelope (analysis purpose, plant types, and transient types) of the EM addressed within the context of this LTR. The constituent phenomena, processes, and key parameters are then identified within the application envelope and their importance is determined.

3.1 *Analysis Purpose, Transient Class, and Power Plant Class (EMDAP Step 1)*

The analysis purpose, transient class, and plant class are defined below in order to define the application envelope (i.e. the target applications). The sections address the major points of each topic. Where necessary, reference is made to more comprehensive descriptions of the plant-class-specific and/or plant-specific details.

3.1.1 Analysis Purpose

The analysis purpose is to demonstrate compliance of plant operations with relevant GDC stipulated in Appendix A of 10 CFR 50 (Reference 1). This is done by confirming or establishing operational constraints that ensure all relevant acceptance criteria delineated in the plant licensing basis are satisfied during plant operations for the plants and scenarios analyzed with this EM.

3.1.2 Transient Class

The range of transient classes includes selected events defined in SRP Chapter 15 applicable to BWRs, as delineated in the subsections below. In some instances the licensing basis for a plant may not adhere to the SRP, or may refer to prior revisions of the SRP. Provided that the licensing basis of the plant does not significantly depart from the SRP bases, the AURORA-B EM supports the licensing basis of each plant to which it is applied by analyzing the plant-specific scenarios, consistent with the criteria defined in the licensing basis documents for the plant. The framework defined by the SRP provides a reasonable common basis for discussion of the events of interest in this LTR.

The operating domain (allowable combinations of core thermal power and total core flow rate) from which events may be initiated is delineated in the plant licensing basis documentation for each plant. However, the AURORA-B EM presented in this LTR may be applied in the US

licensing environment up to and including operation at EPU conditions with expanded power and flow windows.

The following sections summarize the target scenarios to which the AURORA-B EM presented in this LTR is applied. Except were indicated, all scenarios are anticipated operational occurrences (AOOs), as defined in SRP Chapter 15. All scenarios are "core wide" events in which the initial excitation is a thermal-hydraulic disturbance. A sequence of events for each scenario is provided in Reference 13. The descriptions in the reference include considerations for equipment configuration depending on the assumed state of plant equipment and initial conditions during the analyses.

3.1.2.1 SRP 15.1 Cool Down Events

Cool down events involve an unplanned increase in heat removal by the secondary system. Excessive heat removal, i.e., a heat removal rate in excess of the heat generation rate in the core, causes a decrease in moderator temperature which in turn increases core reactivity and can lead to a power level increase and a decrease in shutdown margin. The events in this category include the following:

- SRP 15.1.1 Feedwater system malfunctions that result in a decrease in feedwater temperature
- SRP 15.1.2 Feedwater system malfunctions that result in an increase in feedwater flow
- SRP 15.1.3 Steam pressure regulator malfunctions or failures that result in increased steam flow

3.1.2.2 SRP 15.2 Heat Up Events

Heat up events are all similar in so far as they result in unplanned decreases in heat removal from the reactor core, and subsequent increase in fuel temperature. Additionally, these events include pressurization events which are initiated by isolation of the reactor through closure of steam line valves. The severity of each event is highly dependent on the initial valve position and valve closure characteristics. In general, a more rapid valve closure will lead to a more severe event. The events in this category include the following:

- SRP 15.2.1 Loss of external load (generator load rejection)
- SRP 15.2.2 Turbine trip
- SRP 15.2.3 Loss of condenser vacuum
- SRP 15.2.4 Closure of main steam isolation valve
- SRP 15.2.5 Steam pressure regulator failure (closed)
- SRP 15.2.6 Loss of non-emergency ac power to the station auxiliaries
- SRP 15.2.7 Loss of normal feedwater flow

3.1.2.3 SRP 15.3 Loss of Coolant Flow Events

Loss of coolant flow events involve a decrease in coolant flow, resulting in a degradation of core heat transfer. The events in this category include the following:

- SRP 15.3.1 Recirculation pump trip
- SRP 15.3.2 Recirculation flow controller malfunction (decreasing flow)
- SRP 15.3.3 Reactor coolant pump rotor seizure
- SRP 15.3.4 Reactor coolant pump shaft break

The reactor coolant pump rotor seizure (SRP 15.3.3) and reactor coolant pump shaft break (SRP 15.3.4) events are classified as accidents rather than AOOs.

3.1.2.4 SRP 15.4 Reactivity Events

Reactivity events are classified as those events which generate a reactivity insertion due to increased recirculation flow or by introduction of cooler water into the core. For the flow induced reactivity insertions, the accompanying decrease in core average void fraction leads to an increase in neutron flux and corresponding core power increase. The events in this category include the following:

- SRP 15.4.4 Startup of an idle recirculation loop
- SRP 15.4.5 Recirculation flow controller malfunction which results in increased core flow rate

3.1.2.5 SRP 15.5 Increasing Inventory Events

Increasing inventory events are those that inadvertently inject colder water directly into the reactor vessel during normal plant operation. The assumption of initiation during plant operation

presumes the injection source is a high pressure makeup system. The specific event scenario (cold water source) is plant dependent. The events in this category include the following:

- SRP 15.5.1 Inadvertent operation of an emergency core cooling system that increases reactor coolant inventory, including high pressure core spray (HPCS), high pressure core flooder, high pressure coolant injection (HPCI), or reactor core isolation cooling system

3.1.2.6 SRP 15.6 Decreasing Inventory Events

Decreasing inventory events are typically classified as loss of coolant accidents (LOCAs). However, an exception is the inadvertent opening of a pressure relief valve which results in a decrease in reactor coolant inventory and pressure vessel pressure. The events in this category include the following:

- SRP 15.6.1 Inadvertent opening of a pressure relief valve

3.1.2.7 SRP 15.8 Anticipated Transients without Scram

The ATWS scenarios are AOOs in which a reactor scram is demanded but fails to occur because of a common-mode failure in the reactor scram system. The ATWS scenarios are AOOs that postulate complete failure of the required (single-failure proof) protection system. As such, they are beyond the design basis. There exist four different aspects of any ATWS scenario that are typically considered; protection of the reactor pressure vessel and associated piping from failure due to overpressurization, demonstration that fuel integrity is maintained, demonstration that the secondary means of reactor shutdown is sufficient, and determination of the peak suppression pool temperature with demonstration that containment temperature and pressure limits are not exceeded.

As discussed in Section 8.3, this LTR only addresses the first two aspects of the ATWS scenario, and only through the time at which boron begins arriving at the core. There is a strong similarity between the ATWS scenario and the AOO scenario through this time period, and the same phenomena generally apply.

3.1.3 Power Plant Class

The range of power plant classes includes all forced circulation BWR plant types, including, BWRs equipped with external recirculation pump systems (BWR/2 plants), jet-pump recirculation systems (BWR/3 through BWR/6 plants), and internal recirculation pump systems

(ABWR plants). A detailed description of the BWR plant types is provided in Reference 13. The description not only includes discussion of plant-class hardware such as recirculation system design, but also includes a summary of plant-specific differences that have been observed in operating plants as a result of equipment modernization efforts and evolution of plant operational parameters.

3.2 *Figures of Merit (EMDAP Step 2)*

The figures of merit (FoM) evaluated with the EM are parameters that demonstrate compliance with applicable acceptance criteria defined in the licensing basis of each plant. Specifically, the FoM (also known as acceptance criteria measures) considered are those necessary to demonstrate compliance with the acceptance criteria for the target scenarios described in Section 3.1.2 and that are affected by the fuel system design. The precise role of the AURORA-B EM in calculating FoM for comparison to the applicable acceptance criteria is described in Section 3.2.1. The FoM include:

1. Evaluation of transient change in minimum critical power ratio (ΔMCPR). This FoM is used to provide assurance that the event minimum critical power ratio (MCPR) remains above the safety limit for the applicable AOOs. This FoM is also used in conjunction with other methods to determine radiological consequences of selected infrequent events and postulated accidents.
2. Evaluation of peak system pressure. This FoM is used to provide assurance that peak pressure is maintained below limits for AOOs and the ATWS scenario, where the limits and analysis assumptions differ depending on which scenario is being analyzed.
3. Evaluation of the time dependent nodal power used with fuel thermal-mechanical methodologies. This FoM is used in conjunction with fuel thermal-mechanical methodologies to evaluate cladding strain and fuel melt during the event.
4. Evaluation of maximum cladding temperature and maximum local oxidation. These FoM are used to provide assurance that fuel integrity is maintained for selected events.

The specific acceptance criteria used for demonstrating compliance of plant operations is defined in the licensing basis of each plant. In instances where the plant licensing basis differs from the specific SRP Chapter 15 acceptance criteria, the AURORA-B EM is applied consistent with the licensing basis of plants to which it is applied. However, the framework defined by the SRP provides a reasonable common basis for discussion of the acceptance criteria of interest in this LTR. The following list of acceptance criteria is summarized from the SRP Chapter 15, and is affected by the fuel mechanical, nuclear, and/or thermal hydraulic design. The specific criteria applied to each event are described in Reference 13.

1. Evaluation of the event MCPR and assurance the event critical power ratio remains above the safety limit.
2. Evaluation of the radiological consequences and assurance that the calculated release of radioactivity does not exceed 10 CFR 100 limits for selected infrequent events and postulated accidents. For some events (e.g., recirculation pump seizure) the calculated release does not exceed a small fraction (typically ten percent) of the applicable limits. For plants approved for Alternate Source Term (AST), the limits specified in 10 CFR 50.67, "Accident Source Term," are applicable.
3. Evaluation of peak system pressure and assurance peak pressure is maintained below 110 percent of design values in compliance with American Society of Mechanical Engineers (ASME) limits.
4. Evaluation of peak system pressure and assurance peak pressure is limited such that the maximum primary stress within the reactor coolant pressure boundary does not exceed the ASME Service Level C limits during the ATWS scenario. For boiling water reactors, this is generally a maximum reactor vessel pressure of 1500 psig.
5. Evaluation of the transient strain of the cladding and assurance that it does not exceed one percent. Also, fuel peak pellet temperatures are evaluated to assure they are maintained below melting.
6. The long-term cooling capability is assured by meeting the cladding temperature and oxidation criteria utilized for loss of coolant accidents as specified in 10 CFR 50.46 (i.e., peak cladding temperature not exceeding 2200°F, the local oxidation of the cladding not exceeding 17 percent of the total cladding thickness, and the core-wide metal water reaction not exceeding one percent of the cladding).

The acceptance criteria described above may be revised by USNRC rulemaking activities subsequent to approval of this LTR. As a result, the licensing basis of plants may be modified to reflect the revised criteria through USNRC approved License Amendment Requests that are submitted by the plant licensee. In other situations the licensing basis for a plant may not be consistent with the SRP. In such cases, AURORA-B EM analysis conclusions will address the acceptance criteria found in the licensing basis of plants to which it is applied.

3.2.1 Application Specific Considerations

This LTR describes an EM for confirming or establishing operational constraints that assure compliance of plant operations with applicable GDC through specific acceptance criteria. In some cases, several different classes of analysis capabilities are directly involved in determining an operational constraint. This section defines the context by which this LTR fits into the confirmation or establishment of the operational constraints. In particular, the role of the AURORA-B EM in demonstrating the applicable acceptance criteria are satisfied during plant

operations for the target scenarios is identified. Note, this section addresses the context; Section 9.0 defines the specific activities for which approval is requested.

Figure of Merit 1

Evaluation of event MCPR is performed for two different classes of analyses. The first is for providing assurance the event MCPR remains above the safety limit MCPR for each fuel design. The second class is used in conjunction with other methods to determine radiological consequences of selected events in which the event MCPR is below the safety limit. Both classes are summarized below.

(A) Evaluation of event MCPR and assurance the event MCPR remains above the safety limit MCPR for each fuel design generally necessitates two distinct types of methodologies which are summarized in the AREVA thermal limits methodology (Reference 16). The first type is needed to determine the ΔMCPR for each fuel design over the entire operating domain for which a plant is licensed to operate. This type includes distinct methodologies for evaluating "fast transients" (e.g. turbine trip with no bypass and similar events) and other methodologies for evaluating "slow transients" (e.g. control rod withdrawal error events). The second type is needed for determining the safety limit MCPR that must be protected during AOOs. Examples of the safety limit MCPR process, including the types of and processes for treating uncertainties, are summarized for two different methodologies in Reference 17 and Reference 18.

Compliance with the applicable acceptance criterion is assured through application of operational constraints that are defined during fuel reload licensing activities and monitored during plant operations. These operational constraints are functionally dependent on thermal power and/or core flow, and multiple sets of limits may be defined to provide operational flexibility (e.g. sets for different exposure ranges and equipment configurations). Determining the operational constraints (i.e. the operating limit MCPR) for each fuel design from the ΔMCPR results of transient scenarios is addressed in the thermal limits methodology, Reference 16.

The EM described in this LTR is applied in analyses to determine the event MCPR as quantified through the ΔMCPR. The AURORA-B EM reflects an update to the "Plant Transient Simulation Methodology" described in Section 4.0 of the AREVA thermal limits methodology

(Reference 16). However, the EM described in this LTR applies a deterministic approach for ΔMCPR and not the statistical approach described in Section 4.7 of the reference.

(B) Demonstration that the radiological consequences do not exceed 10 CFR 100 limits, or AST limits in accordance with 10 CFR 50.67 if approved, (or a "small fraction" thereof as applicable) is performed by several distinct elements. The elements are summarized below for those scenarios in which the EM will be applied (e.g. radiological analyses for LOCA and other events not related to this LTR are not addressed). The elements are as follows;

1. Determine dose at the site boundary based on assumptions for the amount of radiological release and its source (from failed fuel rods within the core in this case).
2. Determine the number of failed rods (or assemblies) that are permissible for an accident scenario while still satisfying the assumptions for the amount of radiological release in the first element.
3. Evaluate the ΔMCPR for each fuel design in the applicable events in order to determine the event MCPR. If the event MCPR does not go below the safety limit, then no failures are predicted to occur for the event.
4. Knowing the event MCPR for each fuel design, a safety limit MCPR methodology is used to determine the number of rods assumed to fail (see Section 1.2 of Reference 18). This number of rods is compared to the number of failed rods that are permissible for the scenario. If less than the permissible number is predicted, the radiological consequences of the event are acceptable.

The EM described in this LTR is applied to evaluate the event MCPR experienced in selected events in order to determine if any rods go below the safety limit, and the maximum penetration below the safety limit if applicable.

Figure of Merit 2

Evaluation of peak system pressure is made for two distinct classes of events. The first class of events is analyzed to provide assurance that the peak system pressure remains below applicable ASME limits for AOOs. The second class of events is analyzed to provide assurance that the peak system pressure remains below applicable ASME limits for the ATWS scenario. The applicable limits and analysis assumptions differ depending on which analysis is performed. Both classes are summarized below.

(A) Evaluation of peak system pressure and assurance the peak pressure is maintained below 110 percent of design values in compliance with ASME limits involves analysis of typical

AOO events using a fast transient methodology, but with assumptions that conservatively maximize pressurization. This evaluation is often referred to as an "ASME overpressure analysis."

Compliance with the applicable acceptance criterion is assured by confirming during reload licensing activities that the design and number of safety valves assumed available have sufficient pressure relief capacity and performance to maintain peak pressure below the applicable limits. The plant configuration during plant operations must be in compliance with (or more favorable than) the licensing assumptions.

The EM described in this LTR is applied in evaluation of peak primary system pressure for the "ASME overpressure" scenario.

(B) Evaluation of primary system pressure and assurance the peak pressure does not exceed the ASME Service Level C limits during a postulated ATWS scenario is required. This involves analysis of potentially limiting events using a fast transient methodology with the scram function assumed unavailable. This evaluation is often referred to as an "ATWS overpressure analysis."

Compliance with the applicable criterion is assured by confirming during reload licensing activities that the design and number of relief valves assumed available have sufficient pressure relief capacity and performance to maintain peak pressure below the applicable limits. The plant configuration during plant operations must be in compliance with (or more favorable than) the licensing assumptions.

The EM described in this LTR is applied in the evaluation of peak primary system pressure for the "ATWS overpressure" scenario.

Figure of Merit 3

Evaluation of the transient strain of the cladding and assurance that it does not exceed one percent and evaluation of fuel peak pellet temperatures to assure they remain below melting are primarily the functions of fuel thermal-mechanical analysis methodologies. However, the acceptance criteria oblige consideration of transient conditions. Depending on the bases of the fuel thermal-mechanical analysis methodologies, boundary conditions from "fast transient" and

"slow transient" methodologies (specifically the time dependent nodal power) may be used in part, to demonstrate compliance with the applicable acceptance criteria. Section 6.3 of Reference 7 provides an example of how fast transient methodologies fit into the framework of analyses using RODEX4 for determining the AOO maximum pellet temperature and transient strain criteria.

The EM described in this LTR is applied to predict time dependent nodal power boundary conditions for input to fuel thermal-mechanical codes within the bounds of USNRC approved fuel thermal-mechanical analysis methodologies. With respect to the RODEX4 methodology described in Reference 7, AURORA-B is used as an alternate transient simulator code to provide the time dependent nodal power increase and "a power increment due to the change in the reactor axial profile during the transient" consistent with the description in the reference.

Figure of Merit 4

Long-term cooling capability is assured by meeting the cladding temperature and oxidation criteria utilized for loss of coolant accidents as specified in 10 CFR 50.46 and is performed by two distinct classes of USNRC approved methodologies. The first class is used to perform LOCA analyses over the spectrum of postulated break sizes. The second class uses "fast transient" methodologies to analyze certain non-LOCA events stipulated in SRP Chapter 15 that refer to 10 CFR 50.46 in the specific acceptance criteria.

Depending on the purpose of the non-LOCA analysis, the cladding temperature and oxidation criteria may be the goal of the analysis, or it may contribute as one element of a radiological consequences analysis. In such a role, the cladding temperature and duration of the temperature exceeding some value may be used in conjunction with other methodologies to demonstrate that the radiological consequences of the event do not exceed 10 CFR 100 limits or AST limits specified in 10 CFR 50.67 (or a "small fraction" thereof as applicable). The cladding temperature (and duration) criteria are plant and event specific, and defined in the licensing documentation for each plant.

The EM described in this LTR will be applied to evaluate applicable cladding temperature and local oxidation criteria for infrequent events and postulated accidents (other than LOCA) for

which they may be evaluated based on the applicable criteria defined in the licensing documentation for the plant for specific events.

3.3 *Identify Systems, Components, Phases, Geometries, Fields, and Processes that Must Be Modeled (EMDAP Step 3)*

The capability of an EM to calculate the target applications rests on the characteristics of the EM. Knowing the target applications and FoM (e.g. EMDAP Steps 1 and 2), the characteristics of the EM are now defined. These characteristics are used in later stages of the EMDAP to define the code development activities. A weak or missing capability was addressed through the methodology development process and directed code development. The first step in defining the capabilities is identifying the systems, components, phases, geometries, fields, and processes that must be modeled:

3.4 *Identify and Rank Key Phenomena and Processes (EMDAP Step 4)*

Plant behavior is not equally influenced by all processes and phenomena that occur during a transient. The candidate phenomena for the target scenarios have been reviewed to identify the most important phenomena in order to achieve a manageable set for a wide range of target scenarios. This has been performed by identifying and ranking the phenomena of the target scenarios with respect to their influence on the defined FoM. The information provided in this section summarizes the comprehensive phenomena identification and ranking process that is documented in Reference 15. The indicated reference describes the process by which the phenomena identification and ranking was performed, including how one summary PIRT was developed for application to numerous events and FoM.

Brief descriptions of highly ranked phenomena follow. A detailed description of each item, salient characteristics, the way it contributes to the events of interest and FoM, and a description of how it is connected to other phenomena (where applicable) is provided in

Reference 15 along with phenomena that did not receive a high ranking for the target scenarios.

Note; numbering of the PIRT IDs is consistent with the full PIRT provided in Reference 15.

- **PIRT ID=C01 [**

  ]

- **PIRT ID=C02 [**

  ]

- **PIRT ID=C03 [**

  ]

- **PIRT ID=C04 [**

  ]

- **PIRT ID=C06 [**

  ]

- **PIRT ID=C07 [**

  ]

- **PIRT ID=C09 [**

  ]

- **PIRT ID=C12 [**

  ]

- **PIRT ID=C13 [**

  ]

- **PIRT ID=C15 [**

  ]

- **PIRT ID=B01 [**

  ]

- **PIRT ID=D02 [**

  ]

- **PIRT ID=D03 [**

  ]

- **PIRT ID=FR00 [**

  ]

- **PIRT ID=FR04 [**

  ]

- **PIRT ID=FR11 [**

  ]

- **PIRT ID=JP01 [**

  ]

- **PIRT ID=LP01 [**

  ]

---

* [

  ]

- **PIRT ID=R01 [**

  ]

- **PIRT ID=R02 [**

  ]

- **PIRT ID=S02 [**

  ]

- **PIRT ID=S03 [**

  ]

- **PIRT ID=S04 [**

  ]

- **PIRT ID=SL02 [**

  ]

- **PIRT ID=SL03 [**

  ]

- **PIRT ID=UP02 [**

  ]

- **PIRT ID=SD04 [**

  ]

4.0 Develop Assessment Base (EMDAP Element 2)

This section focuses on the experimental database that is relevant to the scenarios being considered. In addition, the suitability of the experimental scaling of the data is addressed and scaling issues are discussed.

4.1 *Specify Objectives for Assessment Base (EMDAP Step 5)*

The objectives of the assessment base are to provide experimental data to assess the requirements established in Element 1. In particular, BWR components, processes, and phenomena that were identified in Step 3 and ranked as important in Step 4 require assessment. The assessment base includes separate effects experiments needed to develop and assess empirical correlations and other closure models, integral systems tests to assess system interactions and global code capability, and plant transient data that demonstrate the system interactions for scenarios based on full scale plant data.

4.2 *Perform Scaling Analysis and Identify Similarity Criteria (EMDAP Step 6)*

In general, the scaling compromises of test data are minimal and assessments are well-characterized. This is because the assessment base consists of full scale data for all important experiments and applicable plant transient data. Discussion of scaling is provided in Section 6.5 (EMDAP Step 17) and Section 6.6 (EMDAP Step 18) as appropriate.

4.3 *Identify Existing Data and/or Perform Integral Effects Tests and Separate Effects Tests to Complete the Database (EMDAP Step 7)*

Several authoritative works are available in the public domain that survey existing test facilities and available experimental data. These works are more focused on pressurized water reactor loss of coolant accidents, but test facilities and experimental data are identified within these sources for generally applicable facilities and data as well as BWR specific facilities and data. The sources include *The Compendium of ECCS Research for Realistic LOCA Analysis* (Reference 19), *Evaluation of the Separate Effects Tests (SET) Validation Matrix* (Reference 20), *CSNI Integral Test Facility Validation Matrix for the Assessment of Thermal-Hydraulic Codes for LWR LOCA and Transients* (Reference 21), and *TRAC-M Validation Test Matrix* (Reference 22). Additional public domain facilities and experimental data were also

identified by performing a literature search and historical records review. Applicable facilities are selected and included into the assessment database.

In addition to the above, a survey of proprietary technical reports has been performed to identify additional data for inclusion in the database. These reports provide useful data that is specifically applicable to AREVA supplied products as well as component test data that is not publicly available. Also, the USNRC approved LTRs and theory manuals associated with the CCDs mentioned in Section 1.0 have been inspected. The AURORA-B EM is intentionally built upon USNRC approved methodologies in order to take benefit from the prior assessment work.

One motivation of the identification phase was to obtain sufficient data for each development and/or assessment activity such that models were not tuned to a particular data set, and thus make the models appear to be more accurate than they truly are. In addition data covering the full range of conditions for which a model may be used was sought.

A matrix of test facilities (or groups of equivalent facilities) is provided in Table 4-1 that defines the experimental database supporting this LTR versus highly ranked PIRT phenomena listed in Section 3.4. This table defines the assessment matrix for the evaluation model. The use of data from test facilities in evaluating highly ranked PIRT phenomena are indicated in the table. Most commonly, the data was used for detailed development and/or assessment of the phenomena. In this case the facility and data provide sufficient details to permit the detailed investigation. However, in some cases the data was used for independent validation because the facility and/or data did not provide the specific information needed for detailed assessment of the phenomena but they still provided useful information for validating the detailed assessments in other geometries and/or conditions, such as transient scenarios. The type of test is also indicated in Table 4-1, where the types of data are as follows;

- Separate effects tests (SET)
- Component effects tests (CET)
- Integral effects tests (IET)
- Plant transient data (PTD) – tests occurring within actual operating plants
- Foundation methodology assessments (FMA)

Table 4-1: AURORA-B Evaluation Model Assessment Matrix

4.4 *Evaluate Effects of IET Distortions and SET Scaleup Capability (EMDAP Step 8)*

The effects of integral effects test (IET) database distortions and separate effects test (SET) scale-up were evaluated as part of the selection process performed in EMDAP Step 7. For instance, several reduced height IETs are not included in the experimental database because they do not provide any additional experimental evidence over a full height test facility identified in Table 4-1. In addition, the experimental database includes full size prototypic SET or component data for all highly ranked PIRT phenomena and processes that are not treated as initial conditions or plant parameters. In some situations where reduced scale SETs or component tests were used to develop models, full scale data is available to confirm the scale-up of the model.

4.5 *Determine Experimental Uncertainties as Appropriate (EMDAP Step 9)*

Considerations for experimental uncertainty were made during selection of the experimental database. In some instances, measurement errors, experimental biases, or other aspects of experimentation were identified in experimental data that necessitated rejection of the data from the database. Such data is not indicated in Table 4-1. Where applicable, the experimental uncertainty is addressed in conjunction with facility descriptions and presentation of assessment results.

5.0 Develop Evaluation Model (EMDAP Element 3)

As previously discussed, an EM is a collection of calculational devices (computer codes) and procedures developed and organized to meet the requirements established in Element 1. This EMDAP Element describes the integration of the devices into a cohesive package for assessment in EMDAP Element 4.

5.1 *Establish an Evaluation Model Development Plan (EMDAP Step 10)*

A development plan was established at the initiation of the model development and revised as the development progressed to guide the development process. The plan identified methodology requirements and specifies the procedures and work practices to which the development efforts are to adhere. The procedures and work practices define processes for ensuring compliance with applicable quality assurance criteria (including Appendix B to 10 CFR 50).

Taken as a whole, the development plan plus adherence to procedures and work practices ensure that the EM has been developed to specific design requirements, meets expectations for documentation and programming standards, addresses transportability requirements, and is developed within the framework of applicable quality assurance criteria and configuration control procedures.

5.2 *Establish Evaluation Model Structure (EMDAP Step 11)*

The EM structure includes the structure of the CCDs, as well as the structure that combines the devices into the overall EM. This structure is based on the principles of Element 1 (especially Step 3), as well as the requirements established in Element 1 and Step 10 and significant experience with analyzing BWR events. The structure consists of the following six ingredients:

1. *Systems and components:* The EM structure is able to analyze the behavior of all systems and components that play a role in the target scenarios.
2. *Constituents and phases:* The EM structure is able to analyze the behavior of all constituents and phases relevant to the target scenarios.
3. *Field equations:* The field equations are solved to determine the transport of the quantities of interest.
4. *Closure relations:* Correlations and equations that help to evaluate the terms in the field equations by providing code capability to model and scale particular processes are available.

5. *Numerics:* The numerics provide the capability to perform efficient and reliable calculations.
6. *Additional features:* Additional features are available to provide the capability to model boundary conditions and control systems.

The structure defined in this section addresses the systems, components, phases, geometries, fields, and processes described in Section 3.3 (EMDAP Step 3). How each ingredient is addressed in the EM is summarized in the subsections 5.2.1 through 5.2.5. As described in Section 7.0, the EM development was an iterative process until the EM was determined to be adequate for the target applications. The status of the EM structure described in the subsections reflects the final product of the development process, as indicated by having models available for all the required code structures. References 4, 6, and 8 provide more detail on the theoretical descriptions for each of the component calculational devices. Note, because of the importance of selecting proper closure relationships for the governing equations, the specific models are treated separately in EMDAP Step 12, but the basic processes are defined here because the code structure must be able to accommodate the closure relationships.

The way in which the component calculational devices are integrated to form the EM is discussed in Sections 5.2.6 and 5.2.7, including external data transfers and spatial and temporal coupling. A high level description of the nodalization of the plant model is provided in Section 5.2.8. Finally, a single channel model designed to analyze "local" FoM based on results from a system scale calculation is addressed in Section 5.2.9.

5.2.1 Code Structure

To properly model a BWR plant, a code system must have a structure that adequately models the important systems and components of the plant with respect to the target scenarios. As indicated in Table 5-1, the code system has the ability to model all relevant features of the plant. The specific configuration of the structure (e.g. plant nodalization) is described in Section 5.2.8.

Table 5-1: Code Structure

Table 5-1: Code Structure (cont.)

[redacted]

5.2.2 Field Equations

The field and transport equations (conservation of mass, momentum, energy, neutron flux, etc.) possess the capability of addressing phenomena and processes occurring in the plant during the target scenarios for the specified set of constituents and phases. As indicated in Table 5-2, the code system has the ability to model all necessary field equations that have been identified.

Table 5-2: Field & Transport Equations

[redacted]

The thermal-hydraulic and thermal conduction field equations used within S-RELAP5 are the same as used in the RLBLOCA methodology described in Reference 3 and other USNRC approved methodologies based on S-RELAP5. Extensive technical detail related to the field equations is provided in the S-RELAP5 theoretical description (Reference 4).

The neutron kinetics equations contained within the MB2-K 3D kinetics model are described in detail within the MB2-K theoretical description (Reference 6). These field equations solve the transient three-dimensional and two-group equation set with six delayed neutron groups. The advanced nodal methods used in MICROBURN-B2 are also used in MB2-K to solve the spatial neutron flux distribution. A fully implicit numerical scheme is used in the temporal solution in which the neutron flux and the precursor density are factored into a fast varying exponential function and a smoothly varying component.

No field equations are used within the kernel of the RODEX4 fuel thermal-mechanical code that is implemented within S-RELAP5. Instead, RODEX4 calculates the fuel properties based on the temperature predictions of the S-RELAP5 thermal conduction equations.

5.2.3 Closure Relations

Many processes and closure relations are required to support the basic field equations. The thermal-hydraulic, thermal conduction, and neutron kinetics processes and closure relations that model highly ranked PIRT phenomena are summarized in Table 5-3. This table summarizes the processes and closure relations at a high level. The specific processes and closure relations are described separately in Section 5.3 (EMDAP Step 12).

Table 5-3: Processes and Closure Relations

5.2.4 Code Numerics

Numerical solution techniques are available to solve the field equations. The numerical solution techniques contained in S-RELAP5 for the thermal-hydraulic and thermal conduction equations are described in Reference 4, and are the same as used in other S-RELAP5 based methodologies.

Numerical solution techniques are available in MB2-K to solve the neutron kinetics equations, and are partly discussed along with the field equations in Section 5.2.2. The numerical solution techniques are described in detail in Reference 6.

Numerical solution techniques for fuel rod material properties are derived from RODEX4 and are described in Reference 8.

5.2.5 Additional Features

Additional features are available to model boundary conditions and control systems within the EM. These features are summarized in Table 5-4.

Table 5-4: Additional Features

5.2.6 External Data Transfer

External data transfer is an important element of the procedures for treating the input information (particularly the code input arising from the assumed plant state at transient initiation). In addition, analysis of the target scenarios requires input from numerous data sources and engineering disciplines because of the highly coupled neutronic / fuel thermal-mechanical / thermal-hydraulic nature of the events. As a result, the amount and content of data that must be transferred to the EM from external data sources is important in assuring accurate modeling of the BWR plant at the target initial conditions. A summary schematic highlighting important elements of the external data transfer is shown in Figure 5-1.

Preparation and transfer of data requires input from several engineering disciplines. Most important of the input is the MICROBURN-B2 core design that describes how the BWR plant is expected to operate during the fuel cycle(s) being analyzed through the desired cycle exposure point to be analyzed. Definition of the core design and the process for choosing the initial conditions are part of the application methodology outlined in Section 8.0. The MICROBURN-B2 licensing basis core design provides all the necessary cross section and depletion information for input to MB2-K. In addition, a MICROBURN-B2 best estimate core design is used to provide power history and fluence data to best-estimate RODEX4 thermal-mechanical simulations that establish the "permanent effects" in the fuel at the specified time in cycle.

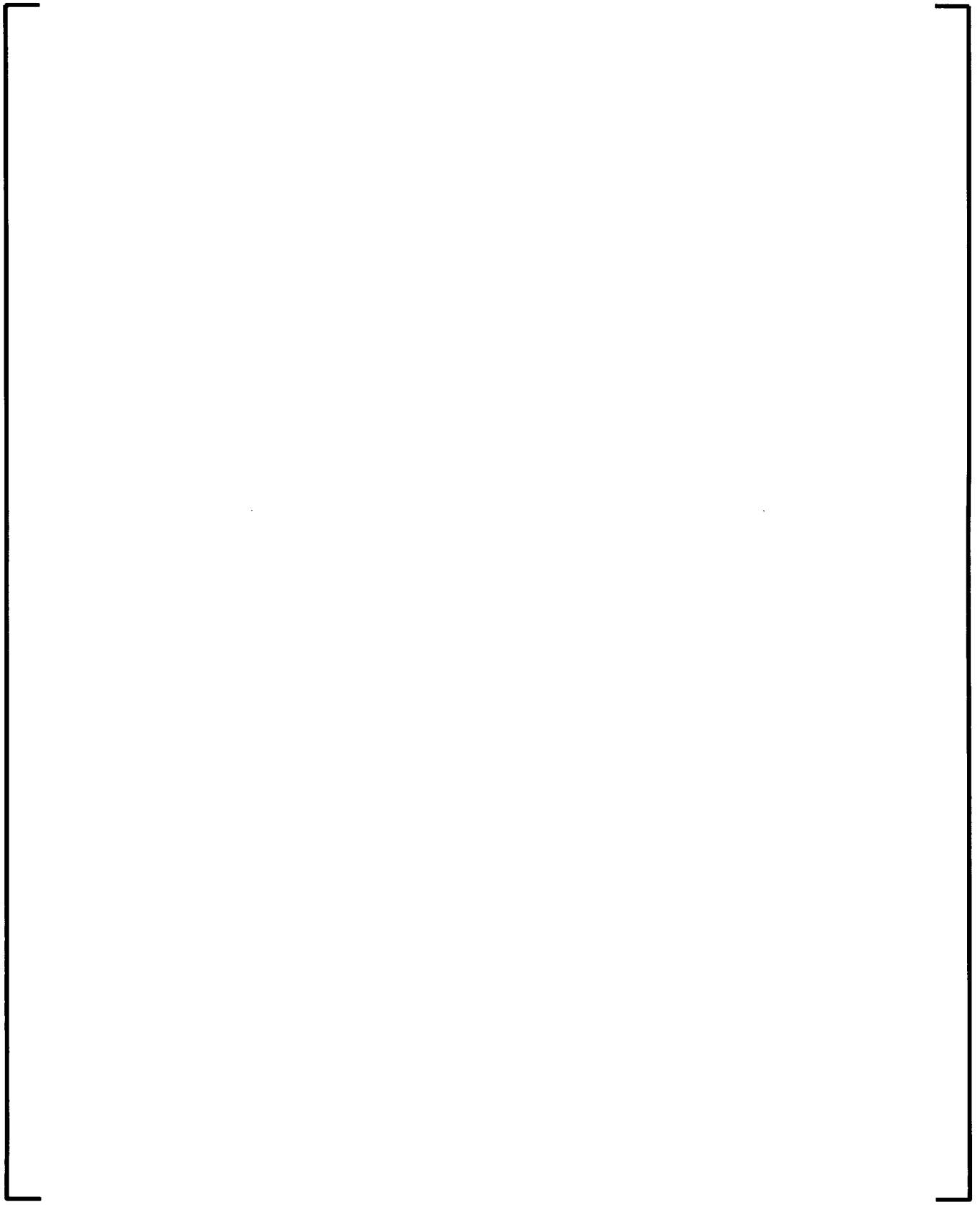

Figure 5-1: External Data Transfer to AURORA-B EM

5.2.7 Coupling of Component Calculational Devices

Coupling of the component calculational devices to create the code system is important to assure the relevant event characteristics are captured in the EM. Modeling the dynamic relationship between the neutron-kinetics, fuel rod models, and core thermal-hydraulics models is a very important aspect in modeling the target scenarios, and the complexity of coupling that has been implemented is consistent with the time scales of the events described in Section 3.0. The coupling between component calculational devices for the system scale calculation is illustrated in Figure 5-2.

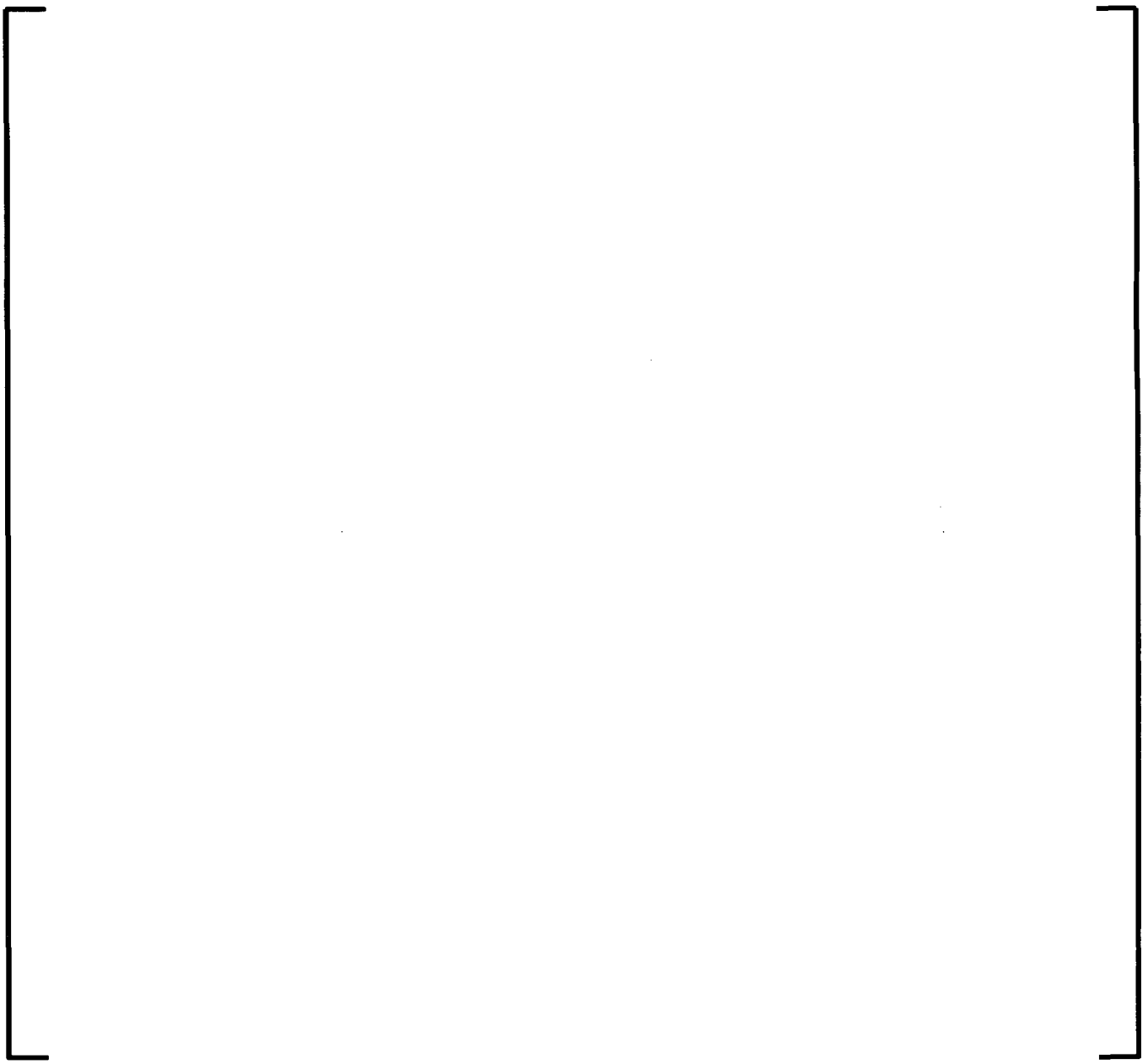

Figure 5-2: Coupling of Component Calculational Devices

In the coupling, the 3D kinetics equations are simulating every fuel assembly in the core at the same level of detail used in the steady state core simulator. Modeling of the water channels/rods and the core bypass are also consistent with the modeling applied in the steady state core simulator.

Coupling from the thermal-hydraulic and thermal conduction equations to the 3D kinetics equations requires passing the active channel, core bypass, and potentially the water channel/rod moderator densities, plus the Doppler effective fuel temperature to the 3D kinetics

[

]

5.2.7.1 Fuel Grouping

All target scenarios in this LTR are "core wide" events, and individual fuel assemblies experience a proportionate hydraulic response to assemblies with similar geometric, hydraulic, thermal power, and fuel thermal properties. Also, an [

] 3D kinetics equations. Therefore, solving the thermal-hydraulic and thermal conduction equations for groups of fuel assemblies is an accurate calculational simplification.

When developing the fuel grouping assignments, an algorithm is applied that ensures all assemblies in a fuel group have identical geometric design, orifice design, nuclear design (e.g. identical nuclear lattice designs), and are part of the same reload batch. Additional characteristics such as exposure, power distribution, and/or the initial CPR predicted by MICROBURN-B2 may be used to define even smaller groups if desired. Typically, the highest power and/or lowest initial CPR fuel assembly of each unique geometry and reload batch is modeled as a single assembly for fuel expected to show a limiting response. [

]

5.2.7.2 Time Step Control and Advancement

A hierarchical scheme is applied in time step control. Each component calculational device determines its optimal time step size based on internal algorithms, and then the coupled code system determines the time step for each device that provides optimal performance for the overall system. The hierarchical scheme allows each device to operate as close as possible to its optimal time step size, which is important because the time scales for the 3D kinetics are typically much longer than those of the hydraulic models for the target scenarios in this LTR.

The internal algorithm for selecting the optimal time step size for the thermal-hydraulic and thermal conduction equations (S-RELAP5) is consistent with the standard RELAP5 algorithm.

FoM. These updated properties are used when solving the thermal conduction equations for fuel rods within S-RELAP5, where the time step size for solving the S-RELAP5 thermal conduction equations was described above.

[

]

5.2.8 Plant Model Nodalization

Modeling of the plant hydraulic components and heat structures is a mathematical mapping from the physical system to the computational framework of the EM. It is recognized that different approaches to the nodalization may yield different results (the "user effect"), particularly in LOCA applications. Though the user effect is not as strong for the target scenarios in this LTR compared to LOCA, the EM relies on a consistent approach to defining the nodalization of the BWR plant to minimize the user effect. Because of the complexity of nuclear power plants and design variations between like plants; the concept of a "standard nuclear power plant nodalization" cannot apply without great simplification and requires clarification.

Nodalization has traditionally referred to the mathematical representation of the physical system (e.g. flow areas, lengths, and volumes), but this is just one element. A "standard nodalization" considers all computer code input necessary to represent the physical plant and any engineered features influencing plant performance. These include trips and control systems, component

dynamics (e.g., pumps), and safety system performance. In addition, computer codes include model options and other plant-independent input for specific phenomenological code models that must be specified to ensure consistency with the assessment base of the EM.

In order to achieve the above, detailed technical guidance has been developed to define the framework under which standardized input models are prepared for the AURORA-B EM. Specifically, the purpose of the technical guidance is to establish a consistent approach for the following parameters;

- Nodalization of hydrodynamic components, heat structures, and their connections, plus flow and pressure boundary conditions
- Modeling practices for components and processes (including selection of phenomenological code models)
- Control variable and trip definition, and their use
- Material properties
- Initialization of the components and structures

The following sections summarize the key aspects of the technical guidance for nodalization of hydrodynamic components and heat structures, as well as the modeling practices for key components and processes. Requirements for establishing the control variables, trip definitions, and their use are provided in Reference 14. Other parameters are less sensitive and are not addressed here.

5.2.8.1 Pressure Vessel Region

The user effect on the plant heat structure and hydrodynamic nodalization is not strong for the target scenarios when compared to LOCA scenarios. This is because little, if any, post CHF heat transfer occurs and flow patterns and chaotic behaviors associated with LOCA are not encountered. The motivation for selecting the heat structure placement and nodalization is to provide adequate modeling of stored energy. The primary motivation in selecting the hydrodynamic nodalization is defining a physically accurate representation of volumes, flow areas, and lengths to ensure accurate modeling of liquid and steam inventory and modeling the fluid momentum or "inertia" in the system. In addition, the nodalization is carefully designed in the regions of quiescent liquid/vapor stratification to ensure stable numerical performance.

The hydrodynamic nodalization of the pressure vessel region (not including the core) is shown in Figure 5-3 through Figure 5-7, and the S-RELAP5 hydrodynamic component type is defined in Table 5-5. [

]

Though not indicated in Figure 5-3 through Figure 5-7, [

] (Note, the drawings are not to scale.)

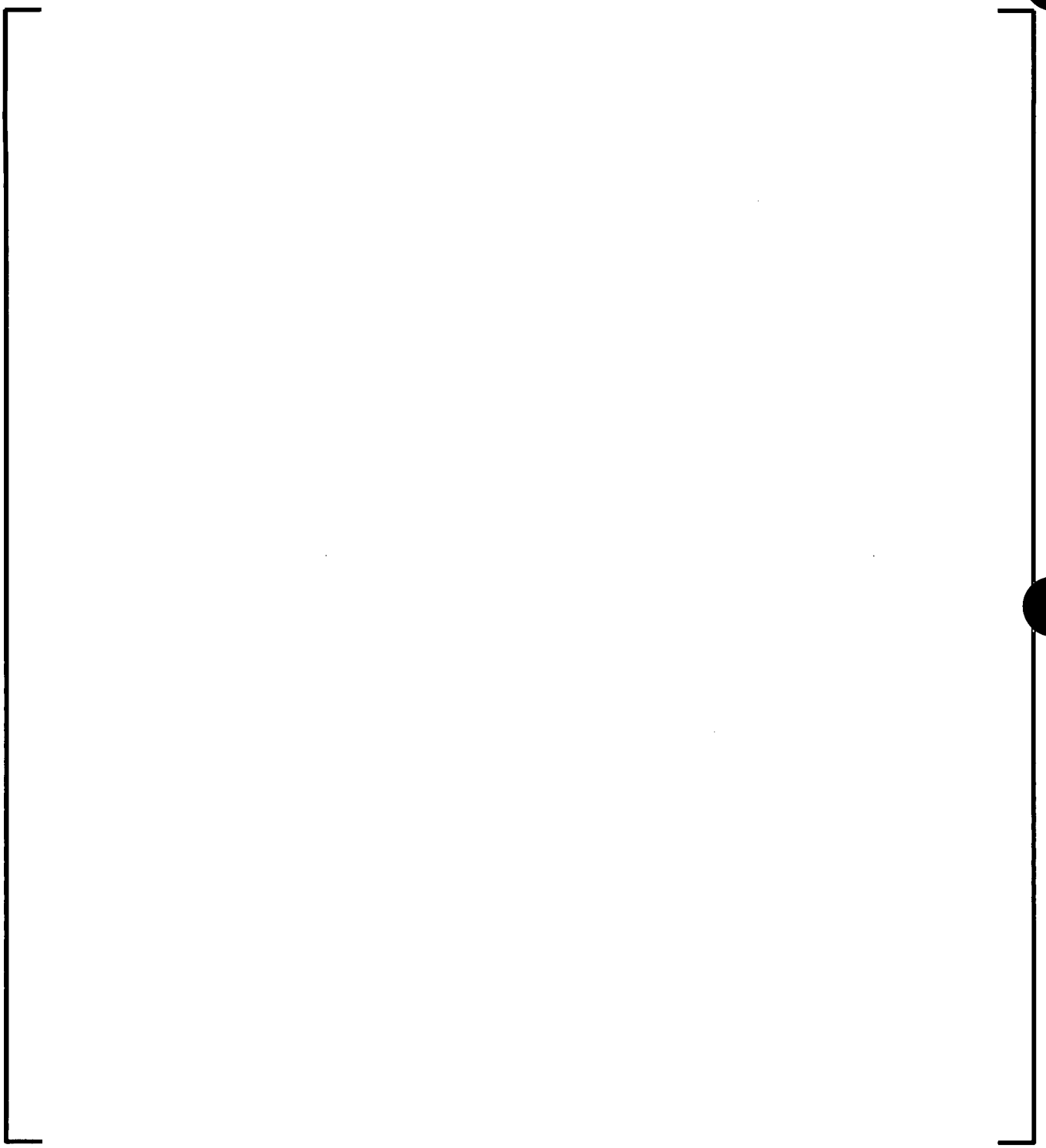

Figure 5-3: Overview of Reactor Vessel Nodalization (Jet-Pump Plant)

Table 5-5: Description of Reactor Vessel Components

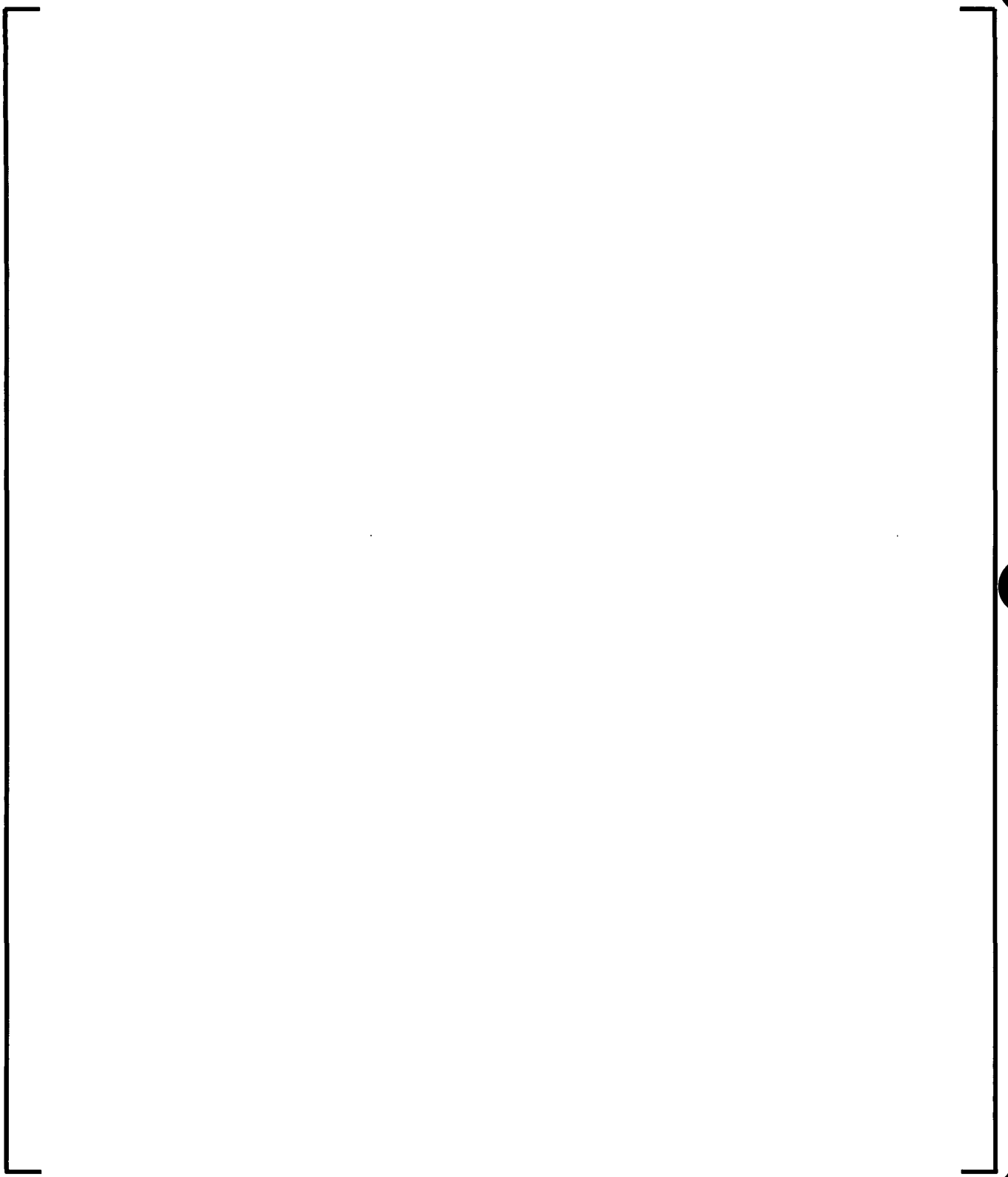

Figure 5-4: Typical Nodalization of Downcomer and Mid-Vessel Region (Jet-Pump Plant)

Figure 5-5: Azimuthal Nodalization of Lower Downcomer Region (Jet-Pump Plant)

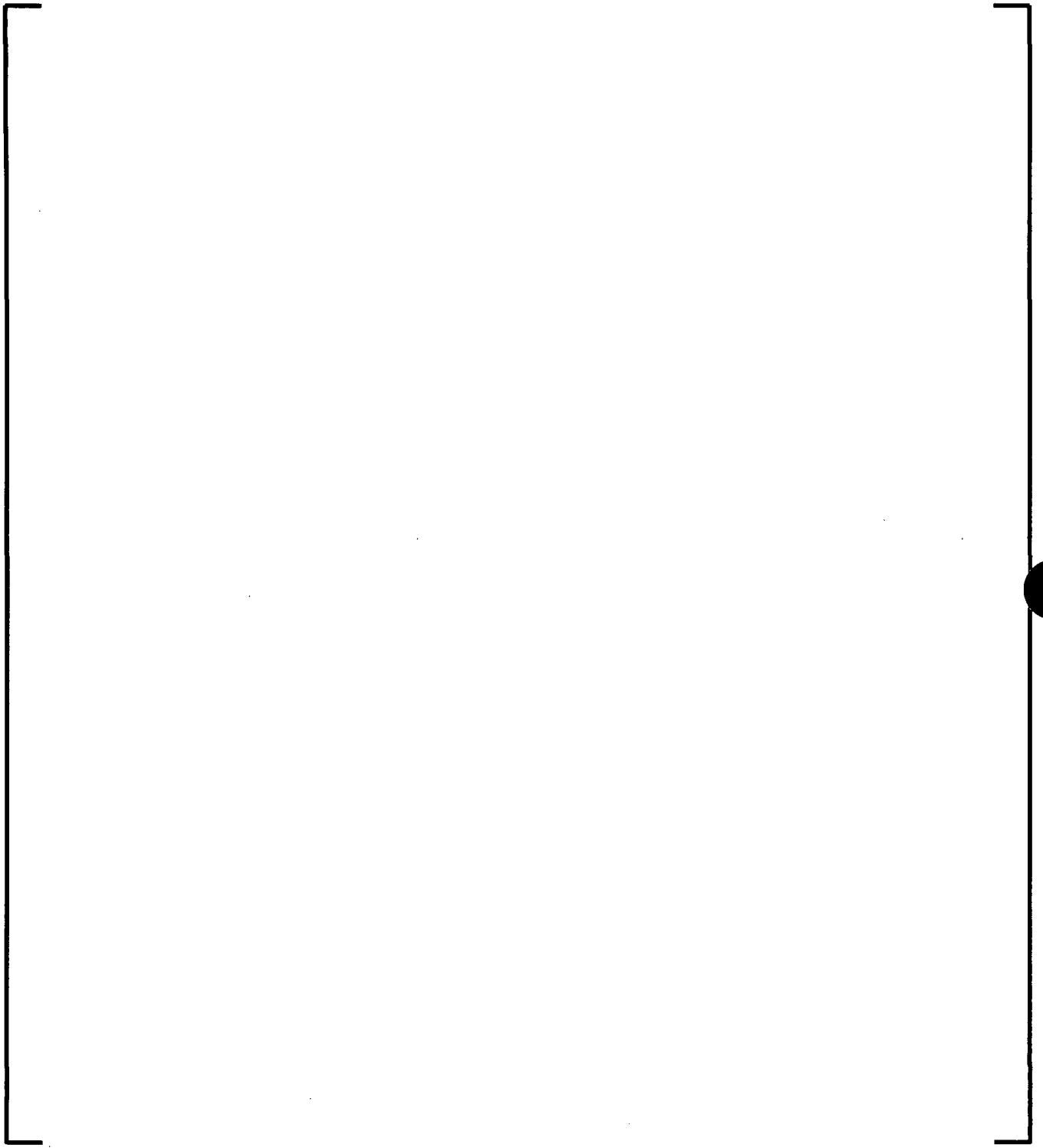

Figure 5-6: Nodalization of Lower Vessel Region (Jet-Pump Plant)

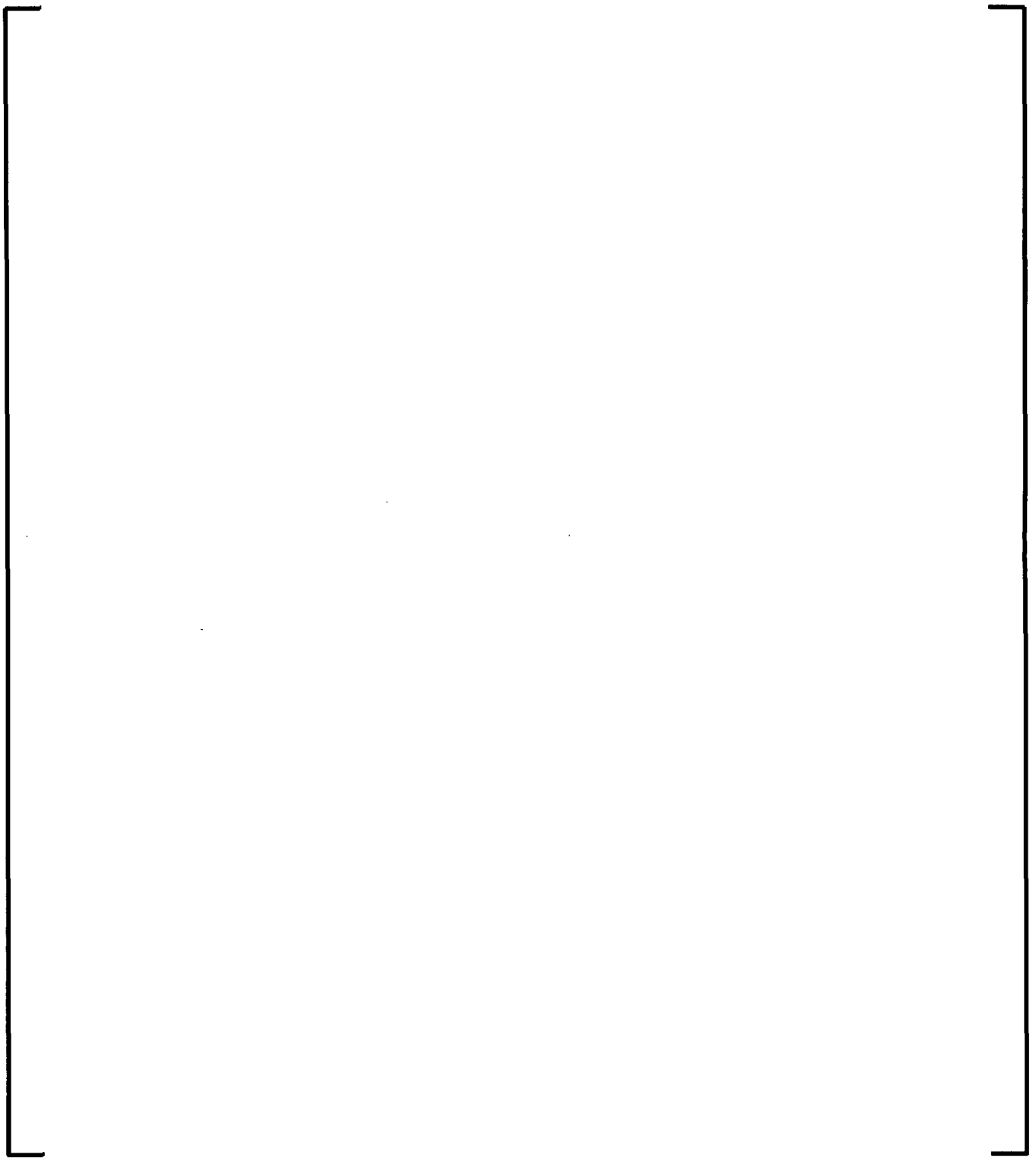

Figure 5-7: Nodalization of Upper Vessel Region (Jet-Pump Plant)

5.2.8.2 Steam Lines

Unlike the reactor pressure vessel internals, which are fairly consistent from plant to plant, the configuration of steam lines in a BWR can vary widely. This is especially true outside of the containment. While varying widely in configuration, preservation of several key physical characteristics in the nodalization of the steam lines ensures good fidelity of numerical predictions. Preservation of these physical characteristics is achieved by respecting the following technical guidance for steam line modeling;

[ ]

5.2.8.3 Recirculation System

There is little sensitivity to the nodalization of the recirculation system piping and pumps for the target scenarios. Nevertheless, technical guidance for modeling this system defines a framework under which standardized input models are prepared that assure the physical characteristics of the piping are modeled. Some key aspects of the guideline are preservation of the total length and volume of recirculation piping, prediction of pressure losses in the piping, and ensuring the rotational inertia, rotational speed, and head produced by the recirculation pumps are consistent with plant data. The best available homologous pump curves are also used to assure accurate modeling.

5.2.8.4 Core Region

The nodalization of the fuel assemblies, flow channels, water channels/rods, core bypass region, and associated heat structures are developed in a manner consistent with the steady state core simulator and fuel design data, except for consideration of "fuel grouping" as described in Section 5.2.7.1. [

]

5.2.8.5 Plant Parameters Data

Plant parameters data are those parameters used in preparing input to the EM that describe the configuration of a given plant that could potentially change from cycle to cycle. A document defining the parameters is prepared jointly by AREVA and the utility customer for each plant and reviewed each fuel cycle. Every value is reviewed and accepted by the utility customer to ensure the most accurate data defining the plant configuration is used in AREVA analyses. This is particularly important to ensure AREVA is aware of values which have been superseded due to plant configuration changes, operation changes, or more recent information. Customer

acceptance of the document validates the parameters within the document. Changes from prior cycles are typically highlighted to ensure analysts are aware of the changes.

The plant parameters data provides necessary information for the physical plant and any engineered features influencing plant performance as part of the "standard nodalization". The data are obtained from plant drawings, plant design data and specifications, component/equipment design data and specifications, plant system manuals, Technical Specifications, startup test data, plant operation data, and other similar sources.

The following list summarizes key plant parameters data used in developing input to the EM;

- Core thermal power, core flow, steam flow, dome pressure at rated conditions, and allowable power/flow map for off rated conditions.
- Heat balance parameters including; feedwater system performance, heat losses to the environment, control rod and cleanup system flow and enthalpy, and pressure loss in the main steam lines from the vessel steam dome to the turbine system.
- Flow capacity and operation of MSIVs, TBVs, TCVs, TSVs, and SRVs.
- Recirculation pump or RIP performance data (including homologous curves and rotational inertia), recirculation flow and allowable mismatch in recirculation flow between loops (jet-pump plants only), and pump speed versus pump capacity.
- Safety system performance and set points including; scram set points for high neutron flux, high dome pressure, scram delays for the instrumentation, control rod insertion speeds, recirculation pump trip set points, water level set points.
- Control system parameters including; sensor time constants, constants and gains for the feedwater system and the pressure regulator system plus the configuration of these systems.

The approach for selecting specific values for plant parameters data that assure plant operations are bounded is described in Section 8.0 for the application methodology.

5.2.9 Single Channel Model

Some FoM are "local" (i.e. related to one particular fuel assembly) and may require special procedures to predict them. [

]

[

]

Application of the single channel model is possible because BWR fuel assemblies [

]

The single channel model complements the system scale calculation because it allows for analysis of any fuel assembly in the core, even assemblies that are included in fuel groups containing more than one fuel assembly. In particular, the model permits analysis of local FoM in any fuel assembly in the core without needing to explicitly model the hydraulic response of every assembly within the system scale calculation.

Implementation of the single channel model within the EM has been made within S-RELAP5. The nuclear response is not reanalyzed within the single channel model; rather the power deposited in the fuel and active moderator per node for a fuel assembly is transferred from the system scale calculation to the single channel model [

] Transfer of the geometric data, initial conditions, hydraulic boundary conditions as a function of time, and the nodal power as a function of time for the fuel assembly of interest is made using data files generated from the system scale calculation.

5.2.9.1 Determination of Event MCPR Response

The single channel model is applied for evaluating the fuel assembly ΔCPR independent from the system scale calculations. [

]

[

]

5.2.9.2 Determination of Peak Cladding Temperature and Maximum Local Oxidation

The single channel model is applied for evaluating peak cladding temperature and maximum oxidation during events where boiling transition is allowable. [

] the transient assembly power response during the event.

Analysis of the cladding temperature and oxidation is only necessary in selected scenarios where boiling transition is permitted, and analysis of the maximum cladding temperature is necessary. [

]

[

]

5.3 *Develop or Incorporate Closure Models (EMDAP Step 12)*

Models and closure relations identified in EMDAP Step 3 that did not already exist within the component calculational devices were developed or incorporated in the EM. The needed closure relations and process models were created, refined and/or assessed based on test data depending on their origin and pedigree.

A large number of models and closure relations are necessary to analyze the target scenarios, many of which are not associated with predicting highly ranked phenomena and processes. The theory manuals for the CCDs provide in-depth descriptions of the models and closure relations. In addition, the validation and assessment of the CCDs address the basis, range of applicability, and accuracy of the models and closure relations. Models and closure relations associated with highly ranked phenomena and processes are summarized in Table 5-6.

Table 5-6: Summary of Models and Closure Relations Associated with Highly Ranked Phenomena

Table 5-6: Summary of Models and Closure Relations Associated with Highly Ranked Phenomena (cont.)

Table 5-6: Summary of Models and Closure Relations Associated with Highly Ranked Phenomena (cont.)

6.0 Assess Evaluation Model Adequacy (EMDAP Element 4)

Evaluation model adequacy was assessed after the previous elements were established and the EM capability was programmed. The process proceeded on an iterative basis between the various elements and steps, though only the final results were documented and are presented in the LTR.

The EM assessment is divided into two parts. The first part (EMDAP Steps 13–15) pertains to the "bottom-up" evaluation of the closure relations for each component calculational device. In this part, important closure models and correlations are examined by considering their pedigree, applicability, fidelity to appropriate fundamental or SET data, and scalability.

The second part (EMDAP Steps 16–19) pertains to the "top-down" evaluations of code-governing equations, numerics, the integrated performance of each code, and the integrated performance of the overall EM. This includes examining the field equations, numerics, applicability, fidelity to integral effects and plant transient data.

Assessment Criteria

The assessment results described in the following sections provide statements about the ability of the EM to predict key parameters of each assessment. Reference 2 suggests how this may be done by defining criteria associated with levels of code-data agreement. The four levels of agreement defined in the reference are used within this LTR. These criteria move from the most desirable correlation of data to the code system to the unacceptable prediction of the data by the code system. For PIRT high-ranked phenomena, the minimum standard for acceptability with respect to fidelity is generally "reasonable agreement." The criteria are:

- Excellent Agreement: Applies when the code exhibits no deficiencies in modeling a given behavior. Major and minor phenomena and trends are correctly predicted. The calculated results are judged to agree closely with data.
- Reasonable Agreement: Applies when the code exhibits minor deficiencies. Overall, the code provides an acceptable prediction. All major trends and phenomena are predicted correctly. Differences between calculated values and data are greater than are deemed necessary for excellent agreement.
- Minimal Agreement: Applies when the code exhibits significant deficiencies. Overall, the code provides a prediction that is not acceptable. Some major trends or phenomena are not predicted correctly, and some calculated values lie considerably outside the specified or inferred uncertainty bands of the data.

- Insufficient Agreement: Applies when the code exhibits major deficiencies. The code provides an unacceptable prediction of the test data because major trends are not predicted correctly. Most calculated values lie outside the specified or inferred uncertainty bands of the data.

6.1 *Determine Model Pedigree and Applicability to Simulate Physical Processes (EMDAP Step 13)*

The physical basis of closure models, assumptions and limitations attributed to the models, and details of the adequacy characterization at the time the models were developed are captured in the software quality assurance documentation associated with the component calculational devices. Much of the information is also captured in the theoretical descriptions of the devices (References 4, 6, and 8).

6.2 *Prepare Input and Perform Calculations to Assess Model Fidelity or Accuracy (EMDAP Step 14)*

The fidelity and accuracy of the closure relations and process models have been assessed using separate effects test data from numerous facilities. Comparison to separate effects tests demonstrates the capability of the EM to predict the important phenomena and processes. The nodalization and option selections used in the separate effects tests are consistent (as far as achievable) with those used in plant analyses. Table 4-1 lists the assessment matrix which includes the SETs, and the phenomena and processes from the PIRT to be addressed by each SET. In addition to the SETs assessments, a description of the closure relations and process models assessment for MICROBURN-B2 and RODEX4 that are performed in the respective CCDs is summarized and references are provided to more detailed assessment descriptions.

The following sections provide the results of the assessments. The results demonstrate the accuracy of the EM to predict key parameters of each assessment. The impact of biases and uncertainties in the predictions is quantified via sensitivity analyses provided in Section 6.8.

6.2.1 Rod Bundle Void Tests

Assessed phenomena and processes

This section addresses the following highly ranked PIRT phenomena identified in Table 4-1;

[ ]

Assessment conclusions

Direct measurement of the highly ranked PIRT phenomena cannot be made in the tests, so the assessment is performed via measured and predicted void fraction. The assessment data base includes a total of [ ] from 3 different test facilities. These tests were performed for a wide range of system pressures (725 to 1260 psia) and flow conditions that cover the typical operating BWR conditions. The S-RELAP5 calculation with a prediction uncertainty band of [ ] These assessment results show excellent code-data agreement for these rod bundle void tests. From this, it is inferred that the EM makes excellent predictions of the indicated PIRT phenomena. Specific conclusions are drawn for the result of each test facility below.

Assessment description

The S-RELAP5 models [ ] have been improved and the range of assessment expanded over what was described in the RLBLOCA methodology (Reference 3). The characteristics of the rod bundle void fraction tests used to assess the models are summarized in Table 6-1.

Table 6-1: Rod Bundle Void Fraction Test Characteristics

	FRIGG2	FRIGG3	ATRIUM*-10A
Axial Power Shape	uniform	uniform	[
Radial Power Peaking	uniform	mild peaking	
Bundle Design	circular array with 36 rods + central thimble	circular array with 36 rods + central thimble	
Pressure (psia)	725	725, 1000, and 1260	
Inlet Subcooling (^{0}F)	4.3 to 40.3	4.1 to 54.7	
Mass Flow Rate (lbm/s) *(calculated from mass flux assuming ATRIUM-10 inlet flow area)*	14.3 to 31.0	10.1 to 42.5	
Equilibrium Quality at Measurement Plane [fraction]	-0.036 to 0.203	-0.058 to 0.330	
Max Void at Measurement Plane [fraction]	0.828	0.848	
Reported Instrument Uncertainty [fraction]	±0.025	±0.016	
Number of Data	27 tests, 174 points	39 tests, 157 points	]

The FRIGG2 and FRIGG3 experiments have been included in the database because of the broad industry use of these experiments in benchmarking activities, including TRAC, TRACE, and RETRAN. These experiments include a wide range of system pressures, subcooling, and quality from which to validate the general applicability of the models. The reported instrument uncertainty on the void fraction for these tests is provided in Table 6-1 based on mockup testing. However, the total uncertainty of the measurements (including power and flow uncertainties) is expected to be larger than the indicated values.

* ATRIUM is a trademark of AREVA NP

The ATRIUM-10A void fraction tests were performed at the KATHY test facility. This experiment used prototypical BWR fuel assembly geometry, part length fuel rods, mixing vane grids, and a prototypic axial/radial power distribution. The range of test conditions for the ATRIUM-10A void data covers the typical reactor operating conditions, including the EPU conditions.

[

] Specific assessment results from the rod bundle void tests are presented in the following subsections.

6.2.1.1 FRIGG2 Void Tests

The FRIGG2 void distribution experiments were performed in the FRIGG Loop Facility in the late 1960s (Reference 24). The test section had 36 heated rods with uniform axial and radial power distribution, and was designed to give a full-scale simulation of a boiling channel for the Marviken reactor. The void distribution was measured for pre-CHF flow regimes at several axial locations by the multi-beam gamma method and the range of tested conditions is indicated in Table 6-1. The FRIGG2 void distribution experiments were used initially to support S-RELAP5 code assessment for the RLBLOCA methodology (Reference 3), though code improvements have been made since being reported in that reference. Additional details about the test can be found in Reference 25.

Figure 6-1 compares the calculated void fraction against the measured void fraction for all 27 tests with a total of 174 points. [

]

Based on this code-data comparison and the criteria described in Section 6.0, the FRIGG2 void test assessment results show excellent agreement between the predicted and measured void fraction.

Figure 6-1: Calculated vs. Measured Results for all FRIGG2 Void Fraction Tests

6.2.1.2 FRIGG3 Void Tests

The FRIGG3 void distribution experiments were performed as a follow-on test after the FRIGG2 tests (References 26 and 27). The test section was essentially the same as the earlier test, except that a mild radial power peaking was introduced. The range of tested conditions is indicated in Table 6-1, of notable interest was the increase in tested pressure and slight increase in maximum measured void fraction.

Figure 6-2 compares the calculated void fraction against the measured void fraction for all 39 tests with a total of 157 points. [

]

Based on this code-data comparison and the criteria described in Section 6.0, the FRIGG3 void test assessment results show excellent agreement between the predicted and measured void fraction.

Figure 6-2: Calculated vs. Measured Results for all FRIGG3 Void Fraction Tests

6.2.1.3 ATRIUM-10A Void Tests

The ATRIUM-10A void fraction tests were performed at the KATHY test facility using a prototypical BWR CHF test assembly. The test assembly used part length fuel rods, mixing vane grids, a [ ], and a radial power peaking typical of CHF tests. Void measurements were made at one of three different elevations in the assembly for each test point: just before the end of the part length fuel rods, midway between the last two

spacers, and just before the last spacer. A scanning gamma apparatus was used to measure the void fraction.

Figure 6-3 compares the calculated void fraction against the measured void fraction for all [

] Based on this code-data comparison and the criteria described in Section 6.0, the ATRIUM-10A void test assessment results show excellent agreement between the predicted and measured void fraction.

Figure 6-3: Calculated vs. Measured Results for all ATRIUM-10A Void Fraction Tests

6.2.2 Christensen Void Tests

Assessed phenomena and processes

This section addresses the following highly ranked PIRT phenomena identified in Table 4-1;

[

]

Assessment conclusions

Direct measurement of the highly ranked PIRT phenomena cannot be made in the tests, so the assessment is performed via measured and predicted void fraction. The assessment data base includes a total of 7 tests (or a total of 112 test points) from the Christensen test facility. These tests were performed for a wide range of system pressures (725 to 1260 psia), inlet subcooling and flow conditions that cover the typical operating BWR conditions. The S-RELAP5 calculated void fraction with a prediction uncertainty [

] The effect of subcooled boiling is also assessed and the result shows excellent agreement between prediction and data.

This assessment results show excellent code-data agreement for the Christensen void fraction tests. From this, it is inferred that the EM makes excellent predictions of the indicated PIRT phenomena.

Assessment description

The Christensen void fraction tests were used in the development of the Lahey subcooled models implemented in the RELAP5 family of codes, including S-RELAP5. These tests also provide a good model assessment for [

]

The Christensen void fraction tests were performed in a test apparatus at the Argonne National Laboratory in 1961 (Reference 28). The test section for these experiments was a stainless steel

uniformly heated vertical rectangular tube. The primary purpose of these tests was to study void oscillations and stability in BWR systems, but the experiments also provided data on steady state axial void distributions, particularly for the subcooled boiling region. The void measurements were made using the gamma-ray attenuation technique and the void fraction at 16 axial locations.

Seven tests were reported in Reference 28 with 16 measurement points for each test along the axial length of the heated section. The boundary conditions for the tests are summarized in Table 6-2.

Table 6-2: Christensen Test Characteristics

Axial Power Shape	uniform
Radial Power Peaking	uniform
Bundle Design (inch)	0.437x1.748 - duct
Test Section Height (inch)	50
Pressure (psia)	400-1000
Inlet Subcooling (^{0}F)	2.2 to 27.4
Mass Flux (Mlbm/ft^2-hr)	0.472 to 0.693
Equilibrium Quality at Measurement Plane [fraction]	-0.044 to 0.040
Max Void at Measurement Plane (fraction)	0.65
Reported Instrument Uncertainty (fraction)	± 0.025 (tests 9-13) ± 0.050 (tests 15-16)
Number of Data	7 tests, 112 points

Figure 6-4 compares the calculated void fraction against the measured void fraction for all 7 tests with a total of 112 points. This figure also compares the measurement uncertainty and the [

]

Based on this code-data comparison and the criteria described in Section 6.0, the Christensen void test assessment results show excellent agreement between the predicted and measured void fraction.

Figure 6-4: Calculated vs. Measured Results for all Christensen Tests

Figure 6-5 compares the calculated and measured void fraction as a function of equilibrium quality, for Tests 11, 12 and 13 (a total of 48 points). These three tests used the same pressure, inlet flow rate, and power level – the only variable between them being the inlet subcooling. The inlet subcooling was 27.4 ^{0}F, 14.2 ^{0}F, and 2.2 ^{0}F for Tests 11, 12, and 13

respectively. Figure 6-5 shows excellent code-data agreement and the ability of S-RELAP5 to accurately predict the phenomena associated with subcooled boiling.

Figure 6-5: Christensen Tests at 600 psia with varying Subcooling

6.2.3 Allis-Chalmers Large Diameter Void Tests

Assessed phenomena and processes

This section addresses the following highly ranked PIRT phenomena identified in Table 4-1;

[

]

Assessment conclusions

Direct measurement of the highly ranked PIRT phenomena cannot be made in the tests, so the assessment is performed via measured and predicted void fraction. The selected test facilities for this assessment covered 3 different sizes in diameter (2.9, 18 and 36 inches) and length/diameter ratios (16.5, 7.85 and 3.92), for a total of 162 data points. The experiments were performed for a wide range of system pressures (615 to 2015 psia) and flow conditions that cover the operating conditions expected in the BWR steam separator standpipes and upper plenum. The assessment results show reasonable agreement between the predicted and measured void fraction. The experimental uncertainty was not provided with the test data, [

] From this, it is inferred that the EM makes reasonable predictions of the indicated PIRT phenomena.

Assessment description

[

]

The S-RELAP5 models affecting these phenomena have been improved and the range of assessment has been expanded to cover these regions. The large diameter adiabatic void fraction tests (References 29, 30, and 31) performed by Allis-Chalmers have been included in the S-RELAP5 assessment database. The characteristics of these void fraction tests are summarized in Table 6-3.

Table 6-3: Allis-Chalmers Large Diameter Void Test Characteristics

	2.9 inch	18 inch	36 inch
Test Section Design	2.9 inch inner diameter circular pipe (Ref. 29)	18 inch inner diameter circular pipe (Ref. 30)	36 inch inner diameter circular pipe (Ref. 31)
Pressure (psia)	615 – 1515	615 – 2015	615 – 1615
Inlet Subcooling (^{0}F)	0	0	0
Mass Flux (lbm/ft^2-sec)	0.26 – 956.	0.786 – 9.43	0.393 – 2.36
Max Void at Measurement Plane [fraction]	0.035 – 0.694	0.255 – 0.687	0.107 – 0.463
Percentage of data covered within the prediction uncertainty band of ± 0.10 (by the Kataoka-Ishii Correlation)	83%	89%	100%
Number of Data	52	56	54
Test Section (Length/Diameter) Ratio	16.5	7.85	3.92

Results from these void fraction tests have been widely used in the industry to develop void correlations, such as the Wilson Bubble Rise model (Reference 32) and the Kataoka-Ishii correlation (Reference 33). Instrument uncertainties on these void fraction tests were not reported. [

]

The S-RELAP5 assessment results from the Allis-Chalmers large diameter void tests are presented in the following subsections.

6.2.3.1 2.9 Inch Void Tests

A series of experiments (Reference 29), designed to measure steady-state void fractions in the vertical flow of steam-water mixtures in a 2.9 inch inside diameter pipe, was performed over a wide range of flow conditions. The experiments covered a range of superficial liquid velocity from 0.0 to 20.0 ft/s, and the system pressures were set at 615, 1015 and 1515 psia. Table 6-3

summarizes the range of tested conditions. Instrument uncertainties on these void fraction tests were not reported. [

]

The void fractions were determined from measurements by a gamma ray attenuation system. The void fractions taken at the axial location corresponding to a length-to-diameter (L/D) ratio of 16.5 are used in the S-RELAP5 assessment calculations.

Figure 6-6 shows the S-RELAP5 results - the comparison of the calculated versus measured void fraction for all 52 data points. This figure also compares the [

] Based on this code-data comparison and the criteria described in Section 6.0, the assessment results show reasonable agreement between the predicted and measured void fraction.

Figure 6-6: Calculated vs. Measured Results for all 2.9 Inch Diameter Void Fraction Tests

6.2.3.2 18 Inch Void Tests

The measurements of void fraction in a bubbling two-phase mixture in an 18 inch vertical pipe (Reference 30) were conducted in a test loop with a 3 ft diameter by 25 ft high pressure vessel located in an electrical power plant in Oak Creek, Wisconsin. The internals of the 3 ft pressure vessel consisted of an 18 inch diameter channel (test section) running the full length of the vessel. The void fraction was determined by differential pressure cells, which were measured at

an axial elevation well below the water level inside the test section. In a typical test run, the vessel pressure and the water level were set at the test conditions. The steam flow was next set to a predetermined rate. When equilibrium conditions were reached, the differential pressure cell readings and the steam flow rate were recorded.

Table 6-3 summarizes the range of tested conditions. Instrument uncertainties on these void fraction tests were not reported. [

]

Figure 6-7 shows S-RELAP5 results - the comparison of the calculated versus measured void fraction for all 56 data points. This figure also compares the [

] Based on this code-data comparison and the criteria described in Section 6.0, the assessment results show reasonable agreement between the predicted and measured void fraction.

Figure 6-7: Calculated vs. Measured Results for all 18 Inch Diameter Void Fraction Tests

6.2.3.3 36 Inch Void Tests

The entire 3 ft diameter vessel discussed in the previous section was used in a follow-up series of void fraction tests. This test series (Reference 31) measured the void fraction in a bubbling two-phase mixture in a 36 inch vertical vessel (test section). The void fraction was determined by differential pressure cells, which were measured at an axial elevation well below the water level inside the test section. In a typical test run, the vessel pressure and the water level were set at the test conditions. The steam flow was next set to a predetermined rate. When

equilibrium conditions were reached, the differential pressure cell readings and the steam flow rate were recorded.

Table 6-3 summarizes the range of tested conditions. Instrument uncertainties on these void fraction tests were not reported. [

]

Figure 6-8 shows the S-RELAP5 results - the comparison of the calculated versus measured void fraction for all 54 test points. This figure also compares the [

] Based on this code-data comparison and the criteria described in Section 6.0, the assessment results show reasonable agreement between the predicted and measured void fraction.

Figure 6-8: Calculated vs. Measured Results for all 36 Inch Diameter Void Fraction Tests

6.2.4 GE Level Swell

Assessed phenomena and processes

This section addresses the following highly ranked PIRT phenomena identified in Table 4-1;

Assessment conclusions

Direct measurement of the level swell process cannot be made in the test because it is defined by several lower level phenomena, particularly interfacial drag and interfacial heat transfer. The assessment is performed via measured and predicted void fraction and their evolution during the event. The level swell test produced excellent code-data comparisons for the void fraction distribution. From this, it is inferred that the EM makes excellent predictions of the indicated PIRT phenomena.

Assessment description

[ ] The GE Level Swell Test 1004-3 was initially used to support S-RELAP5 code assessment of level swell in the RLBLOCA methodology (Reference 3). Code improvements have been made since being reported in that reference with the revised results presented here. Additional details about the test can be found in Reference 25.

The GE Level Swell Test 1004-3 is essentially a small break blowdown of a vertical vessel 14 ft high by 1 ft in diameter (Reference 34). The vessel was initially pressurized to 1011 psi and filled with saturated water up to the 10.4 ft elevation. The test was initiated by blowing down the pressure vessel with the blowdown rate controlled by losses in the blowdown line. The void fraction distribution was measured axially in the test using differential pressure sensors spaced at 1 ft intervals.

The purpose of this assessment is to test the two-fluid interfacial models in predicting the flow regimes and void fraction distributions that occur under level swell in depressurization conditions. The assessment validates the interfacial drag and heat transfer submodels that contribute to predicting level swell. The key model affecting these assessments is the interfacial friction for the bubbly and slug flows.

Comparisons of measured versus calculated axial void fraction distributions are made at two transient times, 40 and 100 sec. Figure 6-9 and Figure 6-10 show the S-RELAP5 calculated void fraction results compared to measured data. Results from S-RELAP5 compare well with the data. The void fractions calculated by S-RELAP5 are within the range of experimental

uncertainty, providing excellent agreement. The calculated flow regimes are bubbly flow below the void fraction of 0.25; slug flow from the void fraction of 0.25 up to the two-phase mixture level position, which occurs at around the void fraction of 0.3 to 0.6; and annular-mist flow (very close to single-phase steam) above the mixture level. The results indicate that, for this slow transient condition, the two-fluid interfacial friction model implemented in S-RELAP5 makes excellent predictions of the indicated PIRT phenomena.

The jump of void fraction from ~0.4 to ~0.99 within neighboring volumes distinctly defines the location of a two-phase mixture level. The interfacial friction models for slug flow, vertical stratification, and annular-mist flow work in harmony to produce a smooth, but sharp transition from a low void fraction region to a very high void fraction (close to 1.0) region.

In a non-equilibrium code such as S-RELAP5, the phase exchange (vapor generation) process during blowdown is calculated through the use of an interfacial heat transfer model. The calculated liquid and vapor (steam) temperatures are close to the saturation temperature. This shows that the interfacial heat transfer submodels, particularly those for the metastable state conditions, are appropriate and adequate for treating the depressurization phenomena.

Figure 6-9: Void Profiles at 40 Seconds for the 1 ft GE Test 1004-3

Figure 6-10: Void Profiles at 100 Seconds for the 1 ft GE Test 1004-3

6.2.5 Summary of MICROBURN-B2 Qualification

Assessed phenomena and processes

This section addresses the following highly ranked PIRT phenomena identified in Table 4-1;

Assessment conclusions

Calculation of the neutron kinetics and other nuclear related properties in the EM is performed by the MICROBURN-B2 core simulator code and underlying cross section generation codes for input to MB2-K. Qualification of the MICROBURN-B2 core simulator code for BWR applications

is described in Reference 5. Direct qualification of some phenomena is achieved in the reference. [

]

The remaining phenomena are indirectly assessed by comparing code calculations to actual plant data. These data include traversing incore probe measurements performed periodically at BWRs supported by AREVA and eigenvalue trending where actual cycle operations are simulated to compare the calculated eigenvalue versus BWR plants in power operation. Comparisons of calculated results indicate reasonable to excellent agreement with these "integral" data. From this, it is inferred that the MICROBURN-B2 core simulator code and underlying lattice physics method provides reasonable to excellent predictions of [

]

Assessment description

MICROBURN-B2 is a modern nodal method for solving the three–dimensional, two group neutron diffusion equation. A high order spatial method based on polynomial expansion of the nodal flux distribution is used to solve the spatial fast and thermal flux distribution within the BWR core. The MICROBURN-B2 code and underlying lattice physics method which together make up the code system have been qualified versus a very broad range of plant operational data, higher order numerical models, and isotopic inventory measurements. Assessment and qualification of the code system is described in Reference 5.

In addition to the qualification described in Reference 5, the code system is assessed versus new data sources on an ongoing basis. This is a necessary element of maintaining and confirming the predictive capabilities of the code system for fuel cycle design, core monitoring, determining shutdown margin, and fuel licensing activities. Since USNRC approval in Reference 5, qualification of the code system has been confirmed for EPU conditions. Confirmation of the qualification for these conditions assures the code system provides accurate

neutron kinetics parameters to MB2-K for target scenarios of the AURORA-B EM in modern fuel cycle design and operating strategies.

6.2.6 Summary of RODEX4 Qualification

Assessed phenomena and processes

This section addresses the following highly ranked PIRT phenomena identified in Table 4-1;

[

]

Assessment conclusions

Thermal-mechanical fuel rod modeling in the EM is performed by the RODEX4 fuel rod code. This code has been developed to perform best-estimate fuel performance predictions considering normal operation and anticipated operational occurrence scenarios as described in Reference 7. [

] As such, a very detailed qualification of the underlying processes and phenomena has been undertaken at a deep level of detail. The overall code performance shows overall excellent agreement with a broad database of fuel rod data, and is capable of accurately modeling heat release rates from the fuel rods to the coolant during target scenarios in this EM.

Assessment description

RODEX4 is a modern realistic thermal-mechanical fuel rod code with the necessary models and correlations to predict fuel rod thermal-mechanical behavior to high burnup (it is currently approved to 62 GWd/MTU peak rod average burnup). The code has been qualified versus a very broad range of data. Also, the processes and phenomena have been USNRC approved to predict transient strain and pellet temperature in typical AOO applications such as feedwater controller failure. With its capability to predict transient conditions, RODEX4 is well qualified for modeling heat release rates from the fuel rods to the coolant during transients. Therefore, RODEX4 is well qualified for use in the AURORA-B EM.

[

]

[

]

6.3 *Assess Scalability of Models (EMDAP Step 15)*

The scalability of the models and correlations that are assessed in EMDAP Step 14 to the configuration and conditions of the plants and transients under evaluation has been confirmed. Specifically, the assessments include separate effects tests that are prototypic in geometry and/or tested conditions, or overlapping prototypic tests confirm the scalability of non-prototypic tests.

6.4 *Determine Capability of Field Equations to Represent Processes and Phenomena and the Ability of Numeric Solutions to Approximate Equation Set (EMDAP Step 16)*

The thermal-hydraulic, thermal conduction, and neutron kinetics equations have been determined to adequately represent processes and phenomena for the selected scenarios. The numerical solutions have also been determined to adequately solve the field equations, including adequate capabilities for solution convergence, property conservation, and stability of code calculations to solve the original equations when applied to the target applications.

The thermal-hydraulic and thermal conduction field equations and numerical solutions contained in RELAP5 have been extensively demonstrated in numerous assessments reported in the open literature. These numerics have been improved in S-RELAP5 as described in Reference 3 and 4. The adequacy of the S-RELAP5 specific field equations and numerics has been demonstrated in the performance of the assessments reported in Reference 25 and within this LTR. One process that requires adequate numerical solution techniques (as well as adequate closure relations) is the resolution of pressure waves. The capability to predict

pressure waves is inherent to the S-RELAP5 numerics and assessment of this capability is demonstrated in Section 6.5.5.

No field equations are solved within the kernel of RODEX4 installed within S-RELAP5. This is because S-RELAP5 solves the thermal conduction equations using its own equations for heat structures. The numerical solutions for determining the thermal-mechanical properties have been well validated and have been determined to provide stable numerical predictions of fuel thermal-mechanical properties.

The performance of the kinetics equations and numerical solutions contained in the MB2-K kinetics model has been assessed through several numerical benchmarks and actual plant transients that are summarized in this LTR. The numerical benchmarks are discussed in this section and the plant transients are addressed in Section 6.6.

Numerical benchmarks provide a useful test of the equations and numerical solutions because the benchmarks are mathematical problems whose solutions are well known. Specifically, they demonstrate the performance of the kinetics equations to simulate industry-standard problems that are specifically designed to test spatial and temporal equations numerical solutions. Results from the 2-D TWIGL seed-blanket reactor problem (Reference 35), the LMW 3-D PWR delayed critical transient problem (Reference 36) and the LRA 2D and 3D BWR Control Blade Drop Transients (Reference 37) are provided in the following subsections.

Section 3.1.2 states the target scenarios to which the AURORA-B EM presented in this LTR is applied are "core wide" events in which the initial excitation is a thermal-hydraulic disturbance. In contrast, the numerical benchmarks are all initiated by a neutronic disturbance in a local region. The benchmarks are useful for two reasons: 1) the capability of the kinetics model to predict a core wide neutron flux response can be inferred by its ability to accurately predict very challenging local neutron flux disturbances, 2) the capability of the kinetics model is demonstrated for predicting the local flux response that may arise during a "core wide" event with non-uniform initial control rod positions and/or non-uniform control rod insertion.

6.4.1 TWIGL 2D Neutron Kinetics Benchmarks

The TWIGL benchmark problems are delayed-critical transients induced by changing the thermal-absorption cross section in several regions of the reactor. The absorption cross section was changed by step and ramp change modes. The TWIGL problems were first introduced in Reference 35.

The problem geometry is given on Figure 6-11. Two types of reactivity perturbations are introduced by a step change and by a linear ramp change (over the range $0 \le t \le 0.2$ sec) of the thermal absorption cross section in four symmetrical seed regions. Two neutron energy groups and one group for delayed precursors are used. The original problem is described in full-core geometry, while many authors have been reporting the results for a quarter-core. MB2-K results are calculated in full-core geometry. Table 6-4 and Table 6-5 provide the summary results of the TWIGL step and linear ramp perturbation reactivity problems calculated with MB2-K and two well-known nodal codes, QUANDRY (analytical nodal method) and SPANDEX (fifth-order polynomial nodal method). The results for CUBBOX (coarse-mesh flux expansion method with cubic functions) are also given for the ramp perturbation problem.

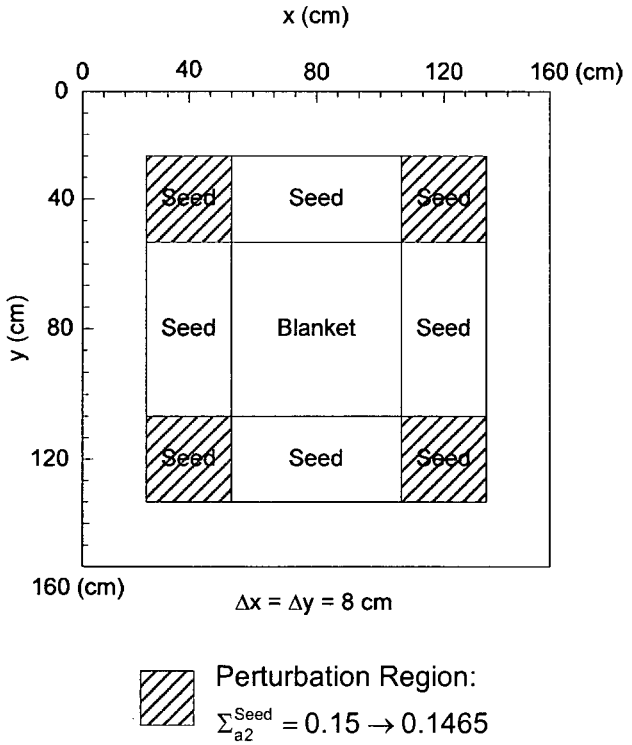

Figure 6-11: Two–Dimensional TWIGL Problem Description

Table 6-4: 2-D TWIGL Problem Number 1 – Step Perturbation Summary

	MB2-K Full-core	QUANDRY[38]	QUANDRY[38]	SPANDEX[38]
Number of Spatial Meshes	[ ]	36	100	400
Initial Eigenvalue	[ ]	0.91323	0.91321	0.91321
Time Step Size (ms)	[ ]	10	2.5	0.1
Number of Time Steps	[ ]	50	200	5000
Relative Power				
0.0 s	[ ]	1.000	1.000	1.000
0.1 s	[ ]	2.064	2.061	2.062
0.2 s	[ ]	2.076	2.078	2.079
0.3 s	[ ]	2.095	2.095	2.096
0.4 s	[ ]	2.112	2.113	2.114
0.5 s	[ ]	2.130	2.131	2.131

Table 6-5: 2-D TWIGL Problem Number 2 – Ramp Perturbation Summary

	MB2-K Full-core	CUBBOX[36]	QUANDRY[38]	SPANDEX[38]
Number of Spatial Meshes	[ ]	121	36	400
Initial Eigenvalue	[ ]	n/a	0.91323	0.91321
Time Step Size (ms)	[ ]	12.5	5	0.1
Number of Time Steps	[ ]	40	100	5000
Relative Power				
0.0 s	[ ]	1.000	1.000	1.000
0.1 s	[ ]	1.321	1.305	1.309
0.2 s	[ ]	1.985	1.954	1.960
0.3 s	[ ]	2.074	2.074	2.075
0.4 s	[ ]	2.092	2.092	2.092
0.5 s	[ ]	2.109	2.109	2.110

Comparisons of the relative power change calculated with MB2-K are provided for the two problems in Figure 6-12 and Figure 6-13, respectively. The TWIGL 2D results obtained with other nodal codes are quoted from References 38, 39, and 40.

Figure 6-12: 2-D TWIGL Problem Number 1 – Step Perturbation: Relative Power Change Calculated with MB2-K

Figure 6-13: 2-D TWIGL Problem Number 2 – Ramp Perturbation: Relative Power Change Calculated with MB2-K

The results for the two TWIGL problems demonstrate the temporal accuracy of the MB2-K code predictions versus numerous other solutions reported in the open literature.

6.4.2 LMW 3D Numerical Benchmark

The LMW problem does not involve a severe flux transient, but is nonetheless interesting to examine temporal convergence because solutions from some well-known kinetics methods are available for varying time step sizes. The reactor geometry for this problem is shown in Figure 6-14. Table 6-6 presents a comparison of temporal convergence of the core average power density for a scenario with a relatively long timescale.

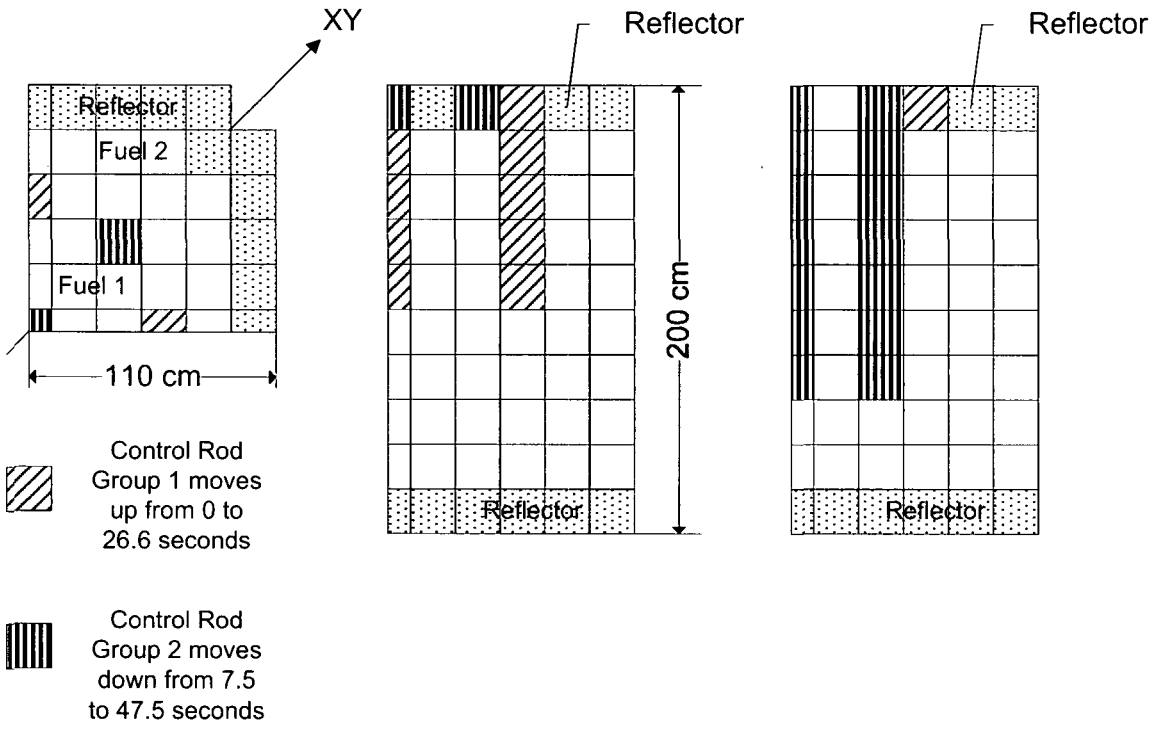

Figure 6-14: Three–Dimensional Model Reactor Geometry for LMW PWR Problem

Table 6-6: Comparison of Time Convergence for LMW PWR Problem

Time (sec)	Core Average Power Density (w/cc) / Error (w/cc)						
	Ref*	MB2-K (Δt=0.5 sec)	MB2-K (Δt=1.0 sec)	CUBBOX (Δt=0.25 sec)[36]	CUBBOX (Δt=0.5 sec)[36]	QUANDRY (Δt=0.25 sec)[41]	QUANDRY (Δt=0.5 sec)[41]
0.0	150.0	[ ]	[ ]	150.0 / 0.0	150.0 / 0.0	150.0 / 0.0	150.0 / 0.0
10.0	202.0	[ ]	[ ]	200.2 / -1.8	198.2 / -3.8	199.6 / -2.4	200.8 / -1.2
20.0	260.5	[ ]	[ ]	259.5 / -1.0	257.8 / -2.7	257.0 / -3.5	260.9 / +0.4
30.0	209.9	[ ]	[ ]	212.6 / +2.7	214.2 / +4.3	205.2 / -4.7	210.2 / +0.3
40.0	123.9	[ ]	[ ]	127.1 / +3.2	129.8 / +5.9	120.9 / -3.0	122.5 / -1.4
50.0	76.5	[ ]	[ ]	77.7 / +1.2	78.8 / +2.3	74.8 / -1.7	75.4 / -1.1
60.0	58.6	[ ]	[ ]	59.2 / +0.6	59.8 / +1.2	57.4 / -1.2	57.8 / -0.8

Note: * Reference Data from Richardson Extrapolation of CUBBOX Solution (41)

As shown in the table, the MB2-K results using a 1.0 second time step follow the reference core average trend with a very high degree of accuracy. Thus the MB2-K time integration method is considered to be well behaved in terms of temporal convergence for scenarios with relatively long time scales. These results are shown graphically in Figure 6-15 where results from other codes are also shown.

Figure 6-15: LMW 3-D Numerical Benchmark: Time dependent MB2-K Core Power Density vs. Other Nodal Codes Results

6.4.3 LRA 2D and 3D BWR Control Blade Drop Transients

The BWR control blade drop transient problem involves a serious spatial flux transient. This problem includes a fuel Doppler feedback and a control blade drop motion. The model core geometry is shown in Figure 6-16. This problem has three versions: ¼-core 2-dimensional, ¼-core 3-dimensional, and, full-core 3-dimensional versions. The last version is defined with asymmetric movement of a single control rod and is the most difficult of the three because it involves severe radial flux asymmetry. The 2-dimensional case is summarized in Table 6-7 along with a few other code results. The ¼-core and full-core 3-dimensional cases are summarized in Table 6-8 and Table 6-9, respectively, along with results from other codes.

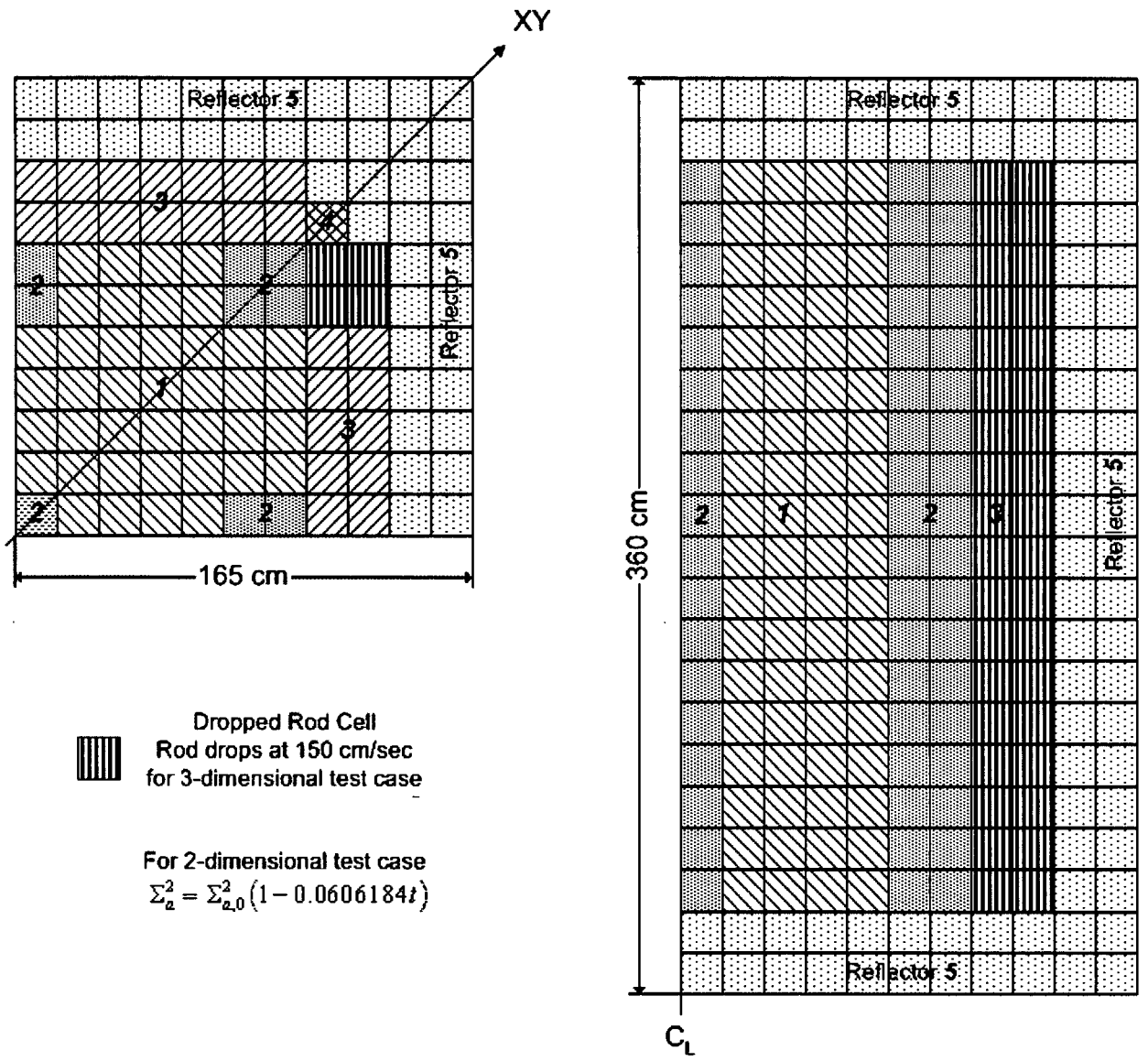

Figure 6-16: Three–Dimensional Model Reactor Geometry for BWR LRA Rod Drop Problem

Table 6-7: LRA 2D ¼-Core BWR Test Problem Summary

	MB2-K	CUBBOX[37,41]	IQSBOX[37,41]	QUANDRY[41]
Mesh Structure	[ ]	(11x11)	(11x11)	(11x11)
Number of Time Steps	[ ]	1200	522	1000
Initial Eigenvalue	[ ]	0.99633	0.99631	0.99641
Time to First Peak (Sec)	[ ]	1.421	1.445	1.435
Average Watts/cc at First Peak	[ ]	5734	5451	5473
Average Watt/cc at Second Peak	[ ]	~830	~800	797
Power at 3.0 Seconds	[ ]	~60	~100	97.5
Average Fuel Temp. at 3.0 Sec	[ ]	1070	1127	1108
Peak Fuel Temp at 3.0 Sec	[ ]	2925	2989	3029

Table 6-8: LRA 3D ¼-Core BWR Test Problem Summary

	MB2-K	CUBBOX[37]	IQSBOX[37]	QUANDRY[41]
Mesh Structure	[ ]	(11x11x14)	(11x11x12)	(11x11x14
Number of Time Steps	[ ]	800	706	410
Initial Eigenvalue	[ ]	0.99626	0.99624	0.99644
Time to First Peak (Sec)	[ ]	0.906	0.894	0.900
Average Watts/cc at First Peak	[ ]	6278	5798	6549
Average Watt/cc at Second Peak	[ ]	~400	~400	408
Power at 3.0 Seconds	[ ]	~70	~70	74
Average Fuel Temp. at 3.0 Sec	[ ]	~1000	~1000	1024

Table 6-9: LRA 3D Full-Core BWR Test Problem Summary

	MB2-K	QUANDRY[41]	PANTHER[38]	SPANDEX[38]
Mesh Structure	[ ]	(13x13x10)	(13x13x10)	(13x13x10)
Number of Time Steps	[ ]	820	820	820
Initial Eigenvalue	[ ]	0.99657	n/a	0.99647
Time to First Peak (Sec)	[ ]	0.950	0.950	0.948
Average Watts/cc at First Peak	[ ]	1435	1514	1509
Average Watt/cc at Second Peak	[ ]	141	170	119
Power at 3.0 Seconds	[ ]	22.6	23.3	23.1
Average Fuel Temp. at 3.0 Sec	[ ]	n/a	n/a	n/a

Time dependent core average power density for the LRA 3D Full-Core BWR Test Problem case with one asymmetric control rod dropped is shown in Figure 6-17 for the MB2-K calculations as well as the results of some other codes. The results of the other codes are taken from References 38, 39, 40, 41, and 42.

Figure 6-17: LRA 3-D Numerical Benchmark: Time dependent MB2-K Core Power Density vs. Other Nodal Codes. One Asymmetric Control Rod is Dropped

Results predicted by MB2-K are in excellent agreement with other published results for all of the problems.

6.5 *Determine Applicability of Evaluation Model to Simulate System Components (EMDAP Step 17)*

The fidelity and accuracy of the system and component models has been assessed by confirming the adequacy of process models for simulating the BWR control systems and reactor protection systems and using component effects test data.

The control systems and reactor protection systems are modeled using the S-RELAP5 control and trip capabilities that have undergone extensive testing and use in other methodologies. The

control system and reactor protection system requirements for modeling BWR events are summarized in Reference 14. Satisfying these requirements ensures the systems can model the BWR plant.

Comparison to component effects tests demonstrates the capability of the EM to predict the relevant characteristics of entire components or regions of the BWR plant, examples being the jet-pumps and steam separator. Table 4-1 is the assessment matrix which shows the component effects tests that were selected, and the highly ranked PIRT phenomena addressed by each. The results of the assessments are summarized in the following sections.

6.5.1 Rod Bundle Pressure Drop

Assessed phenomena and processes

This section addresses the following highly ranked PIRT phenomena identified in Table 4-1;

[

]

Assessment conclusions

The assessment is performed by comparing the calculated and measured pressure drop across prototypical fuel assemblies, which directly addresses the indicated PIRT phenomenon. The broad range of data and reasonable to excellent code-data comparisons for the assembly pressure drop demonstrate that the EM provides excellent predictions of the indicated PIRT phenomena.

Assessment description

The closure relations that define pressure drop within a rod bundle in S-RELAP5 have been assessed to demonstrate their adequacy over a broad experimental database that includes the 7x7, 8x8, 9x9 and 10x10 fuel designs, the egg-crate spacer [

]

The statistical performance of the assessment is tabulated in Table 6-10 as a function of flow quality and graphically in Figure 6-18 through Figure 6-20 for other informative metrics.

Table 6-10: Pressure Drop Benchmark Statistics by Exit Flow Quality (calculated - measured) / measured

[redacted]

Figure 6-18: Histogram of Relative Error

Figure 6-19: Two-Phase Pressure Drop Comparisons

Figure 6-20: Relative Error vs. Exit Void Fraction

6.5.2 Jet-pump Performance Tests

Assessed phenomena and processes

This section addresses the following highly ranked PIRT phenomena identified in Table 4-1;

[ ]

Assessment conclusions

The assessment is performed by comparing the calculated and measured pressure drop across reduced scale and prototypical jet-pumps assemblies over a wide range of flow rates, which directly addresses the indicated PIRT phenomenon. The comparison is made using non-dimensional pressure ratio (n-ratio) and mass flow ratio (m-ratio). The broad range of data and the excellent code-data comparisons for the jet-pump pressure drop demonstrate that the EM provides excellent predictions of the indicated PIRT phenomena.

Assessment description

Jet pump performance tests were analyzed to develop and validate the jet-pump model implemented in S-RELAP5. Test data from 18 jet-pump assemblies was used to develop or assess the performance of the jet-pump model. The data was available from a mixture of sources; bench top tests for reduced scale and production jet-pumps, "component tests" performed within integral test facilities, and in-situ measurements within operating reactors.

The dimensional characteristics for the 18 jet-pump assemblies are summarized in Table 6-11. The diameters are indicated in centimeters, angles are indicated in degrees, and dimensionless lengths (length divided by throat diameter) are presented in the following tables.

Table 6-11: Jet-Pump Characteristic Information

[redacted]

Table 6-11: Jet-Pump Characteristic Information (cont.)

[redacted]

Table 6-11: Jet-Pump Characteristic Information (cont.)

The 18 jet-pump assemblies represent the full spectrum of jet-pump designs found in operating jet-pump BWR plants, from BWR/3 through BWR/6 and reduced scale facilities such as the Two Loop Test Apparatus. The results for selected jet-pump designs are presented in the following sections.

The results are presented in these sections using the classical presentation format for jet-pump performance. The format consists of plotting the non-dimensional pressure ratio versus the mass flow ratio. The pressure ratio (alternatively called head ratio or n-ratio) is determined from the pressure differential between the lower plenum and downcomer divided by the pressure differential between the drive line and lower plenum, where elevation head is typically removed from the pressure differences. The mass flow ratio (alternatively called flow ratio or m-ratio) is the flow rate of liquid passing directly from the downcomer into the jet-pump assembly (the suction flow rate) divided by the flow rate entering from the recirculation system.

6.5.2.1 EGG-LTSF 1/6 Scale Tests

The LOFT Test Support Facility (LTSF) operated at Idaho National Laboratory was used to collect data for a 1/6 scale Browns Ferry type jet-pump. This data spanned all six potential operating flow regimes (e.g. permutations of steady flow direction in the legs of a Tee) in a BWR jet-pump, and represents the reference data set for validation of virtually all jet-pump models

developed to date. The EGG-LTSF data has been used to develop and assess the performance of the jet-pump model implemented in S-RELAP5.

Assessment of the jet-pump model with best-estimate model coefficients (indicated as "Optimal Params") versus the measured data is shown in Figure 6-21. The measured 2σ data uncertainties for the pressure ratio and mass flow ratio of each data point are also shown on the figure.

[

]

Figure 6-21: NM Plot of 1/6 Scale Jet-Pump Results

This figure shows the jet-pump model predicts the data with excellent agreement and within the range of experimental uncertainty for the operating flow regimes typically experienced in the events of interest, particularly the normal (1+) regime for which flow is entering the jet-pump volume from the downcomer and from the recirculation system. The capability of the jet-pump model to predict all operating regimes is important in transitory conditions and cases where one recirculation system is not operating. [

]

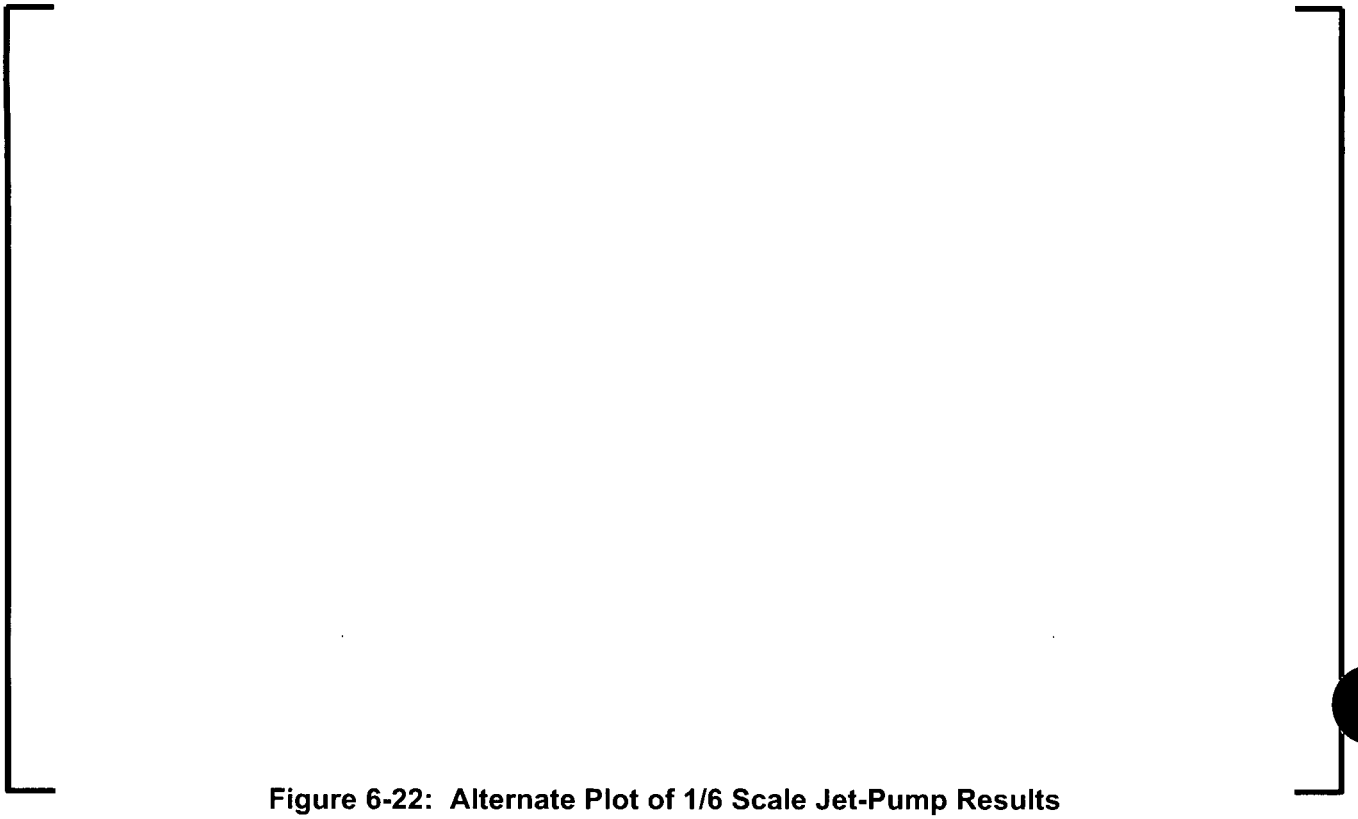

Figure 6-22: Alternate Plot of 1/6 Scale Jet-Pump Results

This figure shows the jet-pump model predicts the data with excellent agreement and within the range of experimental uncertainty for the operating flow regimes not clearly indicated in the earlier figure.

6.5.2.2 Other Jet-pump Tests

Test data from 17 additional jet-pump assemblies was used to develop and assess the performance of the jet-pump model implemented in S-RELAP5 in addition to the EGG-LTSF data. Use of these data to develop and assess the jet-pump model assures the scalability of the jet-pump model from reduced scales, through a wide variety of full scale jet-pump designs. Results for two jet-pump designs are provided in Figure 6-23 and Figure 6-24 for the normal (1+) operating regime of a jet-pump. These two designs are representative of the "single nozzle" and "five nozzle" designs found in BWR/3-/4 and BWR/5-/6 plants respectively.

Figure 6-23: NM Plot of Browns Ferry Jet-Pump Results

Figure 6-24: NM Plot of Columbia Generating Station & LaSalle Jet-Pump Results

These figures indicate the jet-pump model is in excellent agreement with the experimental data for full scale jet-pumps in the normal (1+) operating regime. Also indicated in these figures are upper and lower bound predictions where the model coefficients have been set to their joint 97.5% confidence upper and lower values. The impact of the model parameters uncertainty will be demonstrated later for a plant transient.

6.5.3 Steam Separator Tests

Assessed phenomena and processes

This section addresses the following highly ranked PIRT phenomena identified in Table 4-1;

[

]

Assessment conclusions

The assessment is performed by comparing the calculated and measured steam carryover, steam carryunder, and separator pressure drop across prototypical steam separator assemblies for prototypical reactor conditions, which directly addresses the indicated PIRT phenomena. The reasonable code-data agreement for the first phenomenon and excellent agreement for the second phenomenon shows the EM makes reasonable and excellent predictions of the indicated PIRT phenomena, respectively. [

]

Experimental data from full scale production steam separators has been used to develop and assess the performance of the steam separator model implemented in S-RELAP5. Two different separator designs are considered in S-RELAP5. The "two stage" design is used in BWRs through the BWR/5 plant. The "three stage" design is used on BWR/6 and ABWR plants. Data and assessment for both designs are presented in the following sections. A description of the steam separator test facility can be found in Reference 43.

6.5.3.1 Two Stage Steam Separator

An extensive series of full-scale test data is available to develop and validate the steady state performance of the two stage BWR steam separator model for carryover, carryunder, and pressure drop. Assessment of the separator model for two stage BWR steam separators is shown in Figure 6-25 through Figure 6-27 for representative conditions. The conclusions of the assessment are described in the introduction to the section.

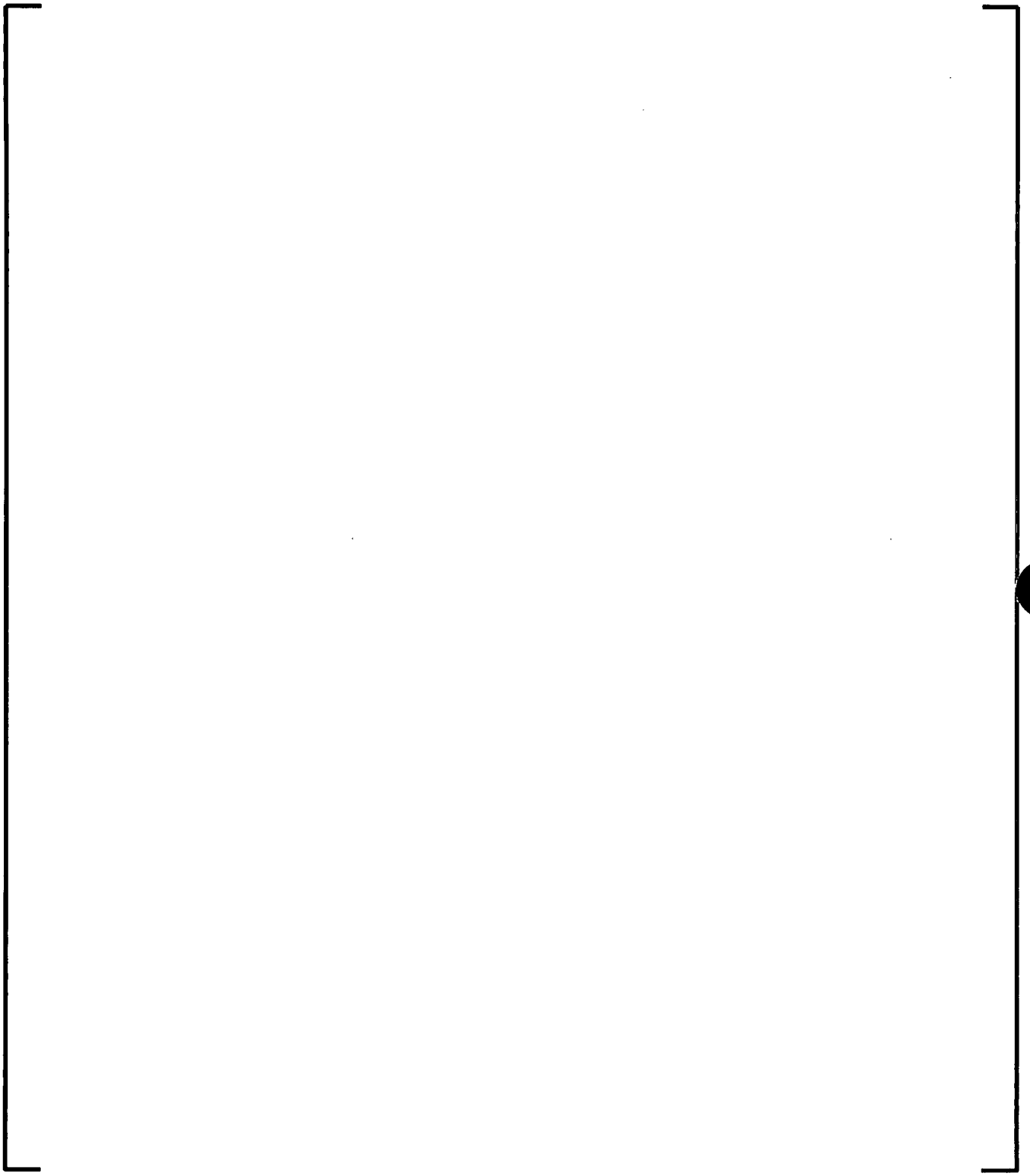

Figure 6-25: Carryover Comparison for 2-Stage Separator

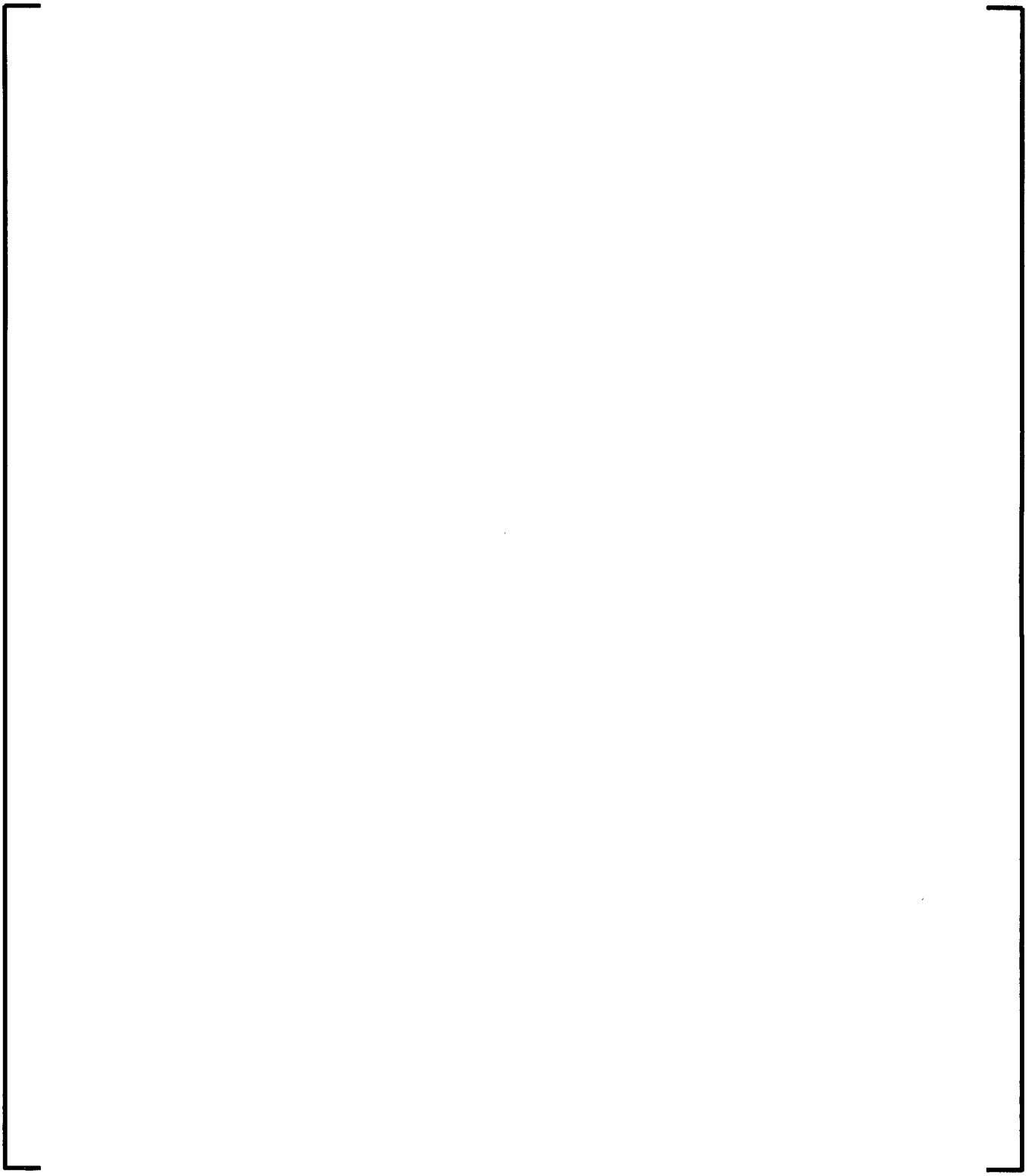

Figure 6-26: Carryunder Comparison for 2-Stage Separator

Figure 6-27: Differential Pressure Comparison for 2-Stage Separator

The units associated with Figure 6-27 are selected because they quantify the separator performance in terms of physical parameters experienced within the actual plant applications over a broad range of conditions. The differential pressure is presented as "differential head in terms of feet of inlet fluid" on the ordinate because the elevation difference of the liquid level inside and outside the separator is a key impact of steam separator pressure drop. Inlet volumetric flow is used on the abscissa to simultaneously quantify the flow conditions as a function of both mass flow rate and inlet quality.

6.5.3.2 Three Stage Steam Separator

An extensive series of full-scale test data is available to develop and validate the steady state performance of the three stage BWR steam separator model for carryover, carryunder, and pressure drop. Assessment of the separator model for three stage BWR steam separators is shown in Figure 6-28 through Figure 6-30 for representative conditions. The conclusions of the assessment are described in the introduction to the section.

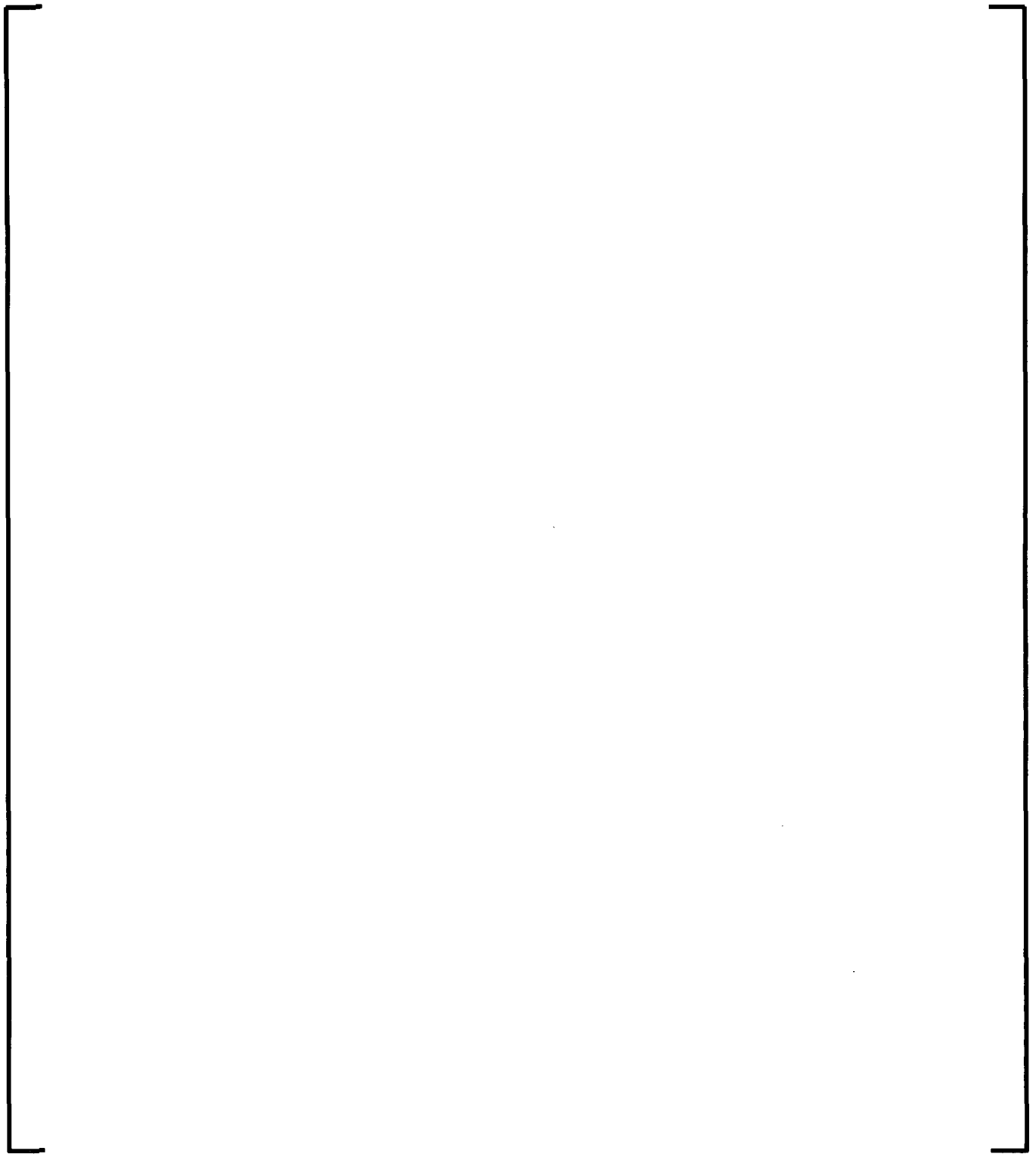

Figure 6-28: Carryover Comparison for 3-Stage Separator

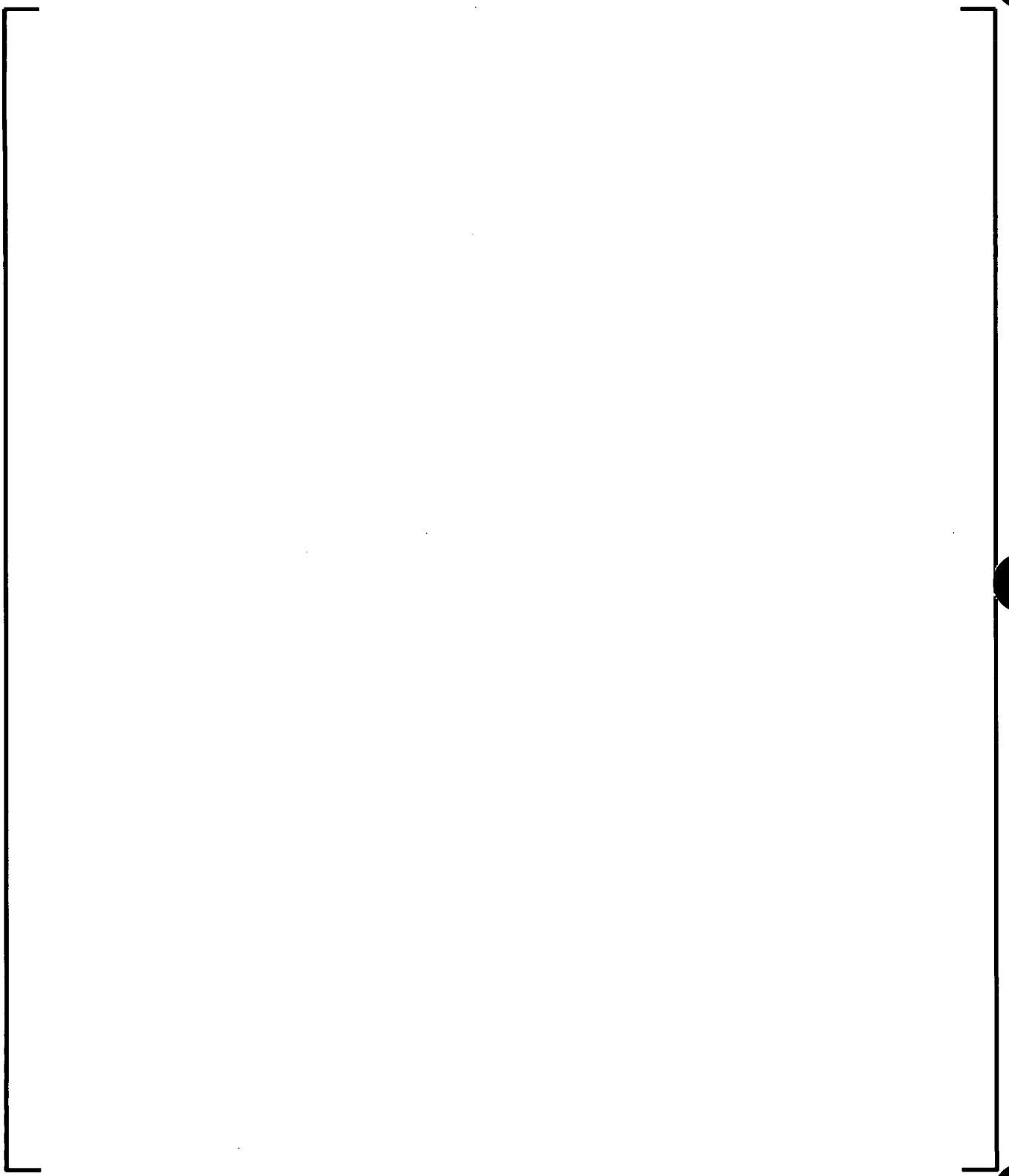

Figure 6-29: Carryunder Comparison for 3-Stage Separator

Figure 6-30: Differential Pressure Comparison for 3-Stage Separator

6.5.4 Critical Power Tests

Assessed phenomena and processes

This section addresses the following highly ranked PIRT phenomena identified in Table 4-1;

Assessment conclusions

Assessment for the determination of CHF is performed by comparing the calculated and measured time to boiling transition for typical transient scenarios using the tested rod-to-rod relative peaking (as it defines the "F-effective" or "K-factor" input to the critical power correlation), [ ]

[

] The reasonable code-data comparisons show the EM makes reasonable predictions of the first three indicated PIRT phenomena.

[

] The acceptable (conservative) code-data comparisons for the transient cladding temperature show the EM makes acceptable (conservative) predictions of the indicated phenomenon.

Assessment description

Critical power correlations such as SPCB (Reference 44) and the ACE correlation (References 45 and 46) are developed using prototypical data for each fuel design. During development, the statistical accuracy is determined for each correlation versus the applicable data. Since S-RELAP5 is used to evaluate the ΔCPR response of fuel assemblies, the applicable correlations are implemented within the code to perform the critical power calculations in a manner consistent with their original development. At the time of installation, the steady state performance of each correlation is tested as implemented within S-RELAP5 for comparison to the original correlation development results to assure the implementation is correct. Therefore, the steady state performance of critical power within S-RELAP5 is consistent with the original correlation development. However, while steady state performance is consistent, the transient performance of critical power correlations may differ from code-to-code depending on the hydraulic equations used in the computer codes. The transient performance of critical power correlations is assessed in this section to demonstrate their performance within S-RELAP5.

An industry-accepted standard in BWR transient analysis is that steady-state critical power correlations are appropriate to use in transient methodologies. Experimental data are often collected for transient scenarios for use in confirming the transient performance of a critical

power correlation and the transient code in which it is implemented. The transient performance of two critical power correlations is provided in the following sections to demonstrate the capability of S-RELAP5 to predict the ΔCPR response of fuel assemblies. The data for the experiments was collected at the KATHY facility in support of developing and assessing the critical power correlations. The performance of SPCB (Reference 44) for ATRIUM-10 and the ACE correlation (Reference 46) for ATRIUM 10XM are demonstrated here, but any approved CPR correlation (including ACE for ATRIUM-10A fuel, Reference 45) may be used in the EM as described in Section 9.1. In addition, selected tests from KATHY are used to demonstrate the ability of S-RELAP5 to conservatively evaluate transient cladding temperature in events where boiling transition is allowable.

6.5.4.1 SPCB CPR Correlation for Application to ATRIUM-10 Fuel

A total of [ ] were performed using S-RELAP5 to confirm the SPCB Critical Power Correlation (Reference 44) transient behavior for the ATRIUM-10 fuel design (with eight part length rods). These transient tests simulated load rejection without bypass (LRNB) events that consist of power and pressure ramps and flow decay; and simulated pump trip events that consist of flow decay and power decay. The flow, pressure, and power are controlled by a function generator. The forcing functions were programmed to produce the transient rod surface heat flux typical of the various events. Additional details about the tests, including plots of representative forcing functions, thermocouple responses, and range of initial conditions can be found in the SPCB Critical Power Correlation topical report (Reference 44).

The transient performance of the SPCB correlation as implemented in S-RELAP5 has been demonstrated through assessment against these transient dryout tests. The assessment calculations compare the measured and calculated time of boiling transition. Table 6-12 summarizes the results of these calculations. The comparisons show that S-RELAP5 conservatively calculates the occurrence of BT and time of BT for [ ], and shows reasonable agreement with [ ] with no measured BT. There are [ ] which is within the range of the defined uncertainties of the correlation documented in Reference 44. The S-RELAP5 results agree very well with those from the XCOBRA-T analyses documented in Reference 44.

Figure 6-31 shows the graphical comparison of the measured and predicted time of BT, for applicable cases in Table 6-12. This figure shows that the S-RELAP5 predictions are conservative but generally show reasonable or excellent agreement with the measurements. These are the indirect code-data comparisons showing that the EM makes at least reasonable predictions of the PIRT phenomena related to [

]

Table 6-12: Assessment Results of SPCB/ATRIUM-10 CPR Correlation

[

]

Figure 6-31: Predicted vs. Measured Time to Dryout for SPCB/ATRIUM-10

6.5.4.2 ACE/ATRIUM 10XM CPR Correlation for Application to ATRIUM 10XM Fuel

A total of [ ] were performed using S-RELAP5 to confirm the ACE/ATRIUM 10XM CPR (Reference 46) transient behavior for the ATRIUM 10XM fuel design (with twelve part length rods). Like the tests for ATRIUM-10, the transient tests simulated load rejection without bypass (LRNB) events and simulated pump trip events. Additional details about the tests, including plots of representative forcing functions, thermocouple responses, and range of initial conditions can be found in the ACE/ATRIUM 10XM topical report (Reference 46).

The transient performance of the ACE correlation as implemented in S-RELAP5 has been demonstrated against these transient dryout tests. The assessment calculations compare the measured and calculated time of boiling transition. Table 6-13 summarizes the results of these calculations. The comparisons show S-RELAP5 conservatively calculates the occurence of BT and time of BT for [ ], and shows reasonable agreement with [ ] with no measured BT. There are [

] which is within the defined uncertainties of the ACE/ATRIUM 10XM correlation. The S-RELAP5 results agree very well with those from the XCOBRA-T analyses documented in Reference 46.

The assessment results also confirm that the calculated time of BT is not sensitive to the time step size for the range of [ ] sec. The impact is small (in the conservative direction) when the time step size is reduced from [ ] sec in the calculation.

Figure 6-32 shows the graphical comparison of the measured and predicted time of BT, for applicable cases in Table 6-13. This figure shows that the S-RELAP5 predictions are conservative but generally are in reasonable or excellent agreement with the measurements. These are the indirect code-data comparisons showing that the EM makes at least reasonable predictions of the PIRT phenomena related to [

].

Table 6-13: Assessment Results of ACE/ATRIUM 10XM CPR Correlation

Figure 6-32: Predicted vs. Measured Time to Dryout for ACE/ATRIUM 10XM

Cladding temperature prediction

The capability of S-RELAP5 to predict the cladding temperature during events where boiling transition is allowable is confirmed by calculating the cladding temperature when boiling transition occurs for comparison to [

]

The FoM of this demonstration is the predicted temperature response that is compared to the measured temperature response. The prediction is made by applying the post boiling transition models described in Section 5.2.9.2 to the ATRIUM 10XM transient analyses models described above. For these test comparisons, the "hot rod" described in Section 5.2.9.2 is set to the tested maximum rod power so the calculated temperature response can be compared to the measured temperature response at the elevation of predicted boiling transition.

[

] Figure 6-33 through Figure 6-36 compare the predicted and measured cladding temperatures for four tests. As shown in these figures, the S-RELAP5 prediction of cladding temperature for cases where boiling transition has occurred is conservative relative to the measured temperature in the tests. The key results of these comparisons are summarized in the following figures.

Figure 6-33: Predicted and Measured Cladding Temperature for Test STS-111.3-H1A.5

Figure 6-34: Predicted and Measured Cladding Temperature for Test STS-111.3-H1B.2

Figure 6-35: Predicted and Measured Cladding Temperature for Test STS-111.3- U1C.4

Figure 6-36: Predicted and Measured Cladding Temperature for Test STS-111.3- U1D.3

As indicated in these plots, the S-RELAP5 prediction of cladding temperature for cases where boiling transition has occurred is reasonable (conservative) relative to the measured cladding temperature in the tests.

6.5.5 Peach Bottom Steam Line

Assessed phenomena and processes

This section addresses the following highly ranked PIRT phenomena identified in Table 4-1;

[

]

Assessment conclusions

Direct measurement of the indicated PIRT phenomena cannot be made in the test, so the assessment is performed via measured and predicted pressure at several locations in the steam line. The excellent code-data pressure comparisons demonstrate that the EM provides excellent predictions of the indicated PIRT phenomena, including little sensitivity to time step size. Also, the thermal-hydraulic field equations and numerical solutions are demonstrated to be adequate for predicting pressure wave propagation in steam flow.

Assessment description

An assessment has been performed using the Peach Bottom Unit 2 Turbine Trip data to evaluate the capability of S-RELAP5 to model the dynamic behavior of steam lines during fast closure of steam line valves, as is characteristic in many events of interest in this LTR. The assessment is focused on [

]

[

] A nodalization diagram is provided in Figure 6-37. This is the same nodalization used in the assessment of the Peach Bottom Turbine Trip tests presented in Section 6.6.2. Other nodalizations (including node size variations and modeling all four steam lines explicitly) were studied during the assessment in addition to the one indicated here.

Figure 6-37: Nodalization for the Peach Bottom Steam Line Model

The measured dome pressure from Turbine Trip 2 is imposed as a boundary condition at Component 100. The TSVs (Component 514) are closed and the TBVs (Component 518) are

opened at the appropriate time based on recorded data. The free parameters in this assessment are measured pressure at two locations within the steam line and within two of four steam lines (steam lines A and D). The "steam line" pressure is recorded by instruments near the flow limiter on the reactor side of the main steam isolation valves. An additional two "turbine inlet" instruments recorded the pressure near the location of the turbine bypass line connection.

The boundary conditions for the calculations are indicated in Figure 6-38 through Figure 6-40. A range of time step sizes are indicated on the plots, and these same time step sizes are carried throughout the assessment. Measured flow rates are not available for comparison in the later two figures. However, the flow rate through the TBV was provided as part of an international standard problem (ISP) that is based on Peach Bottom Turbine Trip 2. The value provided in the ISP is based on RETRAN analyses by the operator of the Peach Bottom plant (Reference 47). The ISP value is provided in Figure 6-40 for comparison to the S-RELAP5 predicted value.

Figure 6-38: Measured Dome Pressure for Peach Bottom Turbine Trip 2 - Imposed as a Boundary Condition on the Calculations

Figure 6-39: Simulated Flow Responses at TSV

Figure 6-40: Simulated Flow Responses at TBV

Comparisons of predicted and measured pressure are provided in Figure 6-41 through Figure 6-42. [

] When comparing the predicted and measured values it is important to recognize that the plant instrumentation was affected by high frequency noise that occurred in the long instrument lines. This issue is discussed in the original data report (Reference 48) and in publications associated with the ISP.

[

]

Figure 6-41: Pressure Response in Steam Line A near the Flow Limiter

Figure 6-42: Pressure Response in Steam Line A near the Turbine Inlet

The previous figures demonstrate the capability of S-RELAP5 to predict all relevant parameters, like frequency and magnitude of the dominant pressurization oscillations, within the accuracy of the experimental data when considering that the plant instrumentation was affected by high frequency oscillations in the instrumentation. Also, the sensitivity of time step size with respect to the system behavior is shown to be small within the range of time step sizes indicated in the figures. The small sensitivity to time step size arises because the pressure waves are created by valves whose elapsed movement time from open to closed position is on the order of 0.1 sec. Compared to the valve stroke time, all the time step sizes used are very small. Therefore, the driving event, which is valve closure, is well represented in any case. Sensitivity to time step size is revisited for integral system behavior in Section 6.8.2.

6.6 *Prepare Input and Perform Calculations to Assess System Interactions and Global Capability (EMDAP Step 18)*

The ability of the EM is assessed in this section for predicting system interactions and the global capability of the EM is demonstrated. First, comparisons to three tests performed in an electrically heated integral test facility are made. Calculations of the thermal-hydraulic response

are compared for the three tests to the measured system response; including dynamic pressure, flow, and void fraction comparisons. Second, comparisons to three plant transients performed at the Peach Bottom Atomic Power Station Unit 2 are made. The three plant transients were turbine trips at reduced power in which the plant was permitted to exhibit a strong coupled neutron kinetics and thermal-hydraulic response typical of the events of interest in this LTR. Finally, demonstration analyses for several target scenarios are provided for three distinct plant types to demonstrate the global capability of the EM to predict the relevant event characteristics. Several of these demonstration analyses will be investigated in more detail in Section 6.8 to determine EM biases and uncertainties.

6.6.1 Full Integral Simulation Test

The test results from the Full Integral Simulation Test (FIST) facility are used to assess the global capability of S-RELAP5 in predicting:

[ ]

In addition to the above, the FIST tests provide sufficient information for validating the capability of S-RELAP5 to predict several PIRT phenomena in dynamic scenarios. These phenomena were only assessed under steady state conditions in earlier sections. Generally, Separate Effects Tests will provide the data for direct assessment of the specific models in the code. However, Integral Test data generally can also be used to validate the capability of the code to predict certain phenomena, and more importantly, the interaction between these phenomena (models in the code) during the transient events. FIST test results are used to validate the PIRT phenomena listed below.

Assessed phenomena and processes

This section addresses the following highly ranked PIRT phenomena identified in Table 4-1:

[ ]

[ ]

Assessment conclusions

Direct measurement of several indicated PIRT phenomena cannot be made in a test; therefore the validation is performed via comparison with parameters that are controlled by the phenomena of interest. Reasonable agreement between measured and predicted dynamic pressure in different regions of the vessel, void fractions in the simulated core and bypass regions, and incipience of flashing and level swell demonstrate the adequacy of the EM in predicting the indicated PIRT phenomena. In addition, this validation demonstrated that S-RELAP5 can adequately predict the dynamic system response and the interaction between different components during pressurization and depressurization events.

Assessment description

The Full Integral Simulation Test (FIST) facility was cosponsored by the USNRC and industry. The FIST facility was designed for simulating large and small break LOCAs and operational transients in jet-pump BWRs. The FIST facility was a full length, 1/624 scale of a BWR/6 and contained one full sized 8x8 test assembly. The assembly consisted of 62 electrically heated rods and several prototypical BWR components including a fuel support piece and a Zircaloy fuel channel.

The facility had two external recirculation loops, two jet-pumps, and all other major nuclear steam supply system components. An extensive facility description (including scaling discussion) is provided in Reference 49, and test results are reported in References 50 and 51 for Phase 1 and Phase 2 of the program, respectively.

The nodalization and selected options used in S-RELAP5 for modeling FIST is consistent, as much as possible, with nodalization and model options used in plant analyses (summarized in Section 5.2.8). However, additional modeling details were necessary to accommodate the

narrow geometry of the test facility and non-prototypical configuration of the downcomer and lower plenum regions. The S-RELAP5 FIST facility vessel nodalization is shown in Figure 6-43. In addition to the vessel, the recirculation loops, the single steam line, and all major heat structures in the vessel are modeled in the S-RELAP5 model. The core is modeled by a single heat structure and 25 heated core volumes consistent with plant modeling practices.

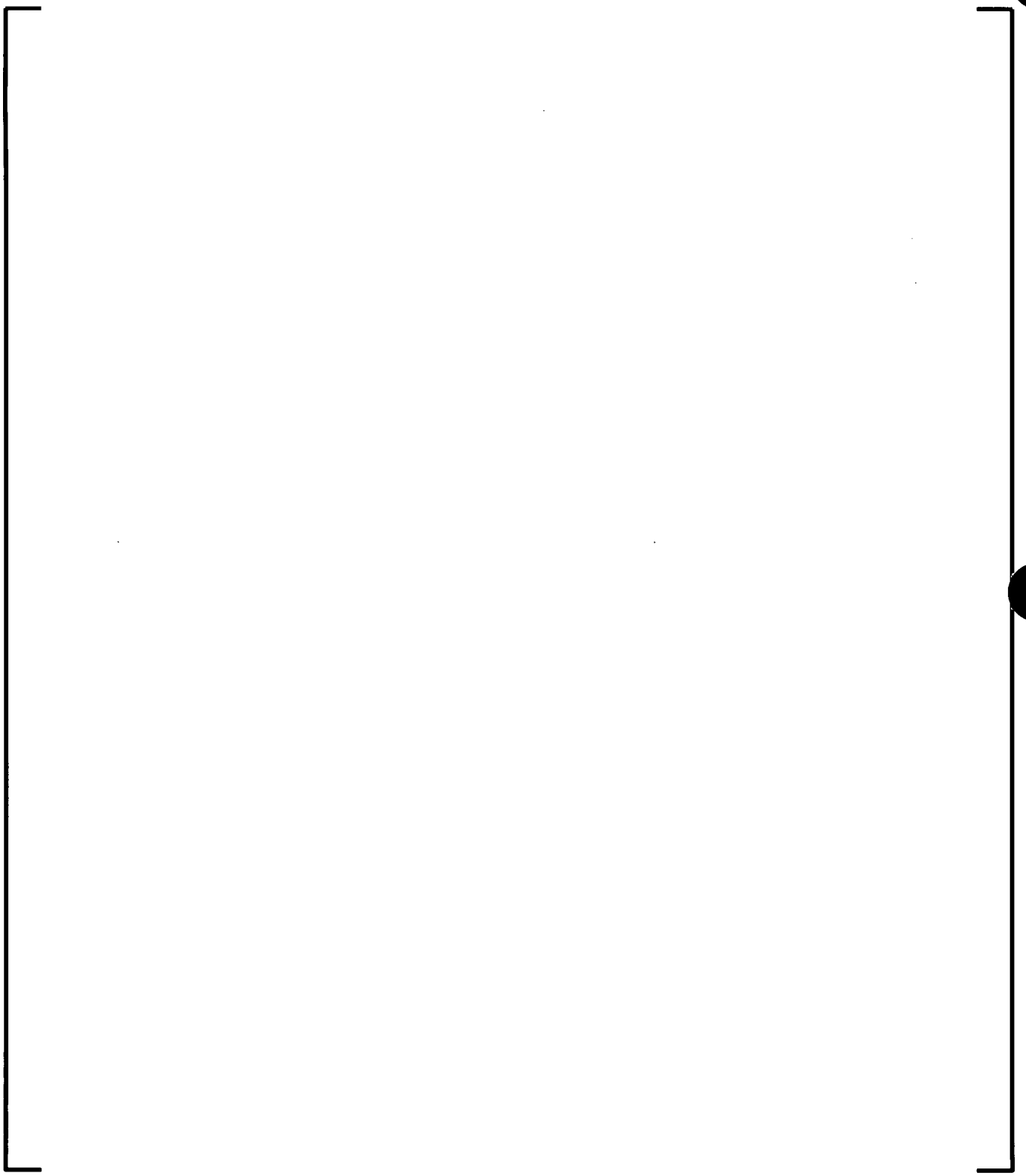

Figure 6-43: S-RELAP5 FIST Vessel Nodalization

A consequence of the full height but volume scaled FIST facility is a narrow downcomer region that distorts the distribution of frictional losses relative to a typical BWR plant. This affects two-phase flow behavior in the downcomer region and results in larger interfacial drag than would be experienced in a BWR. Level swell during a depressurization event would therefore be different than expected in a typical BWR.

In order to maintain the elevation and volume scaling, a large U-tube was used in the facility to model the lower plenum. A cross-piece was included in the facility (indicated by component 214 in Figure 6-43) to maintain a representative fluid transport path from the jet-pumps discharge to the core inlet. As described in the facility design documentation, this lower plenum distortion was a necessary approximation to maintain scaling.

The S-RELAP5 nodalization models the FIST facility, including the geometrical distortions discussed above. The comparison between the prediction and measurement demonstrate the global capability of S-RELAP5 in predicting the specified PIRT phenomena and the system interactions during the modeled transient events.

A diverse set of instrumentation was available in the tests, including absolute and differential pressure sensors, fluid temperature measurements, and flow measurements using differential pressure based devices. In addition, void fraction measurements were made at four different elevations in the assembly using gamma densitometers in the natural circulation and pressurization tests.

Three different FIST tests are simulated with S-RELAP5, a quasi-steady natural circulation test (6PNC2), a pressurization test (4PTT1) that utilized boundary conditions similar to those in the Peach Bottom Turbine Trip 3 event, and a depressurization test (6MSB1) that simulated a main steam line break event. Boiling transition and heat up of the electrically heated fuel rods did not occur in any of the tests. The results from the three tests are summarized in the following subsections.

6.6.1.1 Natural Circulation Test 6PNC2-1

Test description

A series of natural circulation tests have been performed at different assembly powers in the FIST facility. These tests measured the natural circulation core flow rate as a function of power and water level in the downcomer and bypass. These tests were performed under quasi-steady state conditions where power and system pressure were kept nearly constant and the feedwater flow was adjusted such that the level dropped at a slow rate of less than one inch per second. The downcomer was at saturated temperature, the recirculation pumps were disabled, and the loop isolation valves were closed to eliminate any forced or secondary circulation paths. Test Run 6PNC2-1, with a 2.0 MW assembly power and the slowest rate of level decrease, was analyzed with S-RELAP5.

The tests started with the water level above the normal level and ended when the water level reached the top of the jet pumps. The initial water level in the downcomer was higher than the levels in the core, upper plenum, and standpipes. As a result, the difference in levels caused a gravity induced flow (natural circulation) from the downcomer into the core. Another circulation path occurred between the core bypass and the heated assembly depending on their elevation heads. Initially, the core bypass flow was negative, i.e. water flowed from the core bypass into the bottom of the electrically heated test assembly (core region). The flow from the bypass to the core reversed later in the test when the water level in the bypass dropped below the top of active fuel.

Comparison objectives

Comparison to test 6PNC2-1 demonstrates the capability of the EM to predict BWR natural circulation. Most importantly, it demonstrates the global capability of S-RELAP5 to predict transient scenarios and system interactions during events in which the downcomer water level drops significantly below the typical range of operation for BWR plants.

Comparison details

The key parameter in this test is the downcomer water level, which drives the natural circulation flows through the core and bypass. Figure 6-44 and Figure 6-45 compare the calculated and measured downcomer flow and bypass flow, as a function of downcomer water level.

Figure 6-44 shows the relationship between downcomer water level and total flow in the downcomer. The behavior predicted near a water level of 90 to 120 inches is the result of the two-phase boundary passing through a reducer and a non-vertical side-arm simulating the downcomer. Transient variation of natural circulation driving head with varying cross sectional channel area is challenging to model in S-RELAP5. For this test, modeling of the middle downcomer was modified from the one shown in Figure 6-43, by increasing the number of nodes in the region of varying downcomer cross sectional area from 4 to 11. The facility distortion and revised nodalization is not prototypical of a BWR plant and does not adversely affect the conclusions of this assessment.

Figure 6-45 shows the relationship between downcomer water level and core bypass flow. After the downcomer level drops below approximately 30 inches, bypass level controls the flow into the assembly. Downcomer level remains nearly constant and the bypass to assembly flow approaches zero as the bypass level drops.

Result summary

[

]

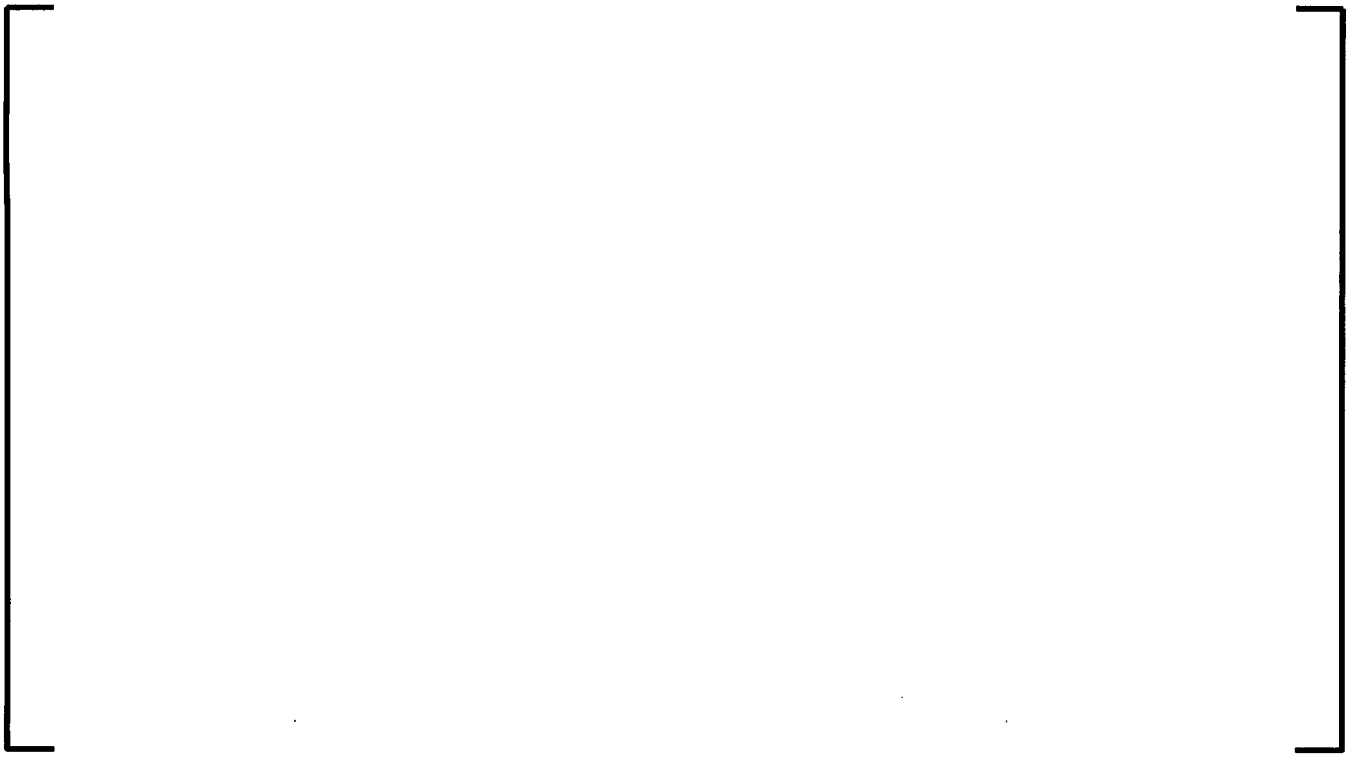

Figure 6-44: Downcomer Level vs Downcomer Flow for 6PNC2-1

Figure 6-45: Downcomer Level vs Core Bypass Flow for 6PNC2-1

6.6.1.2 Turbine Trip Test 4PTT1

Test description

FIST Test 4PTT1 was designed to simulate the Peach Bottom Turbine Trip 3 scenario. Key to this simulation was that the assembly power, feedwater flow, and feedwater temperature were programmatically controlled to simulate the normalized response measured in the Peach Bottom Turbine Trip 3.

For test 4PTT1, the steam line pressure control valve, used to establish the initial pressure, also simulated the turbine stop valve closure. It began to close around 0.1 sec and was completely closed around 0.9 sec. A FIST safety relief valve was fitted with a properly sized orifice and was used to model the opening of the turbine bypass valve. This valve started opening around 0.09 sec and was completely open at approximately 0.9 sec. The turbine bypass valve was tripped to close at 28 sec (based on the time when the Peach Bottom Test reached a low-low water level signal). The recirculation pumps were tripped at 3.5 sec and the recirculation loops were isolated at 23.5 sec to match the plant test conditions. The operation of the BWR feedwater system was not simulated in the FIST test. However, the feedwater flow versus time is controlled in the test to simulate the system response.

Comparison objectives

Comparison to this test demonstrates the capability of the EM to predict the relevant characteristics of a typical BWR plant during a representative pressurization event. In addition, the ability to predict the dynamic pressure and void fraction responses in different regions of the vessel is demonstrated.

Comparison details

For the S-RELAP5 simulation, a steady state is first established at an assembly power of 2.86 MW, a pressure of 991 psia, a water level of 559.3 inch, a downcomer water temperature of 528.5 ^{0}F, and an initial core flow of 37.7 lbm/s. For the transient calculation, the bypass valve characteristics were developed to provide the measured steam flow during the early portion of the transient. The inertias of the recirculation pumps were chosen to match the measured pump coast down transient. The feedwater flow and temperature versus time programmed in the test

were used as boundary conditions to S-RELAP5. Finally, since an accurate estimate of the facility heat losses has not been documented, the measured power history during the transient was used as an input and no consideration for the heat losses was included.

Results from the transient calculation are compared to the corresponding measurements in Figure 6-46 to Figure 6-55.

Figure 6-46 compares the steam dome pressure. The system pressure initially rises following the closure of the TSV. The pressure reaches a maximum shortly after the opening of the turbine bypass valve, and subsequently decreases (around 5 sec into the transient). The depressurization rate is controlled by the balance of the energy addition due to core power and stored energy, and the critical flow through the bypass valve. In the FIST test, the system pressure drops below the saturation pressure in the downcomer region. This causes flashing to occur in the liquid regions including the downcomer, at around 15 sec, and lower plenum, at around 24 sec into the transient. The measured data reported in Reference 51 show that the two phase level in the downcomer reaches the steam line elevation at around 24 sec. The system pressure reaches the minimum and begins to rise shortly after the closure of the turbine bypass valve at 28 sec. Figure 6-46 shows reasonable agreement between the predicted peak dome pressure and the predicted pressure transient history compared to the measurement. The calculated pressures in different regions (Figure 6-47 for lower plenum and Figure 6-48 for the assembly) show reasonable agreement with the measurement.

The total core flow rate in Figure 6-49 matches the data well. The small predicted flow fluctuation at around 18 sec is due to flashing in the lower plenum. The flow coast down is well represented while the flow following the coast down is somewhat over-predicted. The predicted steam line flow rates, as shown by the flow through the turbine bypass valve in Figure 6-50, show a more gradual and less sudden increase in flow due to downcomer level swell and two-phase level reaching the steam line inlet at around 19 sec. It should be noted that the measured data in the steam line is not accurate after two-phase flow reaches the line and the sudden increase in flow around 27 sec is a measurement anomaly.

The predicted jet pump exit flow rate, Figure 6-51, decreases as pressure drops until significant voiding in the lower plenum levels off the predicted flow rate. The measured flow rate continues to decrease until flashing, which occurs later, reverses the flow.

Figure 6-52 through Figure 6-55 compare the predicted and measured void fractions at 4 axial locations in the heated assembly. Gamma densitometer instruments were used to measure the void fractions shown in these figures. The elevation of these instruments is referenced to the beginning of heated length (BOHL) in the assembly. The figures show generally excellent agreement between the predictions and the measurements, particularly for measurements based on gamma densitometers. The apparent under prediction of the void fraction shown in Figure 6-55 near the 137 inch core elevation is believed to be due to a bias in the void fraction measurement device. The device utilized a narrow beam that penetrated a single gap between two heater rods, such devices are known to over predict the void fraction because they cannot detect liquid water on the surface of the heater rods but they can capture the trends in void fraction.

Result summary

[

]

Figure 6-46: Steam Dome Pressure for 4PTT1

Figure 6-47: Lower Plenum (Bottom) Pressure for 4PTT1

Figure 6-48: Assembly Pressure near 16 inch Core Elevation for 4PTT1

Figure 6-49: Side Entry Orifice Flow for 4PTT1

Figure 6-50: Turbine Bypass Valve Flow for 4PTT1

Figure 6-51: Jet Pump 1 Exit Flow for 4PTT1

Figure 6-52: Void in Assembly near 16 inch from BOHL Core Elevation for 4PTT1

Figure 6-53: Void in Assembly near 77 inch from BOHL Core Elevation for 4PTT1

Figure 6-54: Void in Assembly near 81 inch from BOHL Core Elevation for 4PTT1

Figure 6-55: Void in Assembly near 137 inch from BOHL Core Elevation for 4PTT1

6.6.1.3 Steam Line Break 6MSB1

Test description

FIST Test 6MSB1 was designed to simulate the response of a BWR/6 to a double ended break of a steam line at a location upstream of the flow limiter.

The FIST facility steam discharge equipment consisted of a pressure control valve and five air-operated valves which were used to simulate a variety of steam line functions. The pressure control valve was used to maintain the steam dome pressure and also to simulate a MSIV or turbine stop valve (TSV). In FIST test 6MSB1, the effective break area was simulated by two SRVs which were fitted with appropriate size orifices and the pressure control valve which was maintained at a set position. The test was initiated by opening the SRVs to simulate the break and also by activating the programmed assembly power controller.

In a typical BWR, the turbine is expected to be isolated almost immediately following the break. The effective break area consists of a full steam line area plus the area of a flow limiter, from the header side. After the turbine bypass valve opening at around 1 sec, the effective break area also includes the bypass valve area. The MSIV is closed around 5.5 sec, closing the path from the header side. In the FIST test, one of the SRVs is closed after 5.5 sec to simulate this change in effective break area. The simulated break area was based on the bounding assumption of fully open turbine bypass valve at time zero.

Comparison objectives

Comparison to this test demonstrates the capability of the EM to predict the relevant characteristics of the entire BWR plant for a representative depressurization event. Most importantly, comparisons with test 6MSB1 results demonstrate the ability of the EM to address phenomena that occur during system depressurization. In addition, the ability to predict the dynamic pressure and void fraction responses within the vessel is demonstrated.

Comparison details

The test was initiated by opening the SRVs to simulate the break and also by activating the programmed assembly power controller. Event timing for feedwater flow and high and low

pressure ECCS systems was programmed in the analysis to coincide with the observed timing in the test. The feedwater flow and recirculation pumps were tripped at time zero, and recirculation loops were isolated at 7 sec. HPCS was initiated around 27 sec (based on longest delay), and LPCS and LPCI were initiated based on pressure permissives (depending on the predicted depressurization history). Since core sprays injecting in the upper plenum were active, modeling of the upper plenum was modified from the one shown in Figure 6-43 to use more nodes (3 nodes compared to 1 node in Figure 6-43) in order to capture phenomena associated with ECC injection into the upper plenum. The revised nodalization does not adversely affect the conclusions of this assessment.

Steady state with the S-RELAP5 FIST model is established at an assembly power of 4.53 MW, a pressure of 1040 psia, a water level of 553 inch, a downcomer water temperature of 533 °F, and an initial core flow 39.2 lbm/s.

The S-RELAP5 transient simulation for test 6MSB1 is performed for 150 sec. The system pressure response predicted by S-RELAP5 is in excellent agreement with the data, as shown in Figure 6-56 and Figure 6-57 for the steam dome. The system pressure drops rapidly upon break initiation due to steam discharge through the break. The depressurization rate changes around 5.5 sec when the break area is reduced to simulate the MSIV closure. The large depressurization rate results in flashing and level swell in different liquid regions of the vessel. According to Reference 50, the test data has shown that the two-phase mixture level covers the steam line from around 6 to 80 sec into the transient. The predicted void fraction in the steam line, Figure 6-58, shows that the two-phase level reaches the steam line at around 3 sec. The dynamic pressure responses predicted in other regions of the test facility are also in reasonable agreement with data. These figures are similar to the dome pressure prediction and are not shown here.

The predicted break flow rate is shown in Figure 6-59. Since there was no void measurement in the steam line, the reported break flow rate is believed to be based on the local vapor density, rather than the two-phase mixture density. Comparison of the predicted flow rate adjusted for density ratio between the two-phase mixture and single-phase vapor, with the measured flow rate is shown in Figure 6-60. The excellent agreement between the predicted and measured pressures during the time period when the steam line was covered with two-phase flow, 3 to 70

sec, assures that the discharge flow through the break must be in agreement with actual break flow rates.

LPCS and LPCI are tripped at time zero but initiated as the system pressure drops to their pressure permissives. Close prediction of the depressurization history results in LPCS and LPCI initiation around the same time as the experiment. S-RELAP5 predicted LPCS initiation at 82 sec and LPCI at 92 sec, compared to experimental times of 88 sec and 95 sec, respectively.

The test data has shown the existence of two-phase levels in several regions including the jet pumps, lower plenum, and lower downcomer, in addition to the assembly and bypass. After the initial flashing and level swell, a mixture level forms in the jet pump which drops below the jet pump exit at around 70 sec. Strong steam upflow above the mixture level results in Counter Current Flooding Limit at the jet pump entrance which limits the liquid down flow into the lower plenum. Also steam upflow above the mixture level in the lower downcomer results in limiting the liquid down flow from the upper downcomer through the side arm. The current S-RELAP5 model does not predict the level formation in these regions, therefore, the up flow of steam (negative flow) in the jet pump and downcomer regions are not predicted, Figure 6-61 and Figure 6-62. However, this behavior is not relevant to the target scenarios defined in this LTR.

Void fractions in the assembly and bypass are predicted closely by S-RELAP-5 as shown in Figure 6-63 to Figure 6-67. The elevation of these instruments is referenced to BOHL in the assembly. Note, the void fractions in the assembly are measured using differential pressure instrumentation in this test, not the gamma densitometer devices described in the last section. Measurement of zero void fraction at all elevations in the assembly for the first few seconds is attributed to measurement distortion.

Result summary

[

]

Figure 6-56: Steam Dome Pressure for 6MSB1

Figure 6-57: Steam Dome Pressure for 6MSB1 (First 10 Seconds)

Figure 6-58: Void Fraction in Steam Line for 6MSB1 (First 6 Seconds)

Figure 6-59: Predicted Break Flow Rate for 6MSB1

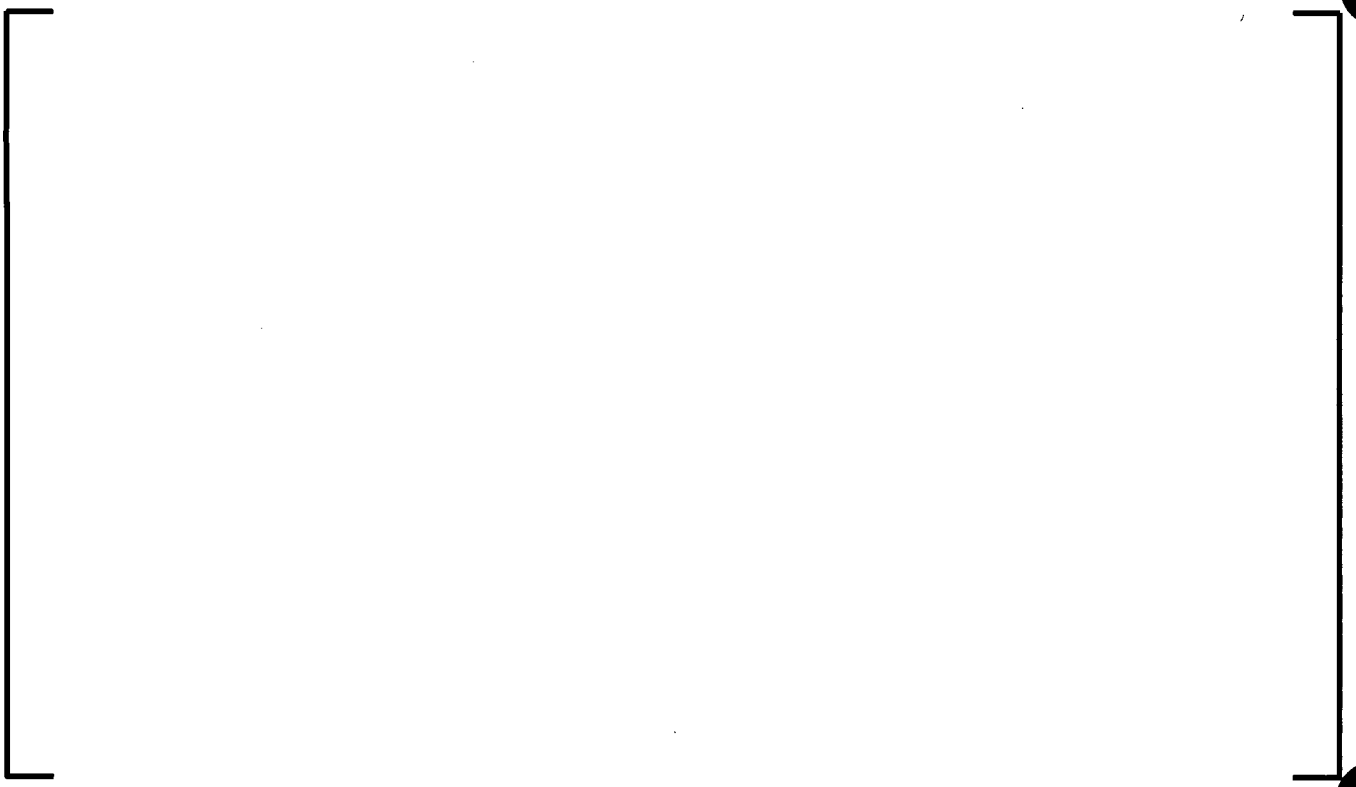

Figure 6-60: Break Flow Rate (Adjusted for Single Phase Vapor Density) for 6MSB1

Figure 6-61: Jet Pump 1 Exit Flow Rate for 6MSB1

Figure 6-62: Downcomer Flow Rate for 6MSB1

Figure 6-63: Void Fraction in Assembly near 37 inch from BOHL for 6MSB1

Figure 6-64: Void Fraction in Assembly near 57 inch from BOHL for 6MSB1

Figure 6-65: Void Fraction in Assembly near 117 inch from BOHL for 6MSB1

Figure 6-66: Void Fraction in Core Bypass near 37 inch from BOHL for 6MSB1

Figure 6-67: Void Fraction in Core Bypass near 117 inch from BOHL for 6MSB1

6.6.2 Peach Bottom Turbine Trips

The test results from the Peach Bottom Turbine Trip tests (Reference 48 and 52) are used to assess the global capability of the EM in predicting the neutron kinetics response to typical pressurization events. In addition, the Peach Bottom tests provide sufficient information for validating the capability of S-RELAP5 in predicting several PIRT phenomena in dynamic scenarios.

Assessed phenomena and processes

This section addresses the following highly ranked PIRT phenomena identified in Table 4-1;

[ ]

Assessment conclusions

Direct measurement of the indicated PIRT phenomena cannot be made in the tests, so the validation is performed via measured and calculated pressure and LPRM response of the plant in three tests. The validation shows reasonable to excellent code-data comparisons of pressure and LPRM response. From this it is inferred that the EM makes excellent predictions of the indicated PIRT phenomena. In addition, the global capability of the EM to predict the events is shown to be excellent.

Assessment description

Three plant transients were performed at Peach Bottom Unit 2 the end of the second cycle of operation in April 1977. The plant transients were turbine trip pressurization events that were intended to expand the experimental database of neutron kinetics and thermal-hydraulics coupled behavior for qualification of BWR transient analysis codes. The three tests, known as Turbine Trip 1 (TT1), Turbine Trip 2 (TT2), and Turbine Trip 3 (TT3), respectively, were performed at reduced power with some control rods positioned within the core to maintain the desired power level. Design and operating characteristics of Peach Bottom Unit 2 at the time of the tests are summarized in Table 6-14.

Table 6-14: Peach Bottom Plant Characteristics

Core thermal rating & power/flow map	3293 MWt – original licensed thermal power and original power/flow map
Cycle design & operating strategy	12 month fuel cycle, "original" operating strategy
Fuel design	576 7x7 and 188 8x8 assemblies
Core lattice configuration	"D lattice", 764 assemblies, 185 control rods
Recirculation system	Jet-pump recirculation system with two external recirculation pumps, 20 jet-pumps of single nozzle design
Scram system	locking piston control rod drives – no pressure dependence of scram speed
Steam Separators	211 "two stage" steam separators
Rated Core Flow	102.5 Mlbm/hr
Steam Flow Rate (Nominal)	13.37 Mlbm/hr
Dome Pressure (Nominal)	1020.0 psia
Turbine Inlet Pressure (Nominal)	965.0 psia
Core Inlet Enthalpy (Nominal)	521.3 Btu/lbm
"Average" assembly characteristics	4.31 MW average power 0.134 Mlbm/hr average flow

Input for modeling the Peach Bottom plant and tests was developed from the best available data sources, including publications by EPRI (Reference 52, 48), the ISP based on the tests

(Reference 47), and AREVA proprietary experience with the tests. Input for the thermal-hydraulic, thermal-mechanical, and neutron kinetics models is based on the same processes and technical guidance with which models for licensing analysis are developed. Specifically, fuel parameters and neutron kinetics (e.g. cross section) data for the thermal-mechanical and neutron kinetics models is based on RODEX4 and MICROBURN-B2 and not data specified in the ISP. The nodalization description provided in Section 5.2 is directly applicable to the Peach Bottom plant model. [

]

6.6.2.1 Event Description

The turbine trip tests began with manual trip of the turbine-generator, causing fast closure of the TSVs. The sudden closure of the valves caused a pressure wave to travel back through the steam lines and to the reactor vessel. The increasing pressure increased the core inlet flow, decreased the core exit flow, and compressed the steam void volume in the core. The net result was an increase in the core reactivity and neutron power. Increased vapor generation, caused by the increase in thermal power released from the fuel rods, and insertion of the control rods rapidly terminated the transient.

To increase the power transient response in the tests, the normal scram signal from the TSVs was delayed. The high neutron-flux trip setpoint was also lowered to limit the power peaking which resulted from the absence of this signal. This combination of operating changes allowed a neutron flux transient to take place while maintaining operating margin to plant safety limits. The sequence of events for all three tests are summarized in Table 6-15.

Table 6-15: Sequence of Events for the Peach Bottom Turbine Trips

	TT1	TT2	TT3
Begin Data Recording	0.0	0.0	0.0
Start of TSV Motion	1.0*	0.996	0.984
Start of TBV Motion	1.312	1.074	1.074
TSV 100% Closed	1.1*	1.086	1.086
APRM Sensed Scram†	1.587	1.551	1.485
Scram Relay Actuation	1.668	1.644	1.566
Start of Rod Motion‡	1.773	1.745	1.672
TBV 100% Open	2.088	1.842	1.872

Special instrumentation and an upgraded data acquisition system recorded the data from the turbine trip tests. This upgrade included direct measurements of 80 local neutron detectors, the position of 31 control rods, and the installation of additional pressure transducers. A total of 160 signals were digitized and recorded on magnetic tape using a 6 millisecond time step.

Though additional instrumentation was installed, the placement of the instrumentation, the type of data measured, and the quality of measurements was limited by virtue of the plant being an operational electric power generation facility. Detailed measurements of the dynamic thermal-hydraulic response were not recorded, particularly within the core region and fuel assemblies. In addition, most pressure sensors were affected by response delays and, in some cases, strong secondary pressure oscillations not related to the actual plant response. Finally, the potential for distortions in the measured neutron flux response via the local power range monitors were observed. These distortions potentially affected the power measurement instrumentation located in the higher elevations of the core that were a result of ionizing radiation interacting with the cabling associated with the local power range monitors. More details and observations for the instrumentation are provided in the test report (Reference 48).

The initial conditions for the three turbine trip tests are shown in Table 6-16.

---

* The actual time the TSVs moved in TT1 was not recorded due to an instrumentation failure

† Timing includes the APRM instrumentation delay

‡ Based on average time of movement for recorded control rods

Table 6-16: Turbine Trip Initial Conditions

	Core Power, MWt (% Rated)	APRM scram Setting, % Rated	Core Flow, Mlbm/hr (% Rated)	Dome Pressure, psia	Calculated core inlet enthalpy, Btu/lbm	Calculated Steam Flow, Mlbm/hr
TT1	1562 (47.4%)	85%	101.3 (98.8%)	991.3	526.4	5.688
TT2	2030 (61.7%)	95%	82.9 (80.9%)	976.3	518.2	7.812
TT3	2275 (69.1%)	77%	101.9 (99.4%)	986.6	522.4	8.891

The eigenvalues predicted by MICROBURN-B2 for TT1, TT2, and TT3 are [ ] respectively. Core-follow benchmarking of MICROBURN-B2 indicates the late Cycle 2 eigenvalue to be [ ] The large deviation of the TT1 eigenvalue from the trend indicates uncertainty in the TT1 simulation (e.g. actual reactor conditions, rod pattern, heat balance, etc.) arising from the brief plant shutdown prior to performing the test. As described later in the detailed results for TT1, this eigenvalue deviation manifests itself in larger deviation of the TT1 initial calculated versus measured axial power distribution.

The Peach Bottom Turbine Trips represent actual plant transients with strong similarity to typical scenarios for which the EM is applied. In addition to validating selected phenomena and processes, the tests demonstrate the ability of the EM to predict system interactions and demonstrate the global capability of the EM for the representative scenario through comparisons of the calculated and measured dynamic system response of core power and pressure at several locations.

One important use for evaluating the Peach Bottom Turbine Trips is the ability to estimate the overall EM conservatism in typical applications. In particular, the tests provide insight to the ability of the EM to predict the ΔMCPR and peak pressure FoM that are described in Section 3.2. The later of these two, peak pressure, is readily quantified by comparing the calculated and measured peak pressure as well as the dynamic pressure response over a period of time. [

]

[

]

A summary of key results from all three tests is provided in the next section, followed by specific results for each of the tests in subsequent sections.

6.6.2.2 Summary of Key Results

The key calculated and measured transient parameters are summarized for all three tests in Table 6-17. The scram signal in the calculations is derived from the APRMs. The calculations are performed using best estimate values for reactor protection system timing and the APRM flux setpoint. An estimate of the APRM instrumentation delay time is made for each test based on the measured data. As shown in this table, the peak power, peak dome pressure, and integral power are all conservatively calculated.

Table 6-17: Key Transient Parameters for the Turbine Trips (APRM scram)

Table 6-17 lists the time of peak power for all three tests. Inspecting TT1 and TT2 shows the time of peak power is [ ] than the peak power determined from the measured data for these tests. In addition, as will be shown later in Table 6-20 and Table 6-21 the start of control rod motion is [ ] in the calculations. The reason for this [

]

Table 6-18 summarizes the key calculated and measured transient parameters for TT1 and TT2, where [ ]
The table shows the peak power, peak dome pressure, and integral power remains conservatively calculated by the EM [

]

[

]

Table 6-18: Key Transient Parameters for the Turbine Trips (Input scram)

The LPRM model in MB2-K has been used to predict the neutron flux response for the 80 LPRM instruments available from plant data. The predicted and measured peak flux response at each axial level is provided in Table 6-19 based on the available instruments. The information is presented as peak average flux response at each level divided by total core peak flux response for both calculated and measured data. This presentation format is chosen to highlight the relative axial peaking and removes any differences in calculated and measured total core power response observed in Table 6-17.

Table 6-19: Relative Axial Power Peaking at Peak Power

A summary of the key characteristics of the transient results for all three tests follows. Plots of pressure and power are provided for each test in subsequent sections.

†

]

The initial pressure rise in the core is significant in determining the core power response, until negative reactivity from control rod insertion and void feedback of heat transmitted from the fuel to coolant can overcome the effects of pressurization. Inspection of the calculated slope of pressure change in the steam dome and upper plenum from 1.5 to 2.0 sec shows excellent agreement to the measured data for all tests. A slight bias in response time observed in the measured data is attributed to instrumentation and data acquisition delays.

The overall pressure response in the steam dome, upper plenum, steam lines, and near the turbine inlet shows reasonable to excellent agreement with data over 8 seconds duration for all three tests. The major oscillations and inflections in the calculated pressure are very consistent with measurements. As described in Section 6.5.5, the plant instrumentation was affected by high frequency noise that occurred in the long instrument lines. The agreement for the pressure response clearly shows that the EM is capable of accurately calculating the dynamic pressure behavior of a BWR plant for rapid pressurization events.

After about 3 sec, the predicted pressure begins trending higher in all three tests, resulting in higher calculated maximum pressure than measured in all the tests. The higher pressure is the result of [

]

6.6.2.3 Turbine Trip 1

Figure 6-68 shows the initial axial power distribution for TT1. As noted earlier, [

]

Figure 6-69 through Figure 6-72 show the pressure response at several locations throughout the plant. The overall pressure response in the steam dome, upper plenum, steam lines, and near the turbine inlet shows reasonable to excellent agreement. Figure 6-73 shows the relative

core power response. The calculated and measured data are based on the LPRM response for about 80 instruments that were recorded during the event.

The timing of actual and simulated key events for TT1 is presented in Table 6-20.

Figure 6-68: Initial Power Distribution for TT1

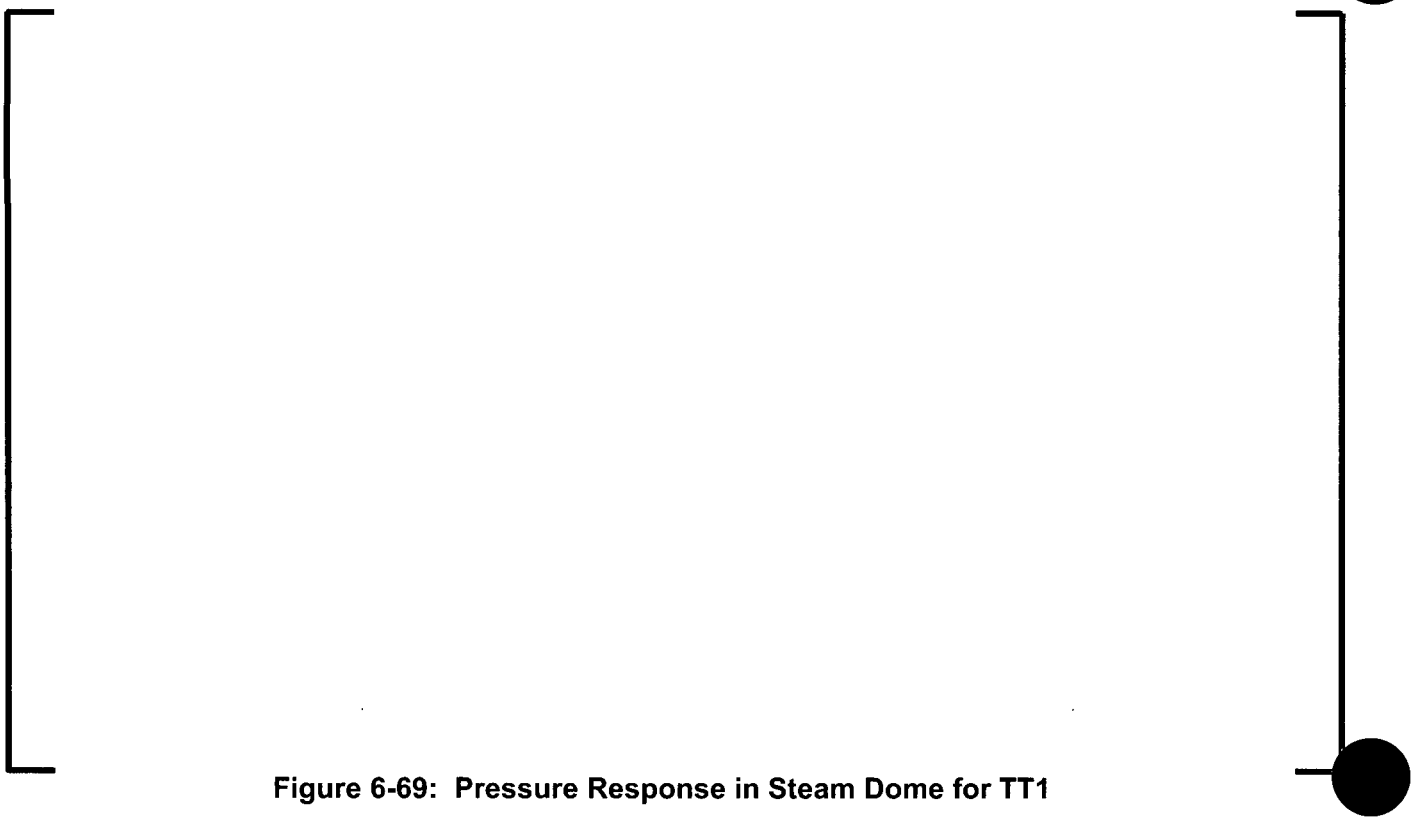

Figure 6-69: Pressure Response in Steam Dome for TT1

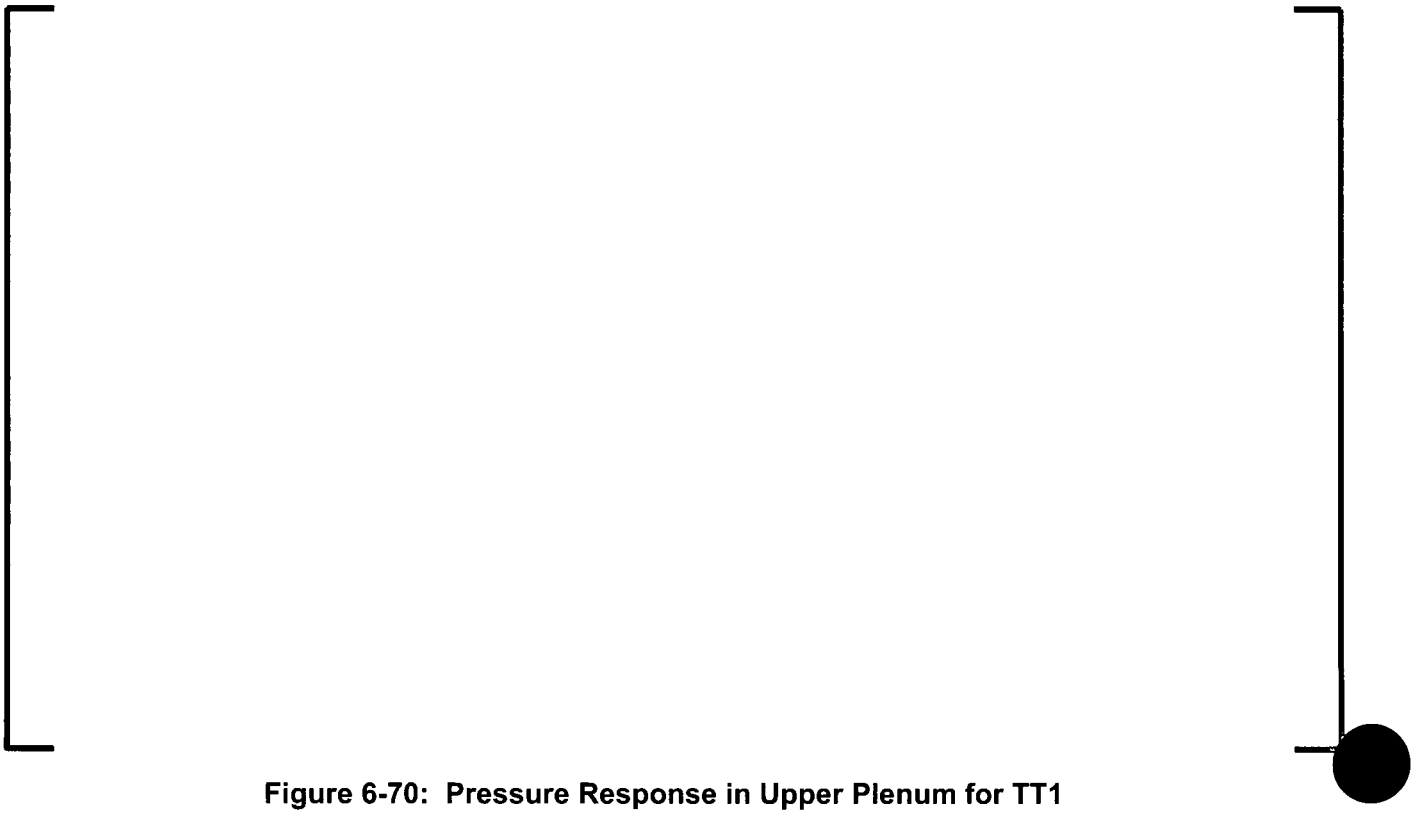

Figure 6-70: Pressure Response in Upper Plenum for TT1

Figure 6-71: Pressure Response in Steam Line A near the Flow Limiter for TT1

Figure 6-72: Pressure Response in Steam Line A near the Turbine Inlet for TT1

Figure 6-73: Relative Core Power Response for TT1

Table 6-20: Actual and Simulated Key Events for Turbine Trip 1

* The actual time the TSVs moved in TT1 was not recorded due to an instrumentation failure

† Timing includes the APRM instrumentation delay

‡ Based on average time of movement for recorded control rods

6.6.2.4 Turbine Trip 2

Figure 6-74 shows the initial axial power distribution for TT2. The calculated axial power shows excellent agreement with data. Figure 6-75 through Figure 6-78 show the pressure response at several locations throughout the plant. As described earlier, the overall pressure response in the steam dome, upper plenum, steam lines, and near the turbine inlet shows reasonable to excellent agreement. Figure 6-79 shows the relative core power response. The calculated and measured data are based on the LPRM response for about 80 instruments that were recorded during the event.

The timing of actual and simulated key events for TT2 is presented in Table 6-21.

Figure 6-74: Initial Power Distribution for TT2

Figure 6-75: Pressure Response in Steam Dome for TT2

Figure 6-76: Pressure Response in Upper Plenum for TT2

Figure 6-77: Pressure Response in Steam Line A near the Flow Limiter for TT2

Figure 6-78: Pressure Response in Steam Line A near the Turbine Inlet for TT2

Figure 6-79: Relative Core Power Response for TT2

Table 6-21: Actual and Simulated Key Events for Turbine Trip 2

* Timing includes the APRM instrumentation delay

† Based on average time of movement for recorded control rods

6.6.2.5 Turbine Trip 3

Figure 6-80 shows the initial axial power distribution for TT3. The calculated axial power shows excellent agreement with data. Figure 6-81 through Figure 6-84 show the pressure response at several locations throughout the plant. As described earlier, the overall pressure response in the steam dome, upper plenum, steam lines, and near the turbine inlet shows reasonable to excellent agreement. Figure 6-85 shows the relative core power response. The calculated and measured data are based on the LPRM response for about 80 instruments that were recorded during the event.

The timing of actual and simulated key events for TT3 is shown in Table 6-22.

Figure 6-80: Initial Power Distribution for TT3

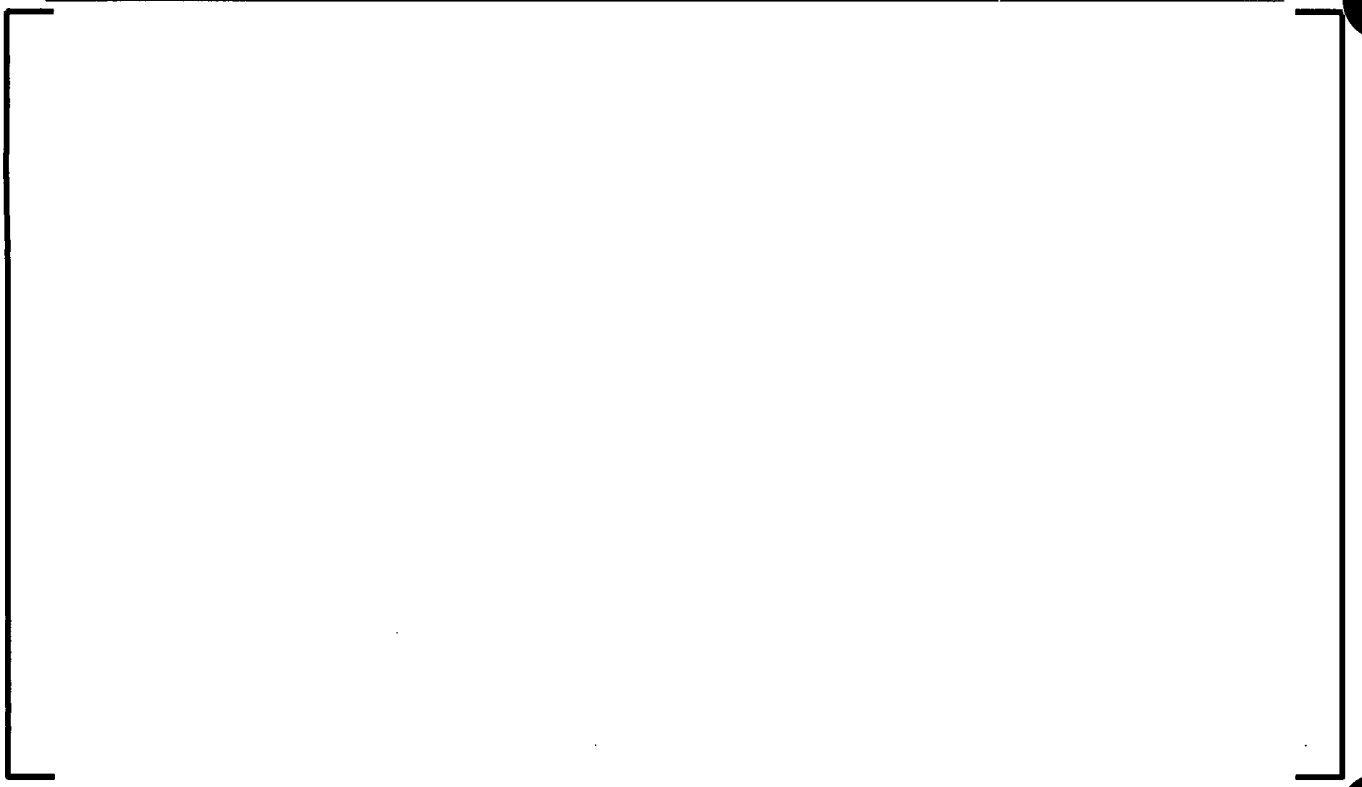

Figure 6-81: Pressure Response in Steam Dome for TT3

Figure 6-82: Pressure Response in Upper Plenum for TT3

Figure 6-83: Pressure Response in Steam Line A near the Flow Limiter for TT3

Figure 6-84: Pressure Response in Steam Line A near the Turbine Inlet for TT3

Figure 6-85: Relative Core Power Response for TT3

Table 6-22: Actual and Simulated Key Events for Turbine Trip 3

* Timing includes the APRM instrumentation delay
† Based on average time of movement for recorded control rods
‡ Initiated by manual operator action

6.6.3 BWR/4 Baseline Analyses

The ability of the AURORA-B EM to model system interactions is demonstrated in this section for typically limiting events in a typical BWR/4 plant. The results are representative of how the EM is applied in licensing calculations, and provide a baseline analysis for subsequent parametric sensitivity evaluations in EMDAP Step 20. Design and operating characteristics of the BWR/4 plant are summarized in Table 6-23.

Table 6-23: BWR/4 Plant Characteristics

The number of safety/relief and turbine bypass valves indicated in Table 6-23 and assumed in the baseline analyses is less than the number actually installed in the plant. The reduced number of valves has been assumed in order to show a stronger pressurization and power response than may otherwise occur if all installed valves were assumed operational. The

nodalization description provided in Section 5.2 is directly applicable to the model. [

]

6.6.3.1 Turbine Trip without Bypass

The turbine trip without bypass (TTNB) event is characterized by fast closure of the TSVs, which in turn creates a compression wave that travels through the steam lines into the vessel causing a rapid pressurization. The increase in pressure results in a decrease in core voids, which in turn causes a rapid increase in power. Closure of the TSV also causes a reactor scram and recirculation pump trip which helps mitigate the pressurization effects. Turbine bypass system operation, which also mitigates the consequences of the event, is not credited in this analysis. The excursion of the core power due to the void collapse is terminated primarily by the reactor scram and revoiding of the core. The revoiding is the result of energy transferred from the fuel rods and by decreasing core flow as a result of the recirculation pump trip.

The reactor is initially operating at 3952 MWt, 100% of rated core flow, and 1050 psia dome pressure in this baseline analysis, with an end of cycle exposure and all control rods fully withdrawn. All control rods are inserted at the Technical Specification scram speed in this analysis. The TSVs move at the fastest closure speed allowable in the Technical Specifications. Key parameters for the event are summarized in Table 6-24 and Figure 6-86.

Table 6-24: Summary of Key Transient Parameters for BWR/4 TTNB

[

]

Figure 6-86: Key Transient Parameters for BWR/4 TTNB

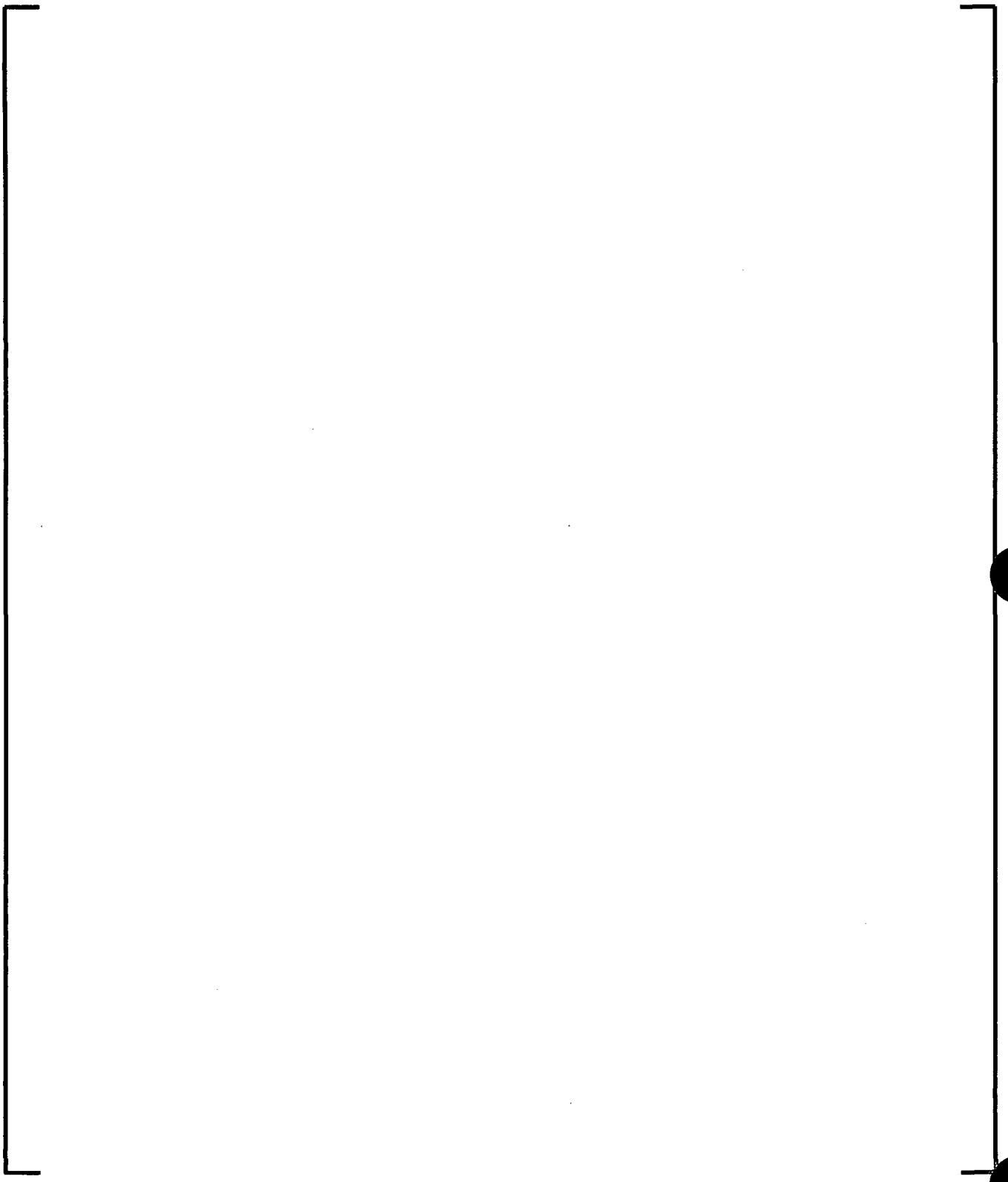

Figure 6-86: Key Transient Parameters for BWR/4 TTNB (cont)

6.6.3.2 Feedwater Controller Failure

The feedwater controller failure – maximum demand event (FWCF) is characterized by an increase in feedwater flow to maximum demand. The reactor is assumed to be operating at steady-state conditions when the feedwater controller fails to maximum demand, initiating an increase in feedwater flow. When the high water level trip setpoint is reached, TSV closure and feedwater pump trip are initiated. The signal that causes the TSV closure also causes a fast closure of the TCV. Reactor scram is initiated on TSV or TCV position. Since the TCV starts to close from a partially closed position it reaches the full closed position before the TSV. Therefore, the TCV fast closure controls the pressurization. Turbine bypass valves are operable during this event. The excursion of the core power due to the void collapse is terminated primarily by the reactor scram and revoiding of the core. The revoiding is the result of energy transferred from the fuel rods and by decreasing core flow as a result of the recirculation pump trip.

The reactor is initially operating at 3952 MWt, 100% of rated core flow, and 1050 psia dome pressure in this baseline analysis, with an end of cycle exposure and all control rods fully withdrawn. One of five turbine bypass valves is assumed out of service. All control rods are inserted at the Technical Specification scram speed in this analysis. The target initial water level is set to the nominal operating level. Key parameters for the event are summarized in Table 6-25 and Figure 6-87.

Table 6-25: Summary of Key Transient Parameters for BWR/4 FWCF

[

]

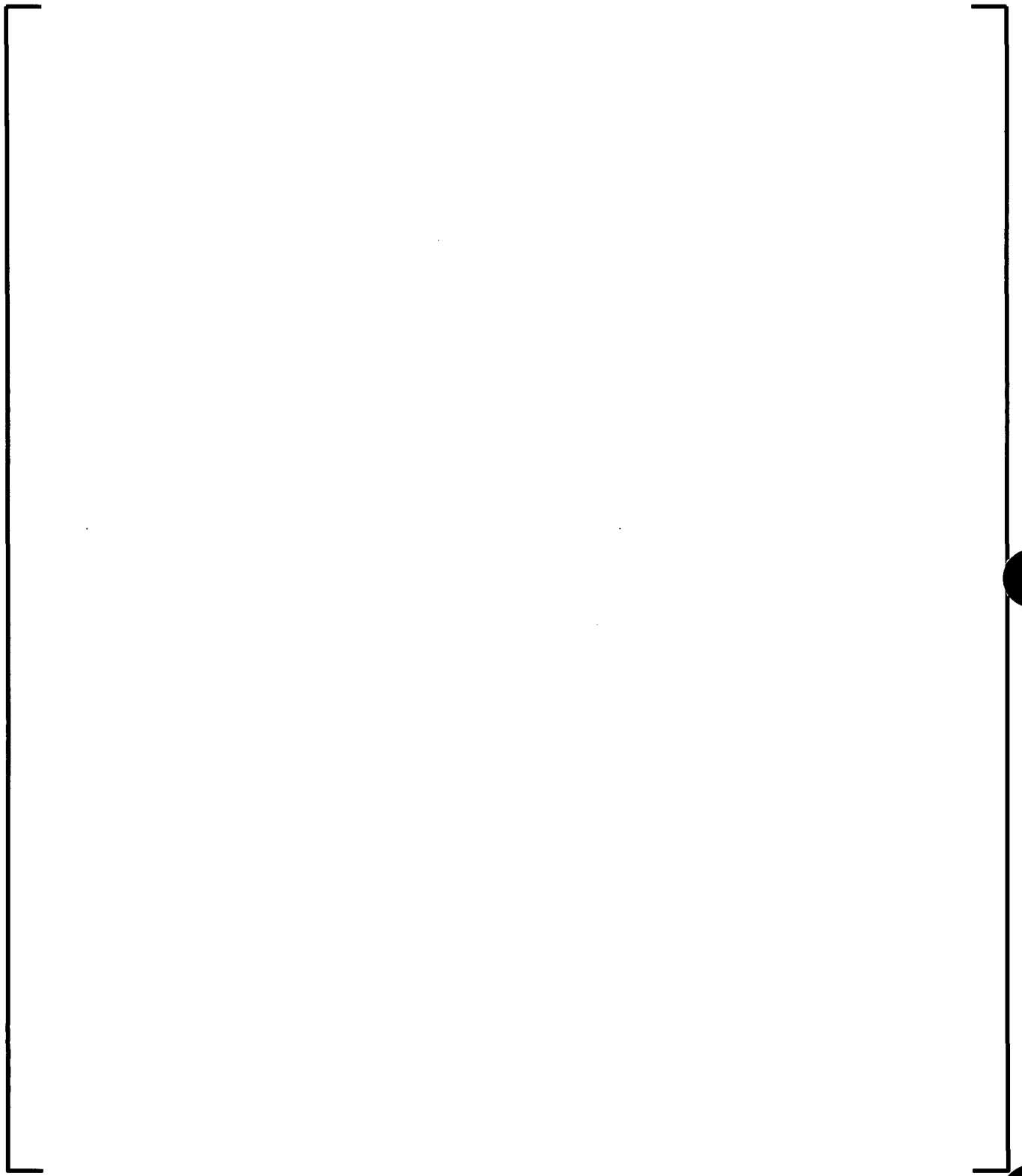

Figure 6-87: Key Transient Parameters for BWR/4 FWCF

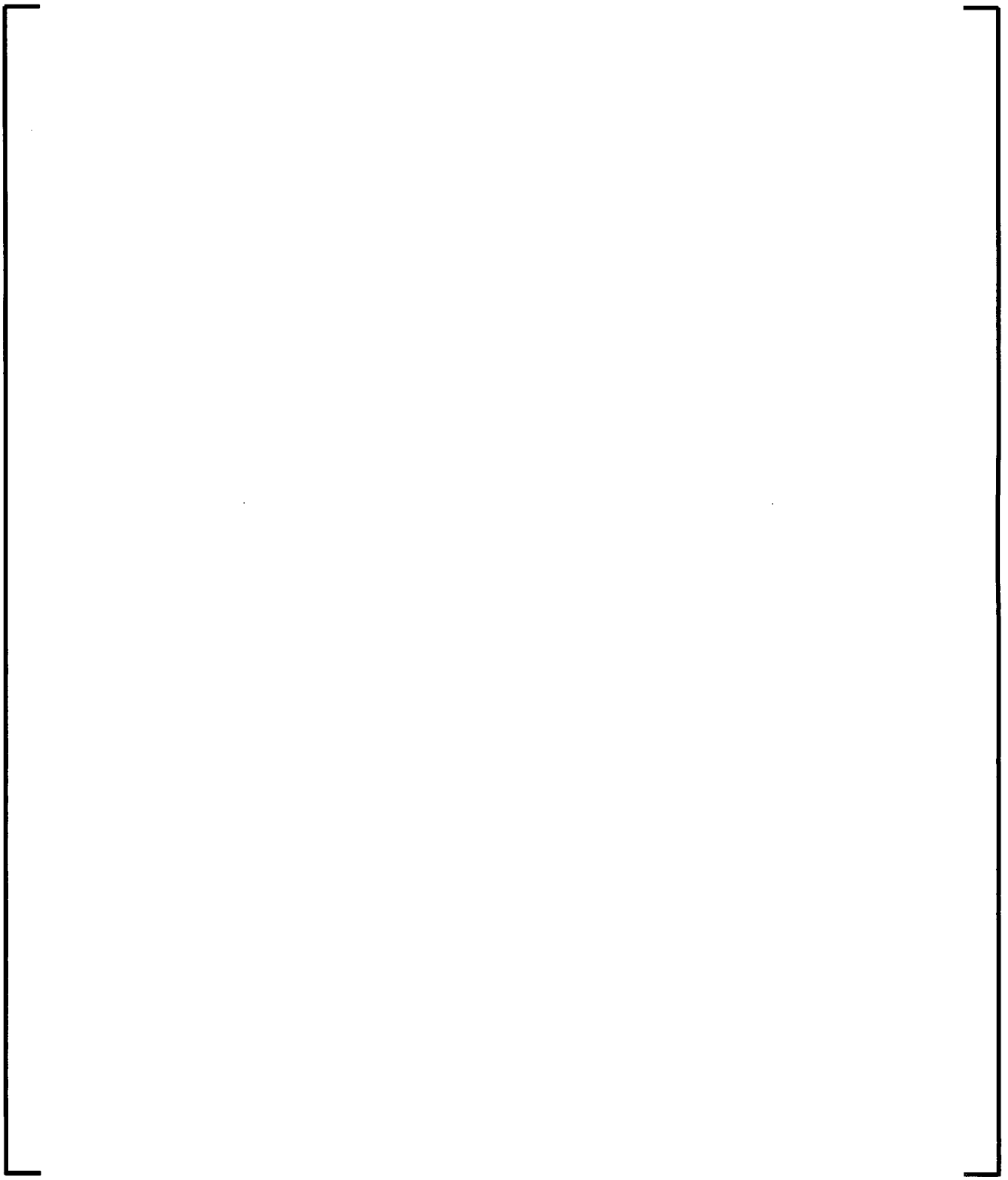

Figure 6-87: Key Transient Parameters for BWR/4 FWCF (cont)

6.6.3.3 Main Steam Isolation Valve Closure with High Flux Scram – ASME Overpressure

The main steam isolation valve closure with scram on high flux (MSIVF) event is analyzed to demonstrate compliance with the ASME overpressure criterion. The event is initiated by an operator error or system malfunction (low steam line pressure, high steam line flow, high steam line radiation, etc.) that initiates a closure of all MSIVs. The MSIV closure generates a compression wave that travels through the steam line into the core creating a rapid pressurization condition. The result is a rapid increase in power. The MSIV closure normally initiates a scram signal when three or more of the valves reach less than the 90% open position. However, this scram signal is assumed disabled for the ASME overpressure analysis. Instead, the scram signal is initiated on neutron high flux. Water level within the vessel initially decreases due to void collapse caused by increasing reactor pressure, until it is restored by feedwater/level controls. A high dome pressure Recirculation Pump Trip (RPT) is initiated as a result of a high reactor vessel pressure signal which produces a trip of the recirculation pumps. The excursion of the core power due to the void collapse is terminated primarily by reactor scram and revoiding of the core. The revoiding is the result of energy transferred from the fuel rods and by decreasing core flow as a result of the recirculation pump trip. Actuation of the safety valves reduce the system pressurization effects and assures peak vessel pressure is maintained below 110 percent of the design value in this scenario.

The reactor is initially operating at 3952 MWt, 100% of rated core flow, and 1050 psia dome pressure in this baseline analysis, with an end of cycle exposure and all control rods fully withdrawn. As described in Section 8.2.4, the ASME overpressure analyses include consideration of the uncertainty in core thermal power. However, this demonstration analysis is performed at the nominal rated core thermal power to maintain consistency with the other BWR/4 demonstration analyses. A small impact on peak pressure occurs when the core thermal power is increased in the analysis to cover the thermal power measurement uncertainty. All control rods are inserted at the Technical Specification scram speed in this analysis. Key parameters for the event are summarized in Table 6-26 and Figure 6-88.

Table 6-26: Summary of Key Transient Parameters for BWR/4 MSIVF

[ ]

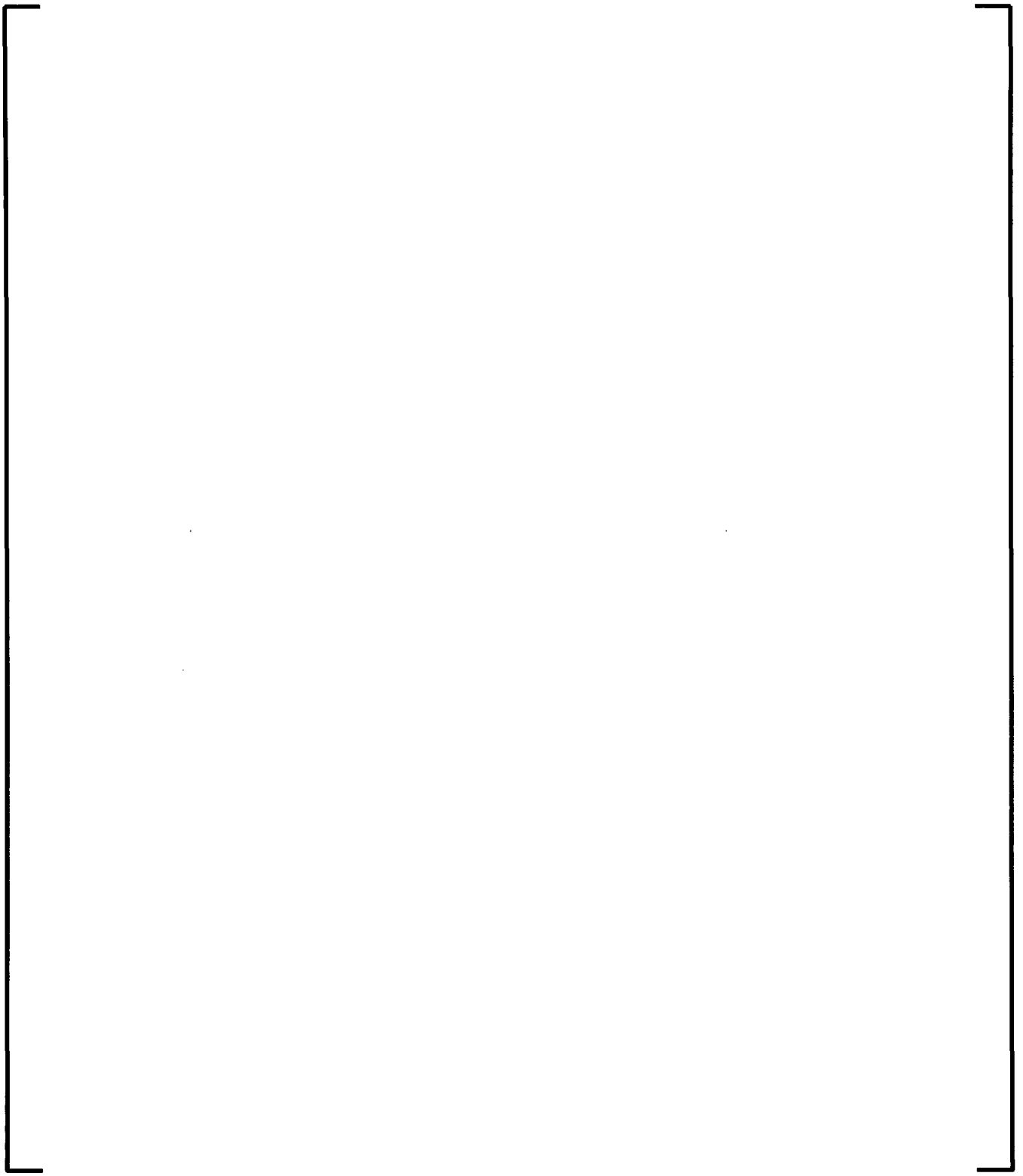

Figure 6-88: Key Transient Parameters for BWR/4 MSIVF

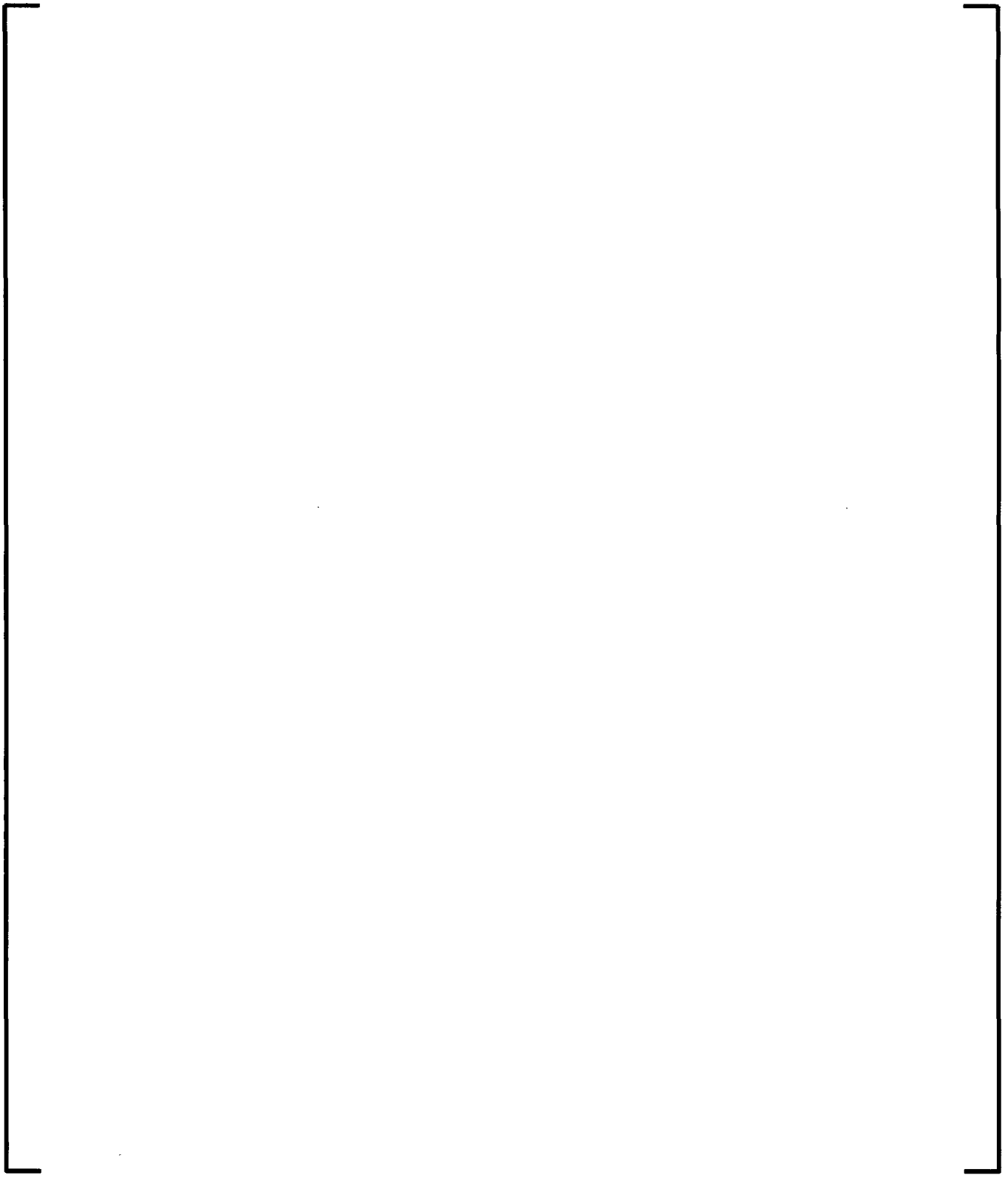

Figure 6-88: Key Transient Parameters for BWR/4 MSIVF (cont)

6.6.3.4 Main Steam Isolation Valve Closure with no Scram – ATWS Overpressure

The main steam isolation valve closure with no scram (ATWSP) event is analyzed to demonstrate compliance with the ATWS overpressure criterion. The event is initiated by an operator error or system malfunction (low steam line pressure, high steam line flow, high steam line radiation, etc.) that initiates a closure of all MSIVs. The MSIV closure generates a compression wave that travels through the steam line into the core creating a rapid pressurization condition. The result is a rapid increase in power. The MSIV closure normally initiates a scram signal when three or more of the valves reach less than the 90% open position. However, the scram signal is assumed to be completely disabled in this analysis. Water level within the vessel initially decreases due to void collapse caused by increasing reactor pressure, until it is restored by feedwater/level controls. An RPT is initiated as a result of a high reactor vessel pressure signal. The excursion of the core power due to the void collapse is mitigated primarily by revoiding of the core as a result of the RPT. The revoiding is the result of energy transferred from the fuel rods and by decreasing core flow as a result of the recirculation pump trip. The feedwater temperature is conservatively assumed to be constant through the duration of this event. Actuation of the relief valves reduces the system pressurization effects and assures peak system pressure is maintained below the maximum reactor vessel pressure of 1500 psig in this scenario.

The reactor is initially operating at 3952 MWt, 100% of rated core flow, and 1050 psia dome pressure in this baseline analysis, with an end of cycle exposure and all control rods fully withdrawn. No control rods are inserted in this analysis. Key parameters for the event are summarized in Table 6-27 and Figure 6-89.

Table 6-27: Summary of Key Transient Parameters for BWR/4 ATWSP

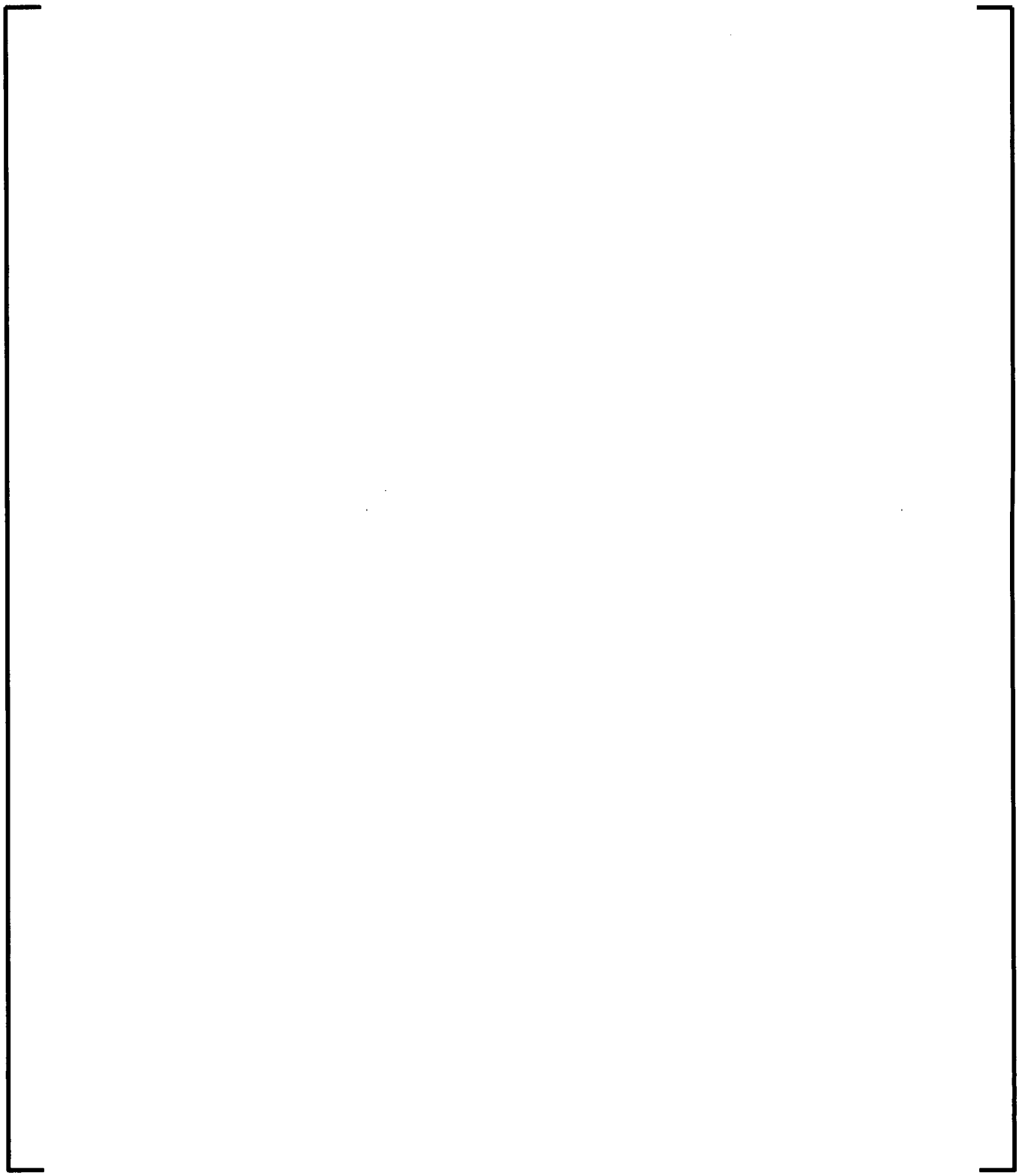

Figure 6-89: Key Transient Parameters for BWR/4 ATWSP

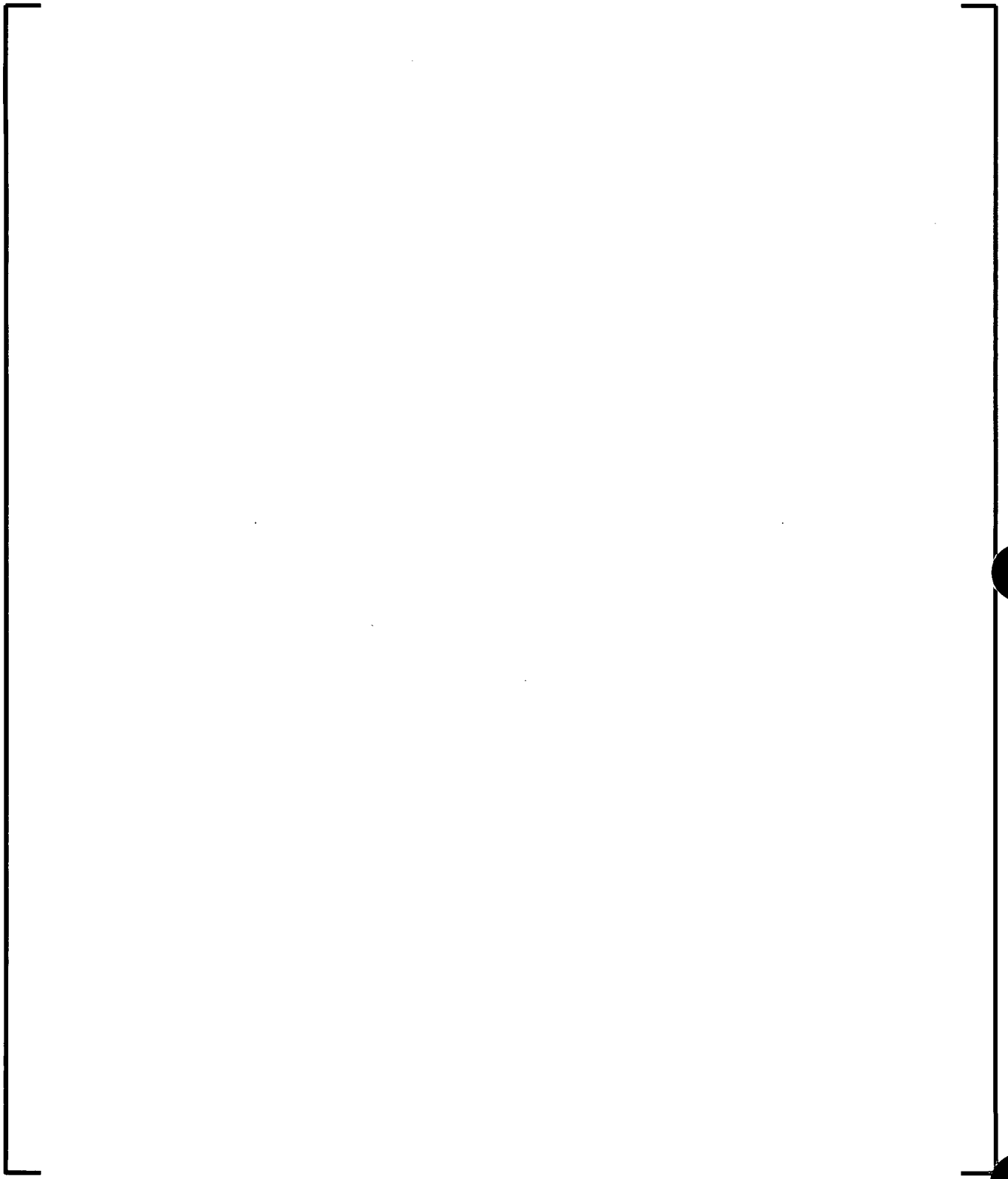

Figure 6-89: Key Transient Parameters for BWR/4 ATWSP (cont)

6.6.3.5 Pressure Regulator Failed Open with no Scram – ATWS Overpressure

The pressure regulator failed open with no scram (PRFO) event is analyzed to demonstrate compliance with the ATWS overpressure criterion. The pressure regulator is assumed to fail, causing the TCVs and turbine bypass valves to open, thereby increasing the steam flow. The steam flow can achieve about 115% - 120% of rated steam flow when the TCVs and bypass valves reach the full open position, causing the system pressure to drop. The MSIVs are signaled to close when the pressure near the turbine header reaches 825 psig. The MSIV closure pressurizes the core and increases the core power. The system pressure increases until the steam line pressure reaches the relief valve(s) opening setpoint and the ATWS RPT occurs. The feedwater temperature is conservatively assumed to be constant through the duration of this event. Actuation of the relief valves reduces the system pressurization effects and assures peak system pressure is maintained below the maximum reactor vessel pressure of 1500 psig in this scenario.

The reactor is initially operating at 3952 MWt, 100% of rated core flow, and 1050 psia dome pressure in this baseline analysis, with an end of cycle exposure and all control rods fully withdrawn. No control rods are inserted in this analysis. Key parameters for the event are summarized in Table 6-28 and Figure 6-90.

Table 6-28: Summary of Key Transient Parameters for BWR/4 PRFO

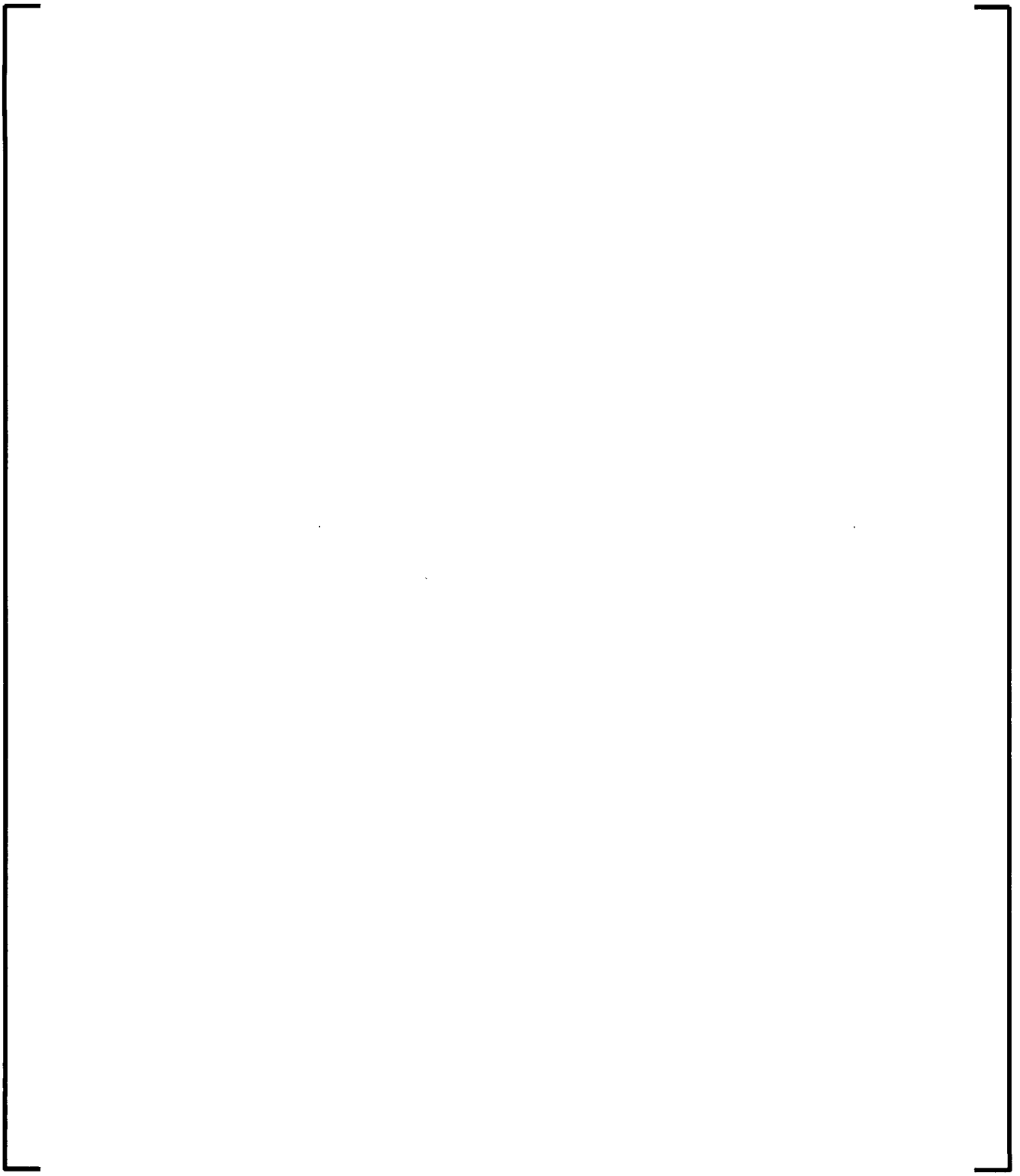

Figure 6-90: Key Transient Parameters for BWR/4 PRFO

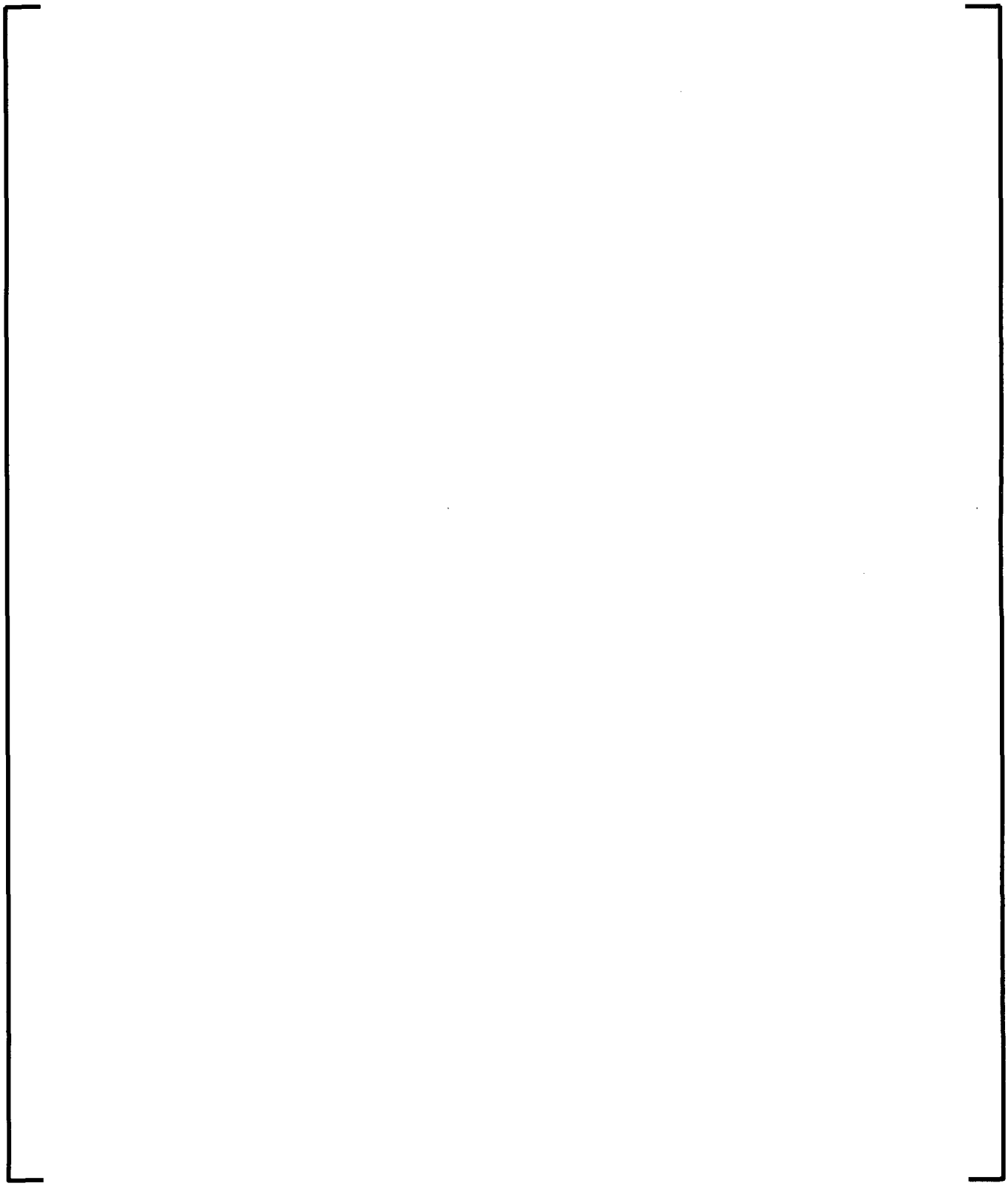

Figure 6-90: Key Transient Parameters for BWR/4 PRFO (cont)

6.6.4 BWR/6 Baseline Analyses

The ability of the AURORA-B EM to model system interactions is demonstrated in this section for three typically limiting events in a typical BWR/6 plant. The results are representative of how the EM is applied in licensing calculations. The selected events are TTNB, FWCF, and ATWSP. These events are provided because they illustrate the impact of the fast scram system on the event scenarios compared to the BWR/4 plant. With the exception of the impact of faster scram, other BWR/6 events show similar characteristics as already demonstrated for the BWR/4 plant type. Design and operating characteristics of the BWR/6 plant are summarized in Table 6-29.

Table 6-29: BWR/6 Plant Characteristics

The number of safety/relief valves indicated in Table 6-29 and assumed in the baseline analyses is less than the number actually installed in the plant. The reduced number of valves has been assumed in order to show a stronger pressurization and power response than may otherwise occur if all installed valves were assumed operational. The nodalization description provided in Section 5.2 is directly applicable to the model. [

]

6.6.4.1 Turbine Trip without Bypass

The sequence of events, phenomena, and processes for the TTNB in a BWR/6 plant are similar to the BWR/4 described earlier. One key difference in the BWR/6 analysis is the faster control rod insertion velocities that mitigate the severity of the event compared to designs used in earlier BWR plants.

The reactor is initially operating at 3898 MWt, 105% of rated core flow, and 1040 psia dome pressure in this baseline analysis, with an end of cycle exposure and all control rods fully withdrawn. All control rods are inserted at the Technical Specification scram speed. Pressure dependence of the insertion velocity is modeled in the neutron kinetics calculations. The TSVs move at the fastest closure speed allowable in the Technical Specifications. Key parameters for the event are summarized in Table 6-30 and Figure 6-91.

Table 6-30: Summary of Key Transient Parameters for BWR/6 TTNB

[

]

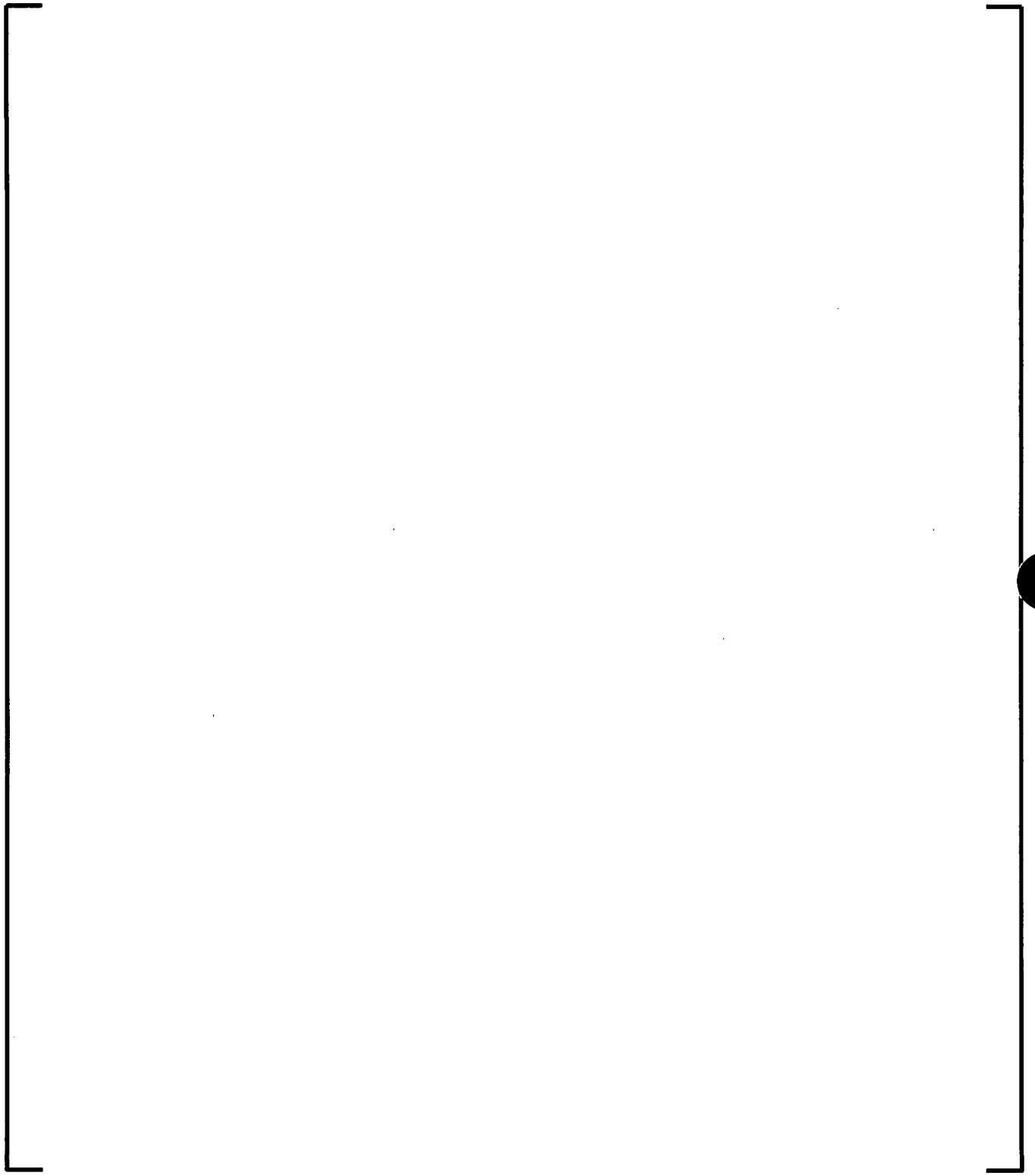

Figure 6-91: Key Transient Parameters for BWR/6 TTNB

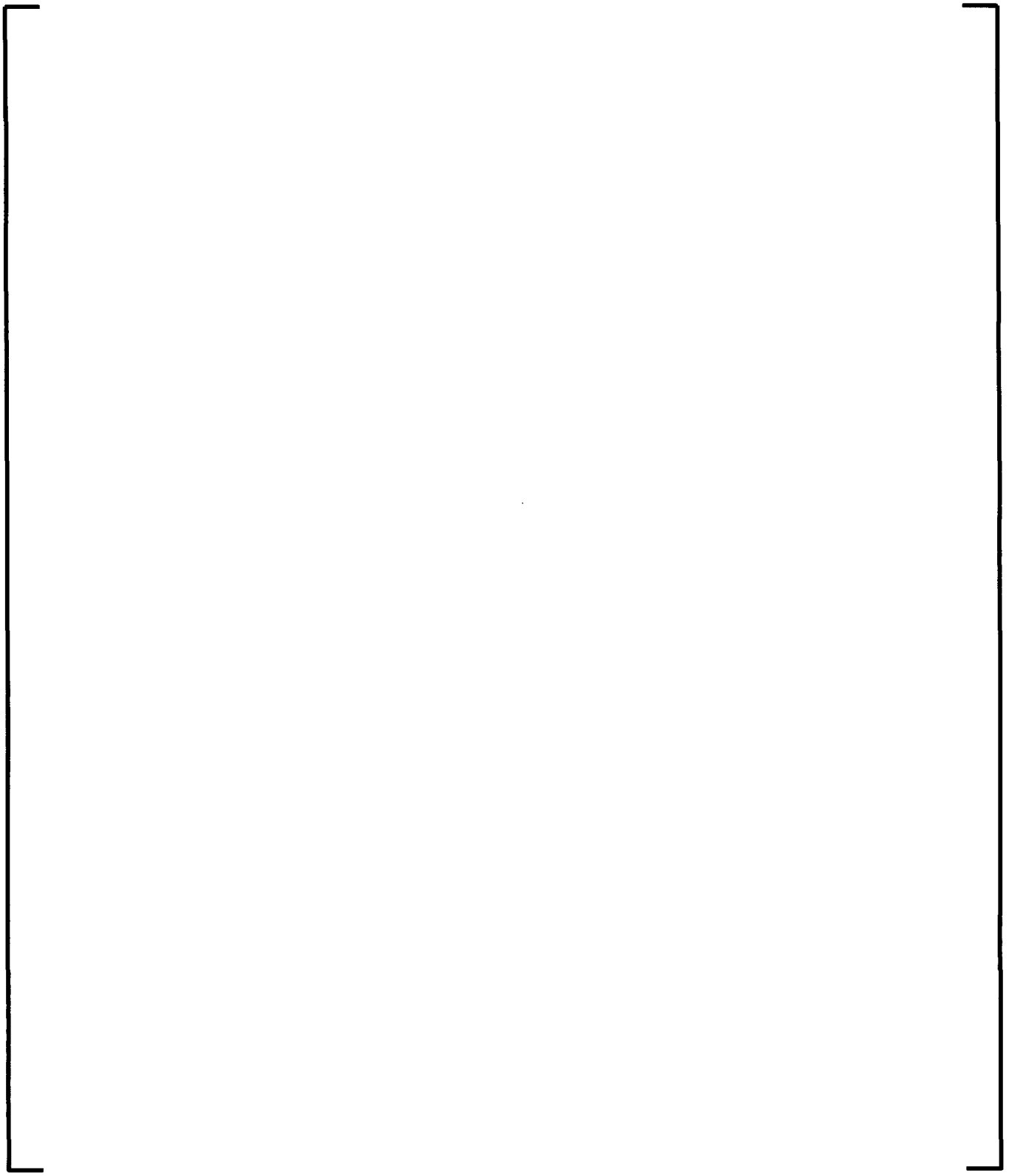

Figure 6-91: Key Transient Parameters for BWR/6 TTNB (cont)

6.6.4.2 Feedwater Controller Failure

The sequence of events, phenomena, and processes for the FWCF in the BWR/6 plant are similar to the BWR/4 described earlier. Again, a key difference in the BWR/6 analysis is the faster control rod insertion velocities that mitigate the severity of the event, compared to designs used in earlier BWR designs.

The reactor is initially operating at 3898 MWt, 105% of rated core flow, and 1040 psia dome pressure in this baseline analysis, with an end of cycle exposure and all control rods fully withdrawn. All turbine bypass valves are assumed in service. All control rods are inserted at the Technical Specification scram speed in this analysis. The target initial water level is set to the nominal operating level. Key parameters for the event are summarized in Table 6-31 and Figure 6-92.

Table 6-31: Summary of Key Transient Parameters for BWR/6 FWCF

[ ]

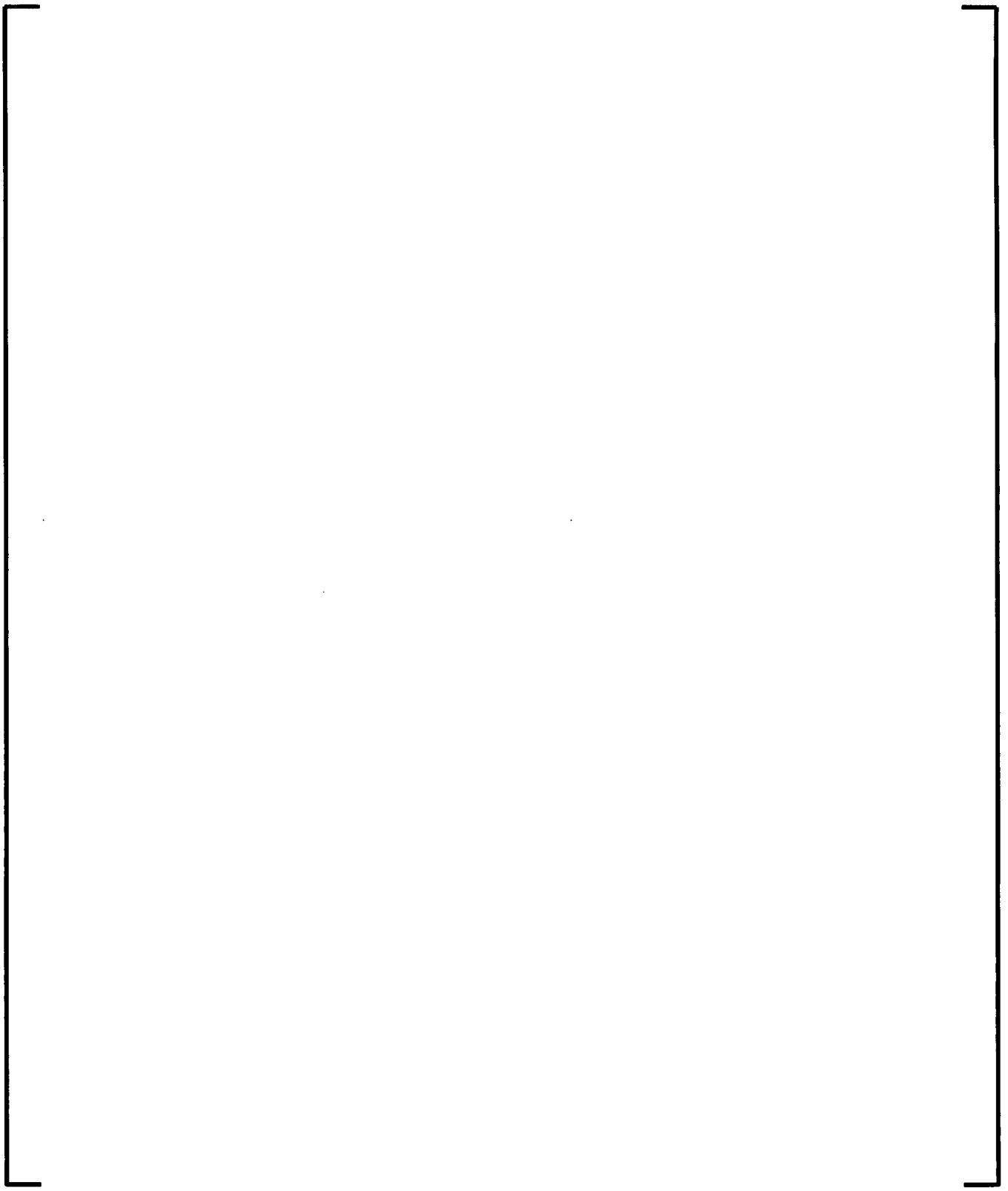

Figure 6-92: Key Transient Parameters for BWR/6 FWCF

Figure 6-92: Key Transient Parameters for BWR/6 FWCF (cont)

6.6.4.3 Main Steam Isolation Valve Closure with no Scram – ATWS Overpressure

The sequence of events, phenomena, and processes for the ATWSP in a BWR/6 plant are similar to the BWR/4 described earlier. Since control rods are not inserted in this analysis, the overall progression of the event is very similar to the BWR/4 ATWSP event. Unlike the BWR/4, the water level exceeds level 8 in this analysis, resulting in a turbine trip and feedwater pump trip. The overall consequence of the feedwater pump trip is to reduce the peak pressure versus not tripping the feedwater system. The plant response to low water level is not modeled in this analysis as it is not important to the determination of peak system pressure.

The reactor is initially operating at 3898 MWt, 105% of rated core flow, and 1040 psia dome pressure in this baseline analysis, with an end of cycle exposure and all control rods fully withdrawn. No control rods are inserted in this analysis. Key parameters for the event are summarized in Table 6-32 and Figure 6-93.

Table 6-32: Summary of Key Transient Parameters for BWR/6 ATWSP

Figure 6-93: Key Transient Parameters for BWR/6 ATWSP

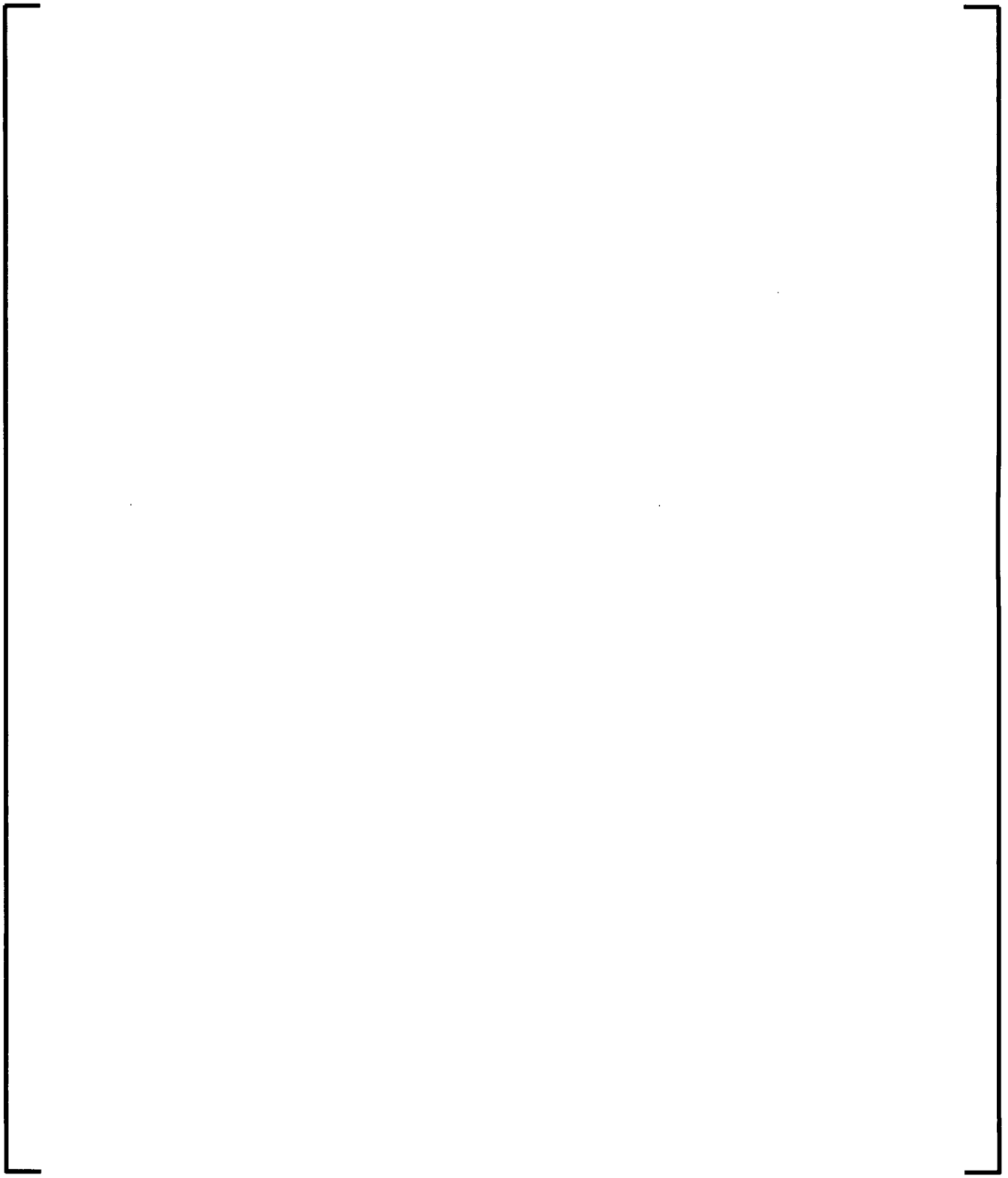

Figure 6-93: Key Transient Parameters for BWR/6 ATWSP (cont)

6.6.5 ABWR Baseline Analyses

The ability of the AURORA-B EM to model system interactions is demonstrated in this section for two events in an ABWR plant. The results are representative of how the EM is applied in licensing calculations. The selected events are TTNB and ATWSP. These events are provided because they illustrate the impact of the RIPs on the event scenarios. With the exception of the impact of RIPs, other ABWR events show similar characteristics as already demonstrated for the other plant types described above. Design and operating characteristics of the ABWR plant are summarized in Table 6-33.

Table 6-33: ABWR Plant Characteristics

The number of safety/relief valves indicated in Table 6-33 and assumed in the baseline analyses is less than the number actually installed in the plant. The reduced number of valves has been assumed in order to show a stronger pressurization and power response than may otherwise occur if all installed valves were assumed operational.

[

]

The nodalization description provided in Section 5.2 is generally applicable to the ABWR plant model. Adaptations of the model are made to address the ten RIPs instead of a jet-pump recirculation system. [

] An overview of the ABWR adapted nodalization indicating the reactor internal pumps is provided in Figure 6-94 (drawing is not to scale).

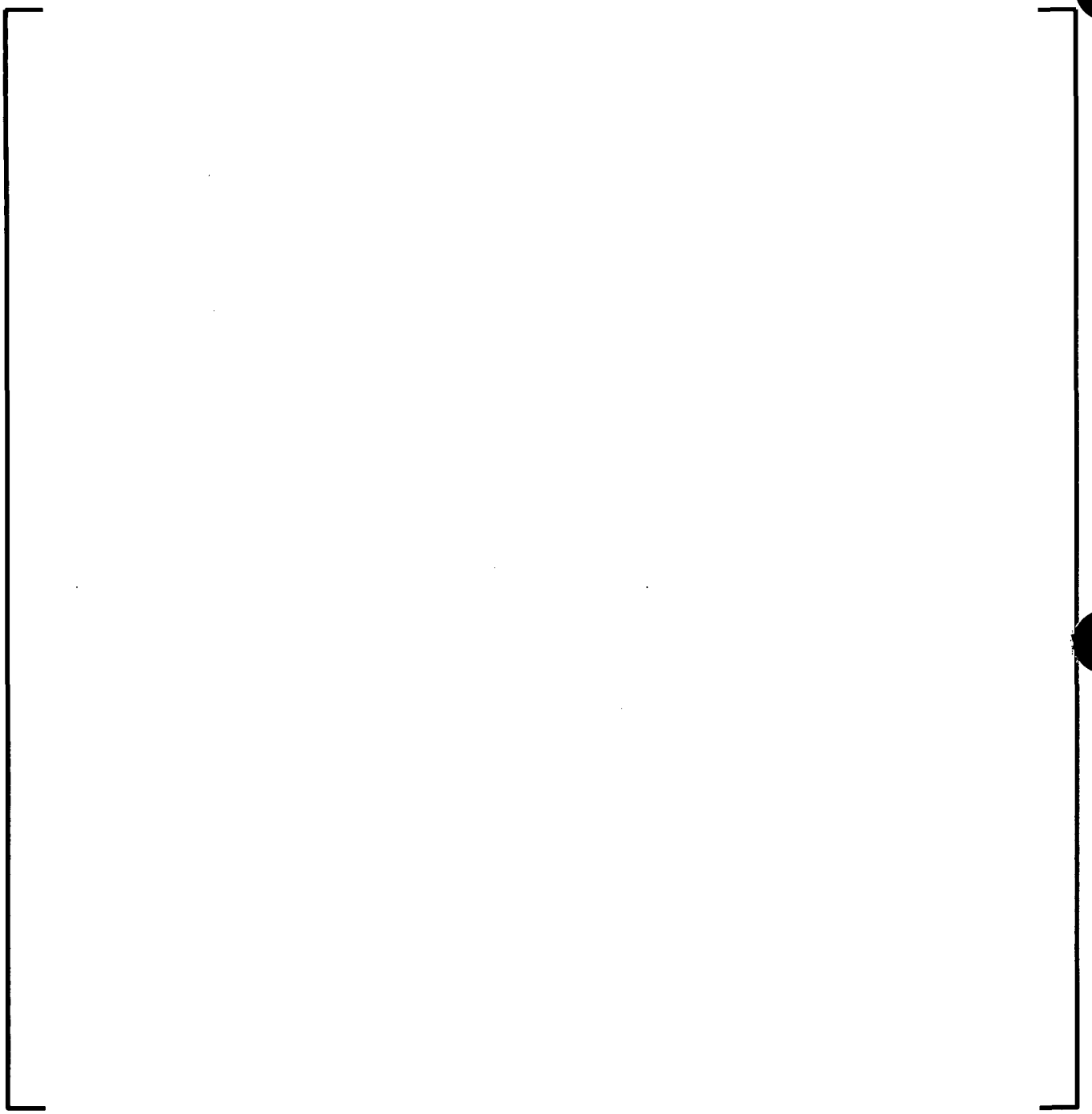

Figure 6-94: Overview of Reactor Vessel Nodalization (ABWR Plant)

6.6.5.1 Turbine Trip without Bypass

The sequence of events, phenomena, and processes for the TTNB in this ABWR baseline analysis have many similarities to the BWR/4 and BWR/6 described earlier. Like the BWR/6,

faster control rod insertion velocities are achieved over the BWR/4 that mitigate the severity of the event. However, unlike the BWR/4 and BWR/6 which trip both recirculation pumps associated with the jet-pump recirculation systems, the ABWR trips only four of ten RIPs. These four pumps have very low inertia and produce a very rapid flow decrease after the trip. The rapid flow decrease produces a quick void-reactivity feedback that mitigates the severity of the event compared to a jet-pump recirculation plant.

The reactor is initially operating at 3926 MWt, 100% of rated core flow, and 1045 psia dome pressure in this baseline analysis, with an end of cycle exposure and all control rods fully withdrawn. All control rods are inserted at the Technical Specification scram speed. The TSVs move at the fastest closure speed allowable in the Technical Specifications. Key parameters for the event are summarized in Table 6-34 and Figure 6-95.

Table 6-34: Summary of Key Transient Parameters for ABWR TTNB

[ ]

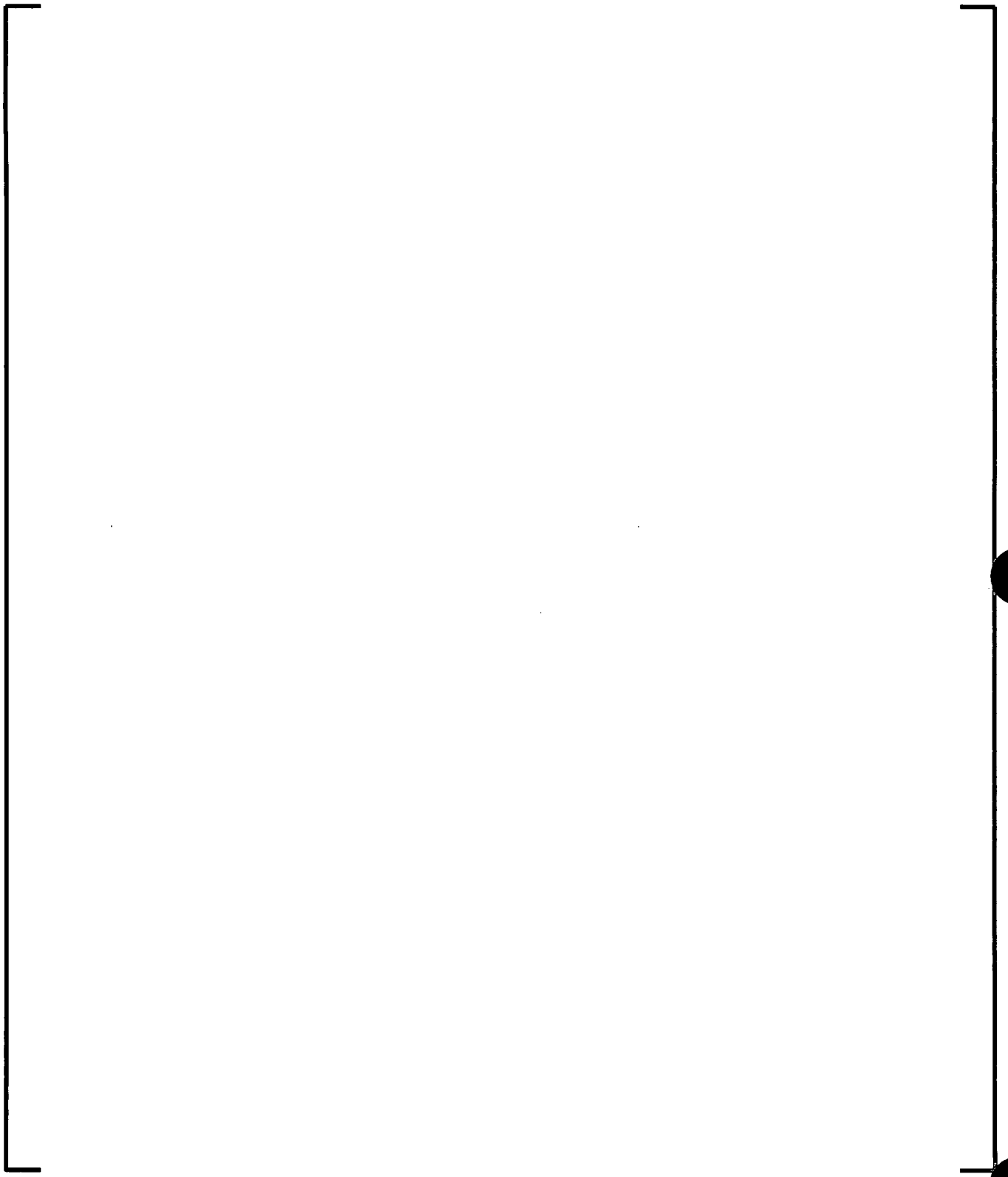

Figure 6-95: Key Transient Parameters for ABWR TTNB

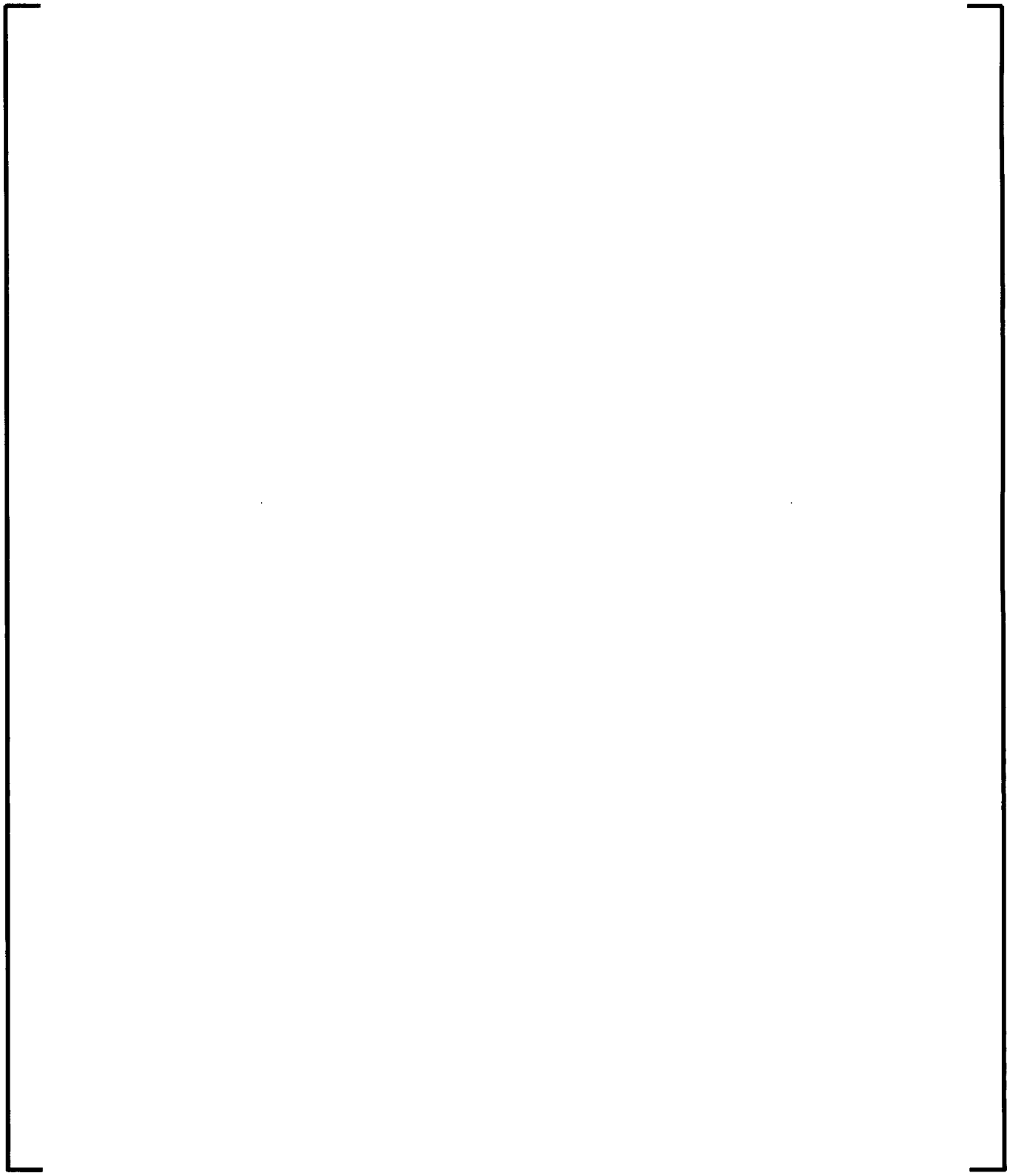

Figure 6-95: Key Transient Parameters for ABWR TTNB (cont)

6.6.5.2 Main Steam Isolation Valve Closure with no Scram – ATWS Overpressure

The sequence of events, phenomena, and processes for the ATWSP in an ABWR plant are similar to the BWR/4 and BWR/6 described earlier. However, unlike the BWR/4 and BWR/6 which trip both recirculation pumps associated with the jet-pump recirculation systems, the ABWR trips only four of ten RIPs. These four pumps have very low inertia and produce a very rapid flow decrease after the trip. The rapid flow decrease produces a quick void-reactivity feedback that mitigates the severity of the event compared to a jet-pump recirculation plant. However, unlike the jet-pump plants where all forced circulation is lost, the remaining six RIPs continue to provide forced flow. A runback is initiated in these six pumps in order to slowly reduce the core flow to natural circulation. This runback is necessary to provide void-reactivity feedback that reduces power and steam production in the long-term (20+ sec).

The reactor is initially operating at 3926 MWt, 100% of rated core flow, and 1045 psia dome pressure in this baseline analysis, with an end of cycle exposure and all control rods fully withdrawn. No control rods are inserted in this analysis. Key parameters for the event are summarized in Table 6-35 and Figure 6-96.

Table 6-35: Summary of Key Transient Parameters for ABWR ATWSP

[ ]

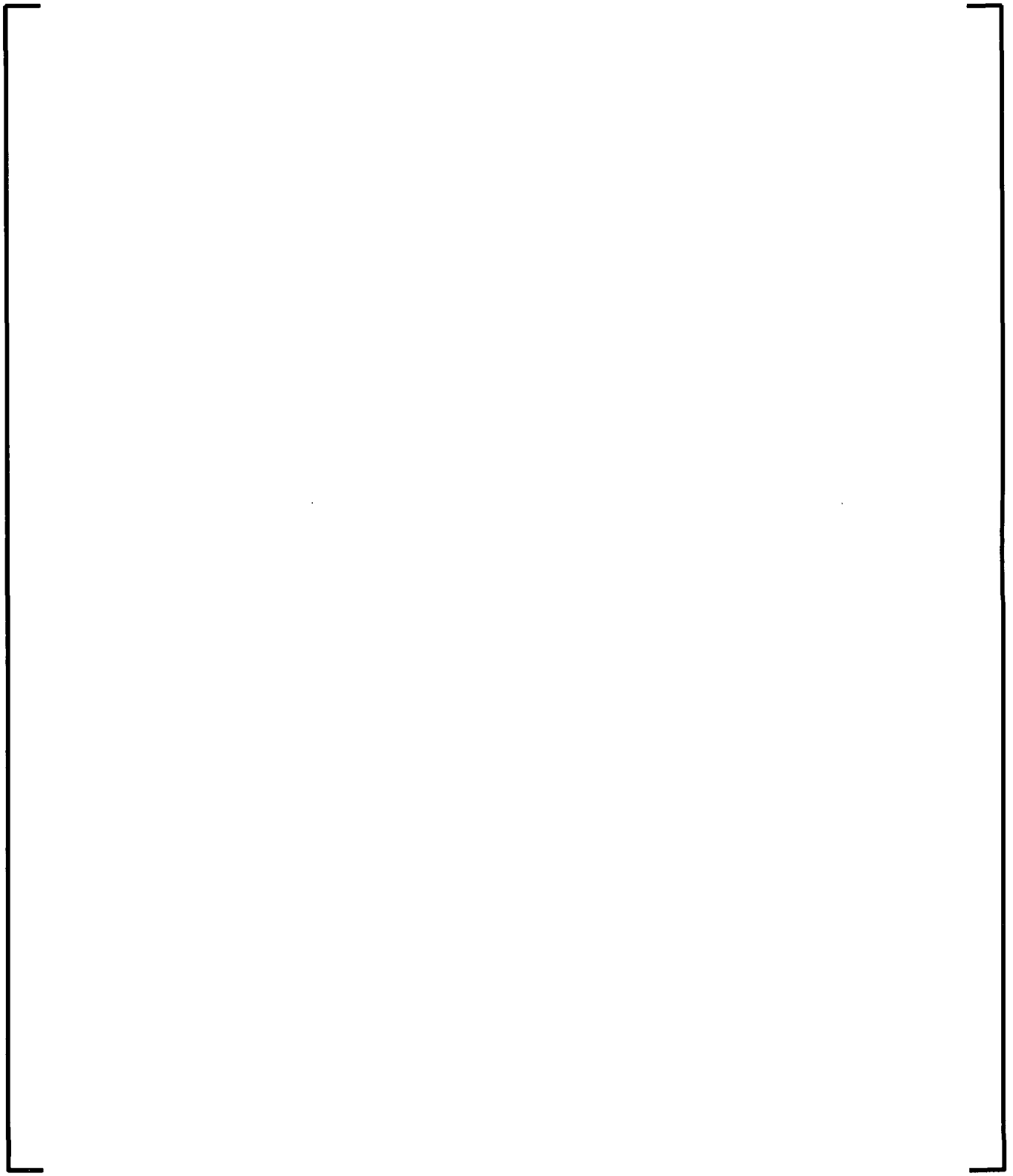

Figure 6-96: Key Transient Parameters for ABWR ATWSP

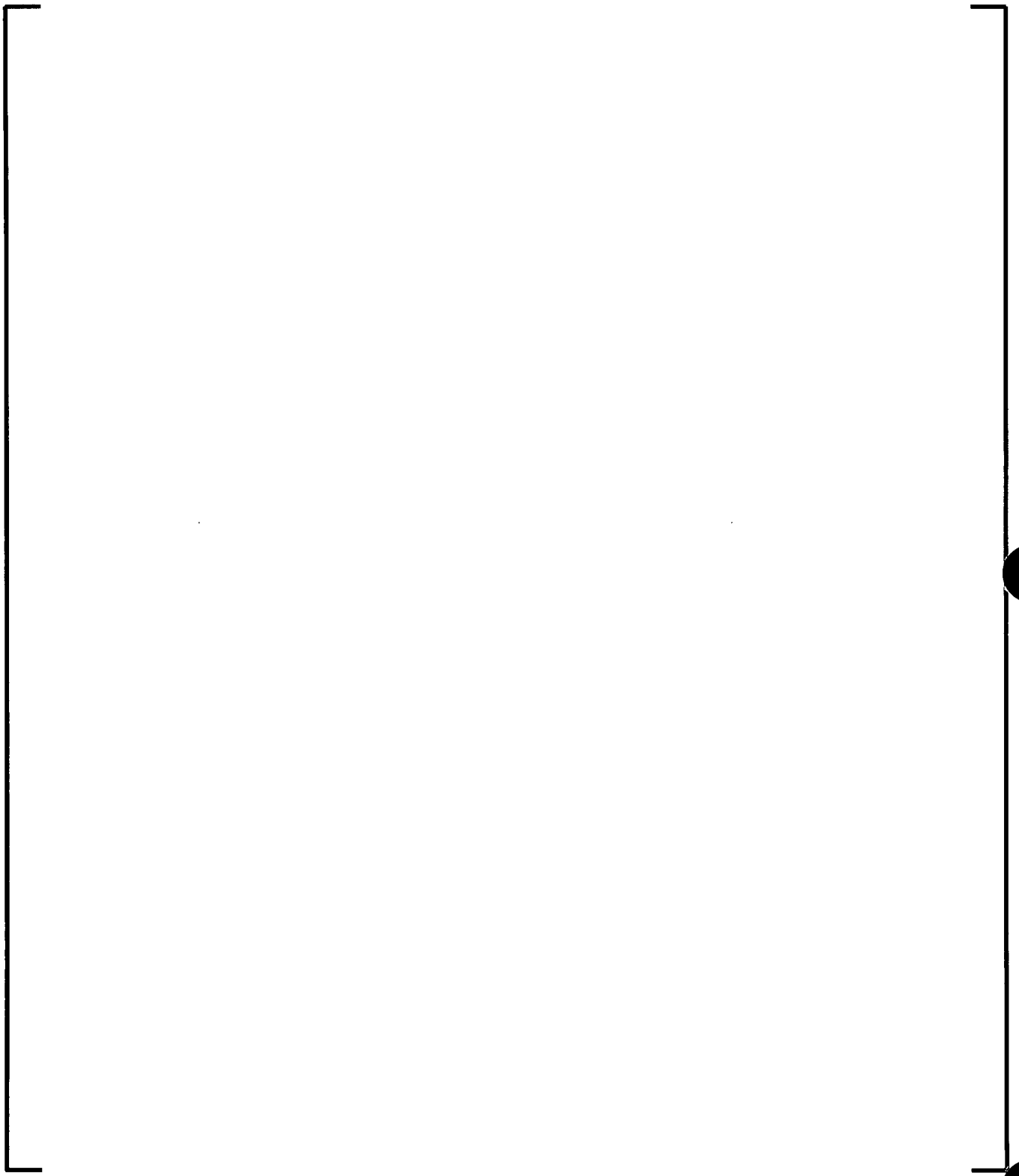

Figure 6-96: Key Transient Parameters for ABWR ATWSP (cont)

6.7 *Assess Scalability of Integrated Calculations and Data for Distortions (EMDAP Step 19)*

The scalability of the integrated calculations and distortions in test facilities and data are addressed in the previous section where they are observed. When observed, their impact and consequences for the noted situation were described.

6.8 *Determine Evaluation Model Biases and Uncertainties (EMDAP Step 20)*

The biases and uncertainties of the EM in predicting the FoM are determined in this section. These biases and uncertainties arise from several factors, including: the EM structure (e.g. coupling strategies between CCDs and time step size sensitivities), selection of plant parameters and initial conditions, and biases and uncertainties in predicting the highly ranked PIRT phenomena. A conservative approach for addressing the biases and uncertainties arising from these factors is different for each factor.

The impact of the EM structure is addressed by applying the EM within a range that assures the FoM experience an insignificant or conservative change in result over the range. As described in Section 5.2.8 the EM structure applies a consistent approach to defining the nodalization that minimizes its impact on the FoM. The impact of coupling strategies between CCDs and time step size sensitivities are described in Section 6.8.2.

The selection of plant parameters such as control system and reactor protection system data are based on a mixture of best estimate and analytical (conservative) values. Parameters such as valve flow capacity and operation characteristics are typically based on values described in the plant Technical Specifications or other requirements. The plant parameters used in the baseline analyses described in Section 6.6 are typical for licensing analyses. Sensitivity analyses of several plant parameters are described in Section 6.8.3. These analyses provide an example of a typical process for determining which plant parameters are important, and how to determine conservative plant parameter values. The selection of initial conditions (e.g. core thermal power, total core flow, and cycle exposure) from which to initiate analyses is a key element of the application methodology described in Section 8.0. Initial conditions such as feedwater system performance and recirculation flow mismatch are related to the plant characteristics and are defined as plant parameters. Selection of other initial conditions such as downcomer water level is described in Section 6.8.3.

Finally, the biases and uncertainties in predicting the highly ranked PIRT phenomena are addressed through a series of sensitivity analyses in Section 6.8.4. These analyses propagate the biases and uncertainties of the highly ranked PIRT phenomena through the EM by modifying the input models. The results of the analyses are then used in Section 6.8.5 to justify conservative measures that are applied when calculating FoM with the EM. The measures are put in place to assure that propagation of the highly ranked PIRT phenomena biases and uncertainties are conservatively accounted for within the framework of a deterministic application methodology.

6.8.1 Sensitivity Analyses

Numerous sensitivity analyses were performed, and key results are summarized in the following sections. The sensitivity analyses have been performed based on the Peach Bottom TT3 analysis summarized in Table 6-17 as well as the five baseline analyses described for the BWR/4 in Section 6.6.3.

[

]

6.8.2 Impact of EM Structure

The impact of specific elements of the EM structure on FoM biases and uncertainties have been evaluated. The evaluations and conclusions are summarized below:

Time Step Sensitivity - System Scale Calculation

[

]

[

]

Time Step Sensitivity – Single Channel Model

[

]

[

]

Hydraulics to Kinetics Coupling Scheme

[

]

Core Flow Distribution

[

]

6.8.3 Plant Parameters and Initial Conditions Selection

Analyses are described below that provide an example of the typical process for classifying the impact of plant parameters and initial conditions on the FoM and used to determine which plant

parameters and initial conditions should use conservative values, as described in Section 8.0. Classifying the impact as insignificant or significant (i.e. small impact or larger) is based on the definitions provided in Section 9.3.

The analyses in this section describe results from the BWR/4 plant. Most sensitivity cases were performed with adjustments producing positive and negative responses in the FoM. However, emphasis is generally placed on the cases with the positive responses (i.e. increases the ΔMCPR or peak pressure).

Scram speed

[

]

Recirculation System Performance

[

]

Elevation of the Level 8 setpoint

[

]

Initial Water Level

[

]

Steam Line Pressure Drop

[

]

TSV Closure Time

[

]

Number of Safety and Relief Valves

[

]

Recirculation Pumps Inertia

[

]

6.8.4 Analysis of Biases and Uncertainties from Highly Ranked PIRT Phenomena

Impact of propagating the biases and/or uncertainties of the highly ranked PIRT phenomena through the EM and into the EM outputs was investigated through a series of sensitivity cases. Key results of the investigation are described in Table 6-36 for Peach Bottom TT3 and the BWR/4 baseline analyses. Extended summaries for several analyses are provided in Sections 6.8.4.1 through 6.8.4.8. The extended summaries describe what parameters are changed relative to the baseline analyses for some key sensitivity cases. In addition, the key parameters that change as a result of the sensitivity are summarized and changes in the initial conditions are quantified where appropriate. Other key points that are important in interpreting the behavior and results of the sensitivity study are also provided.

The sensitivity cases are tied to highly ranked PIRT parameters described in Section 3.4. Where appropriate, [

]

Most analyses were performed with adjustments producing positive and negative responses in the FoM. However, emphasis was generally placed in the positive responses (i.e. increases the ΔMCPR or peak pressure).

Table 6-36: Bias and Uncertainty Evaluation for Highly Ranked Phenomena

Table 6-36: Bias and Uncertainty Evaluation for Highly Ranked Phenomena (cont.)

Table 6-36: Bias and Uncertainty Evaluation for Highly Ranked Phenomena (cont.)

Table 6-36: Bias and Uncertainty Evaluation for Highly Ranked Phenomena (cont.)

6.8.4.1 Sensitivity to interfacial drag in the core region

[

]

[

]

6.8.4.2 Sensitivity to active moderator density feedback

[

]

[

]

6.8.4.3 Sensitivity of system scale results to fuel rod thermal-mechanical models

[

]

6.8.4.4 Sensitivity of ΔMCPR calculations to fuel rod thermal-mechanical models

[

]

6.8.4.5 Sensitivity of Doppler reactivity feedback

[

]

[

]

6.8.4.6 Sensitivity of jet-pump model

[

]

6.8.4.7 Sensitivity of steam separator carryunder

[

]

[

]

6.8.4.8 Sensitivity of steam separator pressure drop

[

]

[

]

6.8.5 Determination of Suitably Conservative Measures

The impact of propagating the biases or uncertainties of the highly ranked PIRT phenomena through the EM and into the EM outputs was described in the previous section. Most sensitivity results were observed to produce an insignificant impact on the results, but some had a small impact. Even though the individual impact is insignificant or small, the cumulative impact on the EM outputs must be addressed using measures that assure conservative results. Suitable conservative measures are defined in this section that assure adequate treatment for

propagation of biases and uncertainties in highly ranked PIRT phenomena. Specific measures to account for uncertainties are defined within the scope of each application methodology. And, the deterministic application methodology described in Section 8.0 makes use of these measures. However, statistically based application methodologies may address uncertainties in a different way.

[

]

The conservative measures for the FoM described in Section 3.2 are now described;

Measures applied to ΔMCPR analyses

[

]

[

]

Measures applied to peak pressure

[

]

Measures applied to the time dependent nodal power used with fuel thermal-mechanical methodologies

[

]

Measures applied to fuel integrity

[

]

7.0 Adequacy Decision

The decision regarding the adequacy of the EM is the culmination of the four EMDAP elements. Throughout the development process, questions concerning the adequacy of the model were asked and numerous iterations were made until the EM was determined to be adequate for the target applications. The final product of the development process is documented in this LTR, which includes showing results from fully certified computer codes using consistent nodalization and modeling options.

The AURORA-B EM has been determined to be adequate for simulating the target applications described in Section 3.0, as demonstrated through completion of the EMDAP documented in this LTR.

7.1 *Code Versions Used in the Adequacy Decision*

Calculations shown in this LTR were generated using computer codes that satisfy the AREVA software quality assurance program and have a "fully certified" status.

- Most separate effects, component effects, and integral effects assessments for the S-RELAP5 thermal-hydraulic and thermal conduction models were performed using the UAPR09 version of S-RELAP5 with the "BWRNL" methodology option* or earlier certified code versions that provide equivalent results.
- The numerical benchmarks for MB2-K were performed using the UAPR09 version of MB2-K in "stand-alone mode" e.g. separate from the coupled code. This is the same version of MB2-K that is coupled within S-RELAP5.
- The fuel rod thermal-mechanical calculations to determine the "permanent effects" on the fuel at the desired level of burnup were performed using the UJUN07 version of RODEX4. This RODEX4 version was developed to support USNRC approval of Reference 7. This is the same version from which the RODEX4 "kernel" was extracted and coupled within S-RELAP5.
- During the evolution of the development several different versions of the lattice physics code CASMO4, the core simulator MICROBURN-B2, and supporting tools were used to generate the cross section information needed by MB2-K. All versions were fully certified and standard production options were used in a manner consistent with the use of these codes in reload analyses.

* Numerous methodologies are based on S-RELAP5. The methodologies use slight variations of the constitutive relations. The methodology option is an input field in S-RELAP5 that selects the specific constitutive relations consistent with the desired methodology.

- Some separate effects assessments and the coupled code calculations using MB2-K were performed using the UOCT09 version of S-RELAP5 with the "BWRNL" methodology option. This version is built upon the UAPR09 version of S-RELAP5 and provides minor updates and corrections.

Going forward, all error corrections and code modifications will be built upon the above described code versions for the purposes of determining the continuity of assessment within the software quality assurance program.

7.2 *Summary of Updates to S-RELAP5 since RLBLOCA Approval*

As described in Section 2.0, the EMDAP was utilized to guide the refinement and extension of the existing tools for use in EM and assure the EM is adequate for addressing the systems, components, phenomena, etc. associated with BWR events. This refinement and extension resulted in refinement of numerous models and correlations found in S-RELAP5 and the installation of two CCDs within S-RELAP5.

The S-RELAP5 computer code is USNRC approved for pressurized water reactor (PWR) large and small break loss of coolant accident (LOCA) analysis and PWR non-LOCA transient analysis (References 3, 10, and 11). This section summarizes the updates made to S-RELAP5 since approval of the RLBLOCA methodology for PWRs. The RLBLOCA methodology is chosen as the reference point because it contains the comprehensive code assessment and documentation and the methodology development followed the CSAU process (Reference 12).

Verification of the S-RELAP5 source coding was extended to support this LTR over what was described in the documentation supporting the RLBLOCA methodology (Reference 25). Specifically, development of a new jet-pump model was made that replaces the original model. Therefore, problems in the original jet-pump model identified in Reference 25 have been addressed. In addition, installation and verification of the MB2-K CCD has been performed to solve the three-dimensional neutron kinetics equations. Finally, installation and verification of a subset of the models in RODEX4 has been performed for predicting BWR specific fuel thermal-mechanical properties in lieu of the PWR fuel models described in earlier documentation.

The range of assessment of S-RELAP5 was expanded and the assessment results are reported in this LTR. A number of improvements were made to physical models compared to the RLBLOCA methodology. Revised results for several assessments described in Reference 25

that were affected by the improvements are provided in this LTR. Specifically, the interfacial drag and interfacial heat & mass transfer models were improved, and the revised results for FRIGG2 and GE level swell are reported in Section 6.2. Assessment versus new sources of data was also provided in Section 6.2 for these two phenomena. Finally, improvements of the mechanistic BWR separator model that was previously available in S-RELAP5 were made and assessment versus data for this revised model is provided in Section 6.5.3.

Several new models were added to S-RELAP5 to address BWR specific issues. These new models included a new jet-pump model and new pressure drop models for BWR fuel assemblies consistent with those in MICROBURN-B2. The new models are described in Reference 4. In addition BWR critical power correlations have also been installed. Assessment results for these new models are provided within this LTR.

Finally, it is important to point out that all of the S-RELAP5 code changes have been implemented without affecting the existing capabilities and approvals of the code. Application of the specific models associated with an approved methodology is controlled through the methodology option selected by the user. The same basic S-RELAP5 code version that supports AURORA-B has the capability to support all of the other approved methodologies described above. Therefore, the S-RELAP5 code qualifications and vast experience from previous methodology applications is generally applicable to the AURORA-B EM, with the exception of the differences arising from improvements summarized in this section.

8.0 Application Methodology Description

The AURORA-B EM will be used to analyze the plant response during specific events over the range of expected plant operating conditions (Section 3.1). Event analyses are performed to determine the transient response of the key plant and fuel parameters (figures of merit) that are used to assess compliance with the applicable event acceptance criteria (Section 3.2). The results of the event analyses are used to establish or confirm operating limits and constraints that are necessary to ensure that acceptance criteria are not exceeded during the event.

The AURORA-B EM development and assessment are described in earlier sections of this LTR. The development and assessment demonstrate the applicability of the EM for analysis of the intended scope of events over the range of expected operating conditions. The development and assessment also demonstrate the accuracy of the EM for calculation of the key figures of merit used to confirm compliance with event acceptance criteria.

The application methodology defines the framework for using the EM to perform the event analyses required to establish or confirm plant operating limits and constraints. The application methodology includes the following elements;

- applicability of the EM for event analysis
- use of analysis results
- addressing EM calculation uncertainty
- determining appropriate analysis conditions
- developing plant input parameters

The application methodology elements define a process that ensures conservative predictions of plant transient response over the entire operating domain. The application methodology combined with the assessments of the EM relative to separate effects and plant test data provide a high degree of confidence that AURORA-B can be used to conservatively demonstrate compliance with event acceptance criteria.

A deterministic application methodology is defined in this LTR; statistical sampling of code model uncertainties, initial conditions, and plant parameters is not performed. Code model uncertainties are addressed either by adjustments to calculation results or by demonstration that the EM has adequate inherent conservatism for the intended application. Uncertainties in initial

conditions or plant parameters that have a significant impact on results are conservatively specified relative to the nominal range of the parameter.

The sections below describe elements of the application methodology that will be used with the AURORA-B EM. The application methodology described is very similar to that used with the currently approved EM (Reference 53); however, the previous EM is replaced with a more detailed and physically based model with reduced calculation uncertainty.

The conservative measures used to account for code calculation uncertainty in the application of the AURORA-B EM are described in the sections below. The adequacy of these measures will be confirmed as part of the initial application of the AURORA-B EM for a plant type. If necessary, the magnitude of the adjustment factors applied to calculated results will be revised consistent with the basis used for the adjustment factors presented in this LTR.

Section 3.1.2 identifies the target scenarios that AURORA-B will be used to analyze. The events identified in Section 3.1.2 are classified as AOOs or Accidents. The classification of the events as either an AOO or an Accident may be slightly different than indicated in Section 3.1.2 in the licensing basis for some plants. In addition, some of the target scenarios in Section 3.1.2 may be classified as Infrequent Events in the licensing basis for some plants. The acceptance criteria, and therefore the application methodology for the EM, are dependent on the event classification. The AURORA-B EM application methodology used for an analysis will be consistent with the current plant licensing basis classification for that event.

8.1 *Application for AOO Analysis*

8.1.1 EM Applicability for Event Analysis

The AOOs that the AURORA-B EM is applicable for are identified in Section 3.1.2.

Generally, an application of the methodology will not require a reanalysis for all the AOOs analyzed in the current plant licensing basis. The impact of a planned change (such as a reload core design) on the AOOs can be assessed and many AOOs will be qualitatively dispositioned as not being impacted by the change or as being inherently bounded by another AOO. In addition, some AOOs can be dispositioned as being less limiting than another AOO based on results from previous analyses provided that the planned plant change would not impact that

conclusion. Generally, the number of AOOs analyzed to support a particular application will be a subset of those identified in Section 3.1.2.

8.1.2 Use of Analysis Results

The primary purpose of the AOO analyses is to establish or confirm the steady state MCPR and LHGR operating limits that ensure that fuel acceptance criteria are not exceeded during the event.

The AURORA-B analysis is used to calculate the ΔMCPR during the AOO. The ΔMCPR is based on the initial MCPR and the minimum MCPR during the AOO that is determined for groups of fuel assemblies of the same design. The ΔMCPR is combined with the safety limit MCPR obtained from a USNRC approved methodology (e.g., Reference 17 and 18) to establish or confirm the plant operating limits for MCPR.

The AURORA-B analysis is used to calculate the fuel rod transient power history during the AOO. The fuel rod transient power history is used as a boundary condition for fuel rod analyses performed with a USNRC approved fuel thermal-mechanical analysis methodology (e.g., Reference 7). The fuel thermal-mechanical analysis methodology is used to confirm or establish the plant operating limits for LHGR.

8.1.3 Calculation Uncertainty

The figures of merit used for the AOO analyses are the ΔMCPR and the fuel rod transient power history. Section 6.8.5 defines conservative measures to be applied with the AURORA-B EM that ensure biases and uncertainties in highly ranked PIRT phenomena are conservatively accounted for in the calculation of these two figures of merit.

[

]

[

]

8.1.4 Plant Operating Conditions Envelope

The plant operating conditions envelope consists of all parameters which define the spectrum of possible initial operating conditions that are allowed during normal operation. The plant operating conditions envelope is used to establish input parameters for the AOO safety analyses. As long as plant operation is within the assumed envelope, the safety analysis is valid.

EM sensitivity analyses are performed to determine the significant plant operating conditions. For significant plant operating conditions, the AOO safety analyses are performed using the limiting values (relative to the calculated figure of merit) within the operating envelope. Nominal or best estimate values are used for operating conditions that are not significant. Performing analyses simultaneously using the limiting value for each significant plant operating condition compounds the overall conservatism of the calculation.

For some situations, improved operating margins can be obtained by partitioning the allowed operating envelope into subregions. Analyses must then be performed for each subregion based on the limiting conditions within the subregion. Operating limits based on these analyses are only valid when operating within the defined subregion.

The approach used for determining analysis values for significant plant operating conditions is demonstrated below.

- **Core Power and Flow:** For a BWR, the allowed combinations of core power and core flow are defined in the power/flow map. The AOO analyses must support operation over the entire power/flow map. Many AOOs are limiting when initiated from maximum core power and flow; however, some AOOs are limiting at reduced power and flow. AOO analyses are performed at multiple state points that span the allowable power/flow combinations. As an alternative, AOO analyses can be performed at a limiting power/flow state point with justification based on previous sensitivity studies. Power- and flow-dependent operating limits can be established to provide improved operating margins.

  Analyses are also performed at state points to bound transition regions that result in changes in the transient scenarios; e.g., above and below the power level at which turbine control or stop valve closure initiates a direct reactor scram.

- **Initial Reactor Operating Conditions:** Based on the core power and core flow at the analysis state point, heat balance calculations are used to determine nominal values for other operating conditions such as dome pressure, feedwater temperature, steam flow, and core inlet enthalpy. If an AOO has a significant sensitivity to a parameter, a conservative value within the nominal operating range is used. If plant operation is planned that varies significantly from nominal conditions (such as reduced feedwater temperature operation), additional analyses are performed to assess the adequacy of the operating limits. If necessary, more restrictive operating limits are established for use when the plant is operating in this manner.
- **Core Design:** The core design includes the core fuel loading plan, control rod patterns, and spectral shift operation planned for the cycle. The core loading plan for the cycle and the control rod positions and core flow through the cycle have a significant impact on the core exposure distribution, core power distribution, and core reactivity characteristics. AOO analyses are performed using neutronics input from a licensing basis core design that results in a conservative prediction of the core power response relative to the response for the planned core design. The licensing basis core design is depleted using adjusted control rod patterns or modified operating conditions that results in scram reactivity characteristics that are conservative relative to the planned core design. The licensing basis core design reflects the planned cycle specific fuel loading configuration.
- **Cycle Exposure:** The severity of an AOO depends on the cycle exposure assumed. Some AOOs are clearly limiting at either beginning of cycle or end of cycle conditions whereas other AOOs do not have a strong dependence on cycle exposure and may be limiting at an intermediate cycle exposure. Unless the limiting cycle exposure is known based on previous sensitivity studies, each AOO analysis is performed at multiple cycle exposures that span the planned cycle exposure range. Exposure-dependent operating limits may be established to provide improved operating margins.

8.1.5 Plant Parameters

The input for the AURORA-B EM is developed using extensive plant specific data to accurately reflect the characteristics of the plant for which the analyses are being performed. The plant data required to prepare the AURORA-B EM input is identified and documented in a Plant Parameters Document that is verified by the utility operating the plant. This process is summarized in Section 5.2.8.5.

Previous experience, engineering judgment, and EM sensitivity analyses are used to determine the plant input parameters that have a significant effect on analysis results. For significant plant parameters, the AOO safety analyses are performed using conservative values (relative to the calculated figure of merit for the event). Nominal or best estimate values are used for plant parameters that are not significant. Simultaneously using the conservative value for each significant plant input parameter compounds the overall conservatism of the calculation.

For some situations, AOO analyses may be performed to support operation with specific plant equipment out of service (EOOS). These analyses address equipment that is normally functioning but that is not required, or is allowed to be out of service, by the plant Technical Specifications. Additional analyses must be performed using input assumptions appropriate for the EOOS plant configuration in order to confirm that the nominal operation limits are valid or, if necessary, to provide a basis for developing operating limits appropriate for the planned operating plant configuration. Operating limits based on these analyses are applied when operating with the specified EOOS.

The EM input is developed using several types of plant data. The types of plant information and the approach for selecting values for significant parameters are demonstrated below.

Plant Safety Systems Characteristics

- **Reactor Protection System (RPS) Setpoints:** The RPS initiates a reactor scram when the signal from a monitored instrument exceeds a specified nominal setpoint. The analyses are performed using conservative analytical setpoints. The analytical setpoints are determined to ensure a high probability that a reactor scram will actually be initiated sooner than predicted by the EM. The analytical setpoints are based on the nominal setpoints and the uncertainties associated with the instruments. The uncertainties considered include measurement uncertainty, instrument drift, and calibration uncertainty. Generally, the analytical setpoints are specified by the utility in the Plant Parameters Document.
- **RPS Response Times:** Bounding delay times are used for RPS response times to conservatively delay the initiation of control rod insertion following a scram signal. The analysis delay times includes conservative values for the instrument response time as well as for the RPS logic processing delay.
- **Control Rod Scram Speed:** The rate at which control rods are inserted into the core after receipt of a scram signal is an important parameter for predicting the core power response during an AOO. Analyses are performed assuming the limiting (slowest) insertion times allowed by the plant Technical Specifications.

  The plant customer may request AOO analyses using specified control rod insertion times based on plant measurements. These analyses are performed in addition to the analyses using Technical Specification control rod insertion times. When MCPR operating limits are provided for alternate control rod insertion times, the plant operators may elect to use the alternate operating limits based on scram time surveillance test data confirming the alternate control rod insertion times.

- **Control Rod Initial Position:** For simplicity and conservatism, transient analyses may assume all control rods are fully withdrawn when the transient is initiated. The benefit of initial control rod positions can be modeled in the EM and credited as long as there is assurance that actual initial control rod positions are not less conservative than those analyzed. Control rods may be fully inserted as a result of Technical Specification requirements or control rods could be administratively maintained at shallow positions to provide increased negative reactivity during scram.
- **Engineered Safety Features Setpoints:** The analyses are performed using conservative analytical setpoints. Important engineered safety features for AOO analyses include the RPT and the ATWS-RPT.
- **Engineered Safety Features Delay Times:** The delay time associated with engineered safety features is assumed to be at the Technical Specification limit (if specified) or the equipment specification limit.
- **Safety and Relief Valve Performance:** Upper bounds for opening setpoints, slowest specified response and opening times, and minimum specified flow capacity are generally used for safety and relief valves in the analyses.

Plant Components and Systems Characteristics

- **Steam Line Valve Closure Times:** The initiating event for several AOOs is the fast closure of a valve in the steam line (MSIV, TCV, TSV) due to a trip signal. For these events, the fastest closure of the valve is conservative and the closure time for the valve is assumed to be at the Technical Specification limit (if specified) or the equipment specification limit.
- **Turbine Bypass System Capacity and Response Time:** For pressurization events, the operation of the turbine bypass system mitigates the consequences. For these events, the slowest response time and minimum rated flow capacity allowed by the Technical Specifications (if specified) or the equipment specifications are used. For some events, the bypass valves are assumed to fail as part of the event assumptions. For depressurization events with bypass failure open, conservatively high flow capacities and fast response times are assumed.
- **Steam Line Pressure Drop:** A low steam line pressure drop is conservative for pressurization events. Plant design and operation data is used to establish the pressure drop for the EM model.
- **Recirculation Pump Inertia:** A conservative high pump inertia (slow coastdown rate) is used for events that initiate an RPT to minimize the benefits of the core flow reduction. A conservative low pump inertia (fast pump response) is used for events assessing a sudden change in pump demand (pump trip or pump runup).
- **Feedwater Pump Maximum Capacity:** The failure of the feedwater control system to maximum demand is often a limiting AOO. The maximum pump capacity identified in the design specifications is used in the analysis.

- **Control System Parameters:** The AURORA-B EM simulates the response of the reactor pressure control system and the reactor water level (feedwater) control system during the events. For most AOOs, the limiting values for the figures of merit occur relatively early in the event before the control systems response can significantly affect the calculated values. Nominal or best estimate values are used for most control system parameters. Some of the AOOs are initiated by postulated failures of the control systems.

Plant Geometry Parameters

The plant geometry parameters are used to define physical characteristics of the plant systems. The plant systems represented in the AURORA-B EM include the reactor vessel, the main steam lines, and the recirculation system. Plant geometry parameters used to develop the EM input are based on the best available data for the plant. The data is obtained from sources that are verified by the plant operator.

- Plant geometry data is obtained from plant design drawings and documents and and/or other sources of information that can be verified. Nominal values from the design information are used to develop the model input and no additional conservatism is required.
- If some plant geometry parameters are not directly available from design drawings or documents, data from similar plants, previous experience, or engineering judgment can be used with justification. In these situations, the input parameter will be biased in a conservative direction if the parameter has a significant impact on analysis results.

8.2 *Application for ASME Overpressure Analysis*

8.2.1 EM Applicability for Event Analysis

The ASME overpressure analysis is performed to demonstrate compliance to ASME code requirements for protection against overpressure of the reactor coolant system. As described in SRP Chapter 5.2.2, the design of safety valves should have sufficient capacity to limit the pressure to less than 110 percent of the reactor coolant system design pressure during the most severe AOO. The ASME overpressure analysis includes conservative assumptions beyond those required for AOO analyses:

- No credit for the first scram initiation signal during the event
- No credit for operation of relief valves or the relief mode of safety/relief valves

The AOOs that the AURORA-B EM is applicable for are identified in Section 3.1.2. The AURORA-B EM is applicable for analyzing these AOOs consistent with the assumptions required for the ASME overpressure analysis.

The limiting AOO for the ASME overpressure analysis is generally the MSIV closure. However, depending on plant specific configuration and performance characteristic, other pressurization AOOs could potentially be limiting. The limiting event for the ASME overpressure analysis is confirmed on a plant specific basis.

8.2.2 Use of Analysis Results

The purpose of the ASME overpressure analysis is to demonstrate that the maximum reactor vessel pressure during the limiting ASME event will not exceed the reactor vessel pressure limit. The analysis is also used to demonstrate that the Technical Specification steam dome pressure safety limit is not exceeded.

The AURORA-B analysis is used to calculate the maximum reactor vessel pressure and the maximum dome pressure during the limiting ASME event. The calculated maximum reactor vessel pressure is compared to the ASME acceptance criterion (110% of vessel design pressure) and the calculated maximum steam dome pressure is compared to the pressure safety limit in the plant Technical Specifications. Meeting the acceptance criteria confirms that the plant safety valve performance (number of valves available, capacity per valve, and setpoints) is acceptable.

8.2.3 Calculation Uncertainty

The figures of merit used for the ASME overpressure analysis are the maximum vessel pressure and the maximum dome pressure. Section 6.8.5 defines conservative measures to be applied with the AURORA-B EM that ensure biases and uncertainties in highly ranked PIRT phenomena are conservatively accounted for in the calculation of these figures of merit.

[

]

8.2.4 Plant Operating Conditions Envelope

The plant operating conditions envelope for the ASME overpressure analysis is the same as described for AOO analyses. The approach used for selecting plant operating conditions for the

ASME overpressure analysis is the same as described for the AOO analyses in Section 8.1.4 with the following exceptions:

- **Core Power and Flow:** The overpressure events are limiting at maximum core power due to the sensitivity to initial steam flow (maximum steam flow at maximum power). The analysis includes an uncertainty associated with core power measurement. The uncertainty value is typically 2%, but is plant specific. The ASME overpressure analysis is performed over the range of core flow allowed at maximum core power unless the limiting conditions have been previously established based on sensitivity studies.

8.2.5 Plant Parameters

The approach used for selecting plant input parameters for the ASME overpressure analysis is the same as described for the AOO analyses in Section 8.1.5 with the following exceptions:

- The first scram initiation signal during the event is disabled. For the MSIV closure ASME overpressure analysis, the scram signal due to MSIV valve closure is disabled and reactor scram will generally be initiated by the high neutron flux (APRM) trip signal.
- Relief valves are not assumed to be operable in the analysis. For plants with dual mode safety/relief valves, only the safety mode is assumed to be operable.
- Some plants have more safety valves than required by the Technical Specifications. For the ASME overpressure analysis, only the minimum number of valves required by the Technical Specifications will be assumed in the analysis. The valves assumed to be unavailable will be those with the most importance to mitigating the event (generally the valves with the lowest setpoint).
- The analysis is performed for the most limiting (relative to maximum pressure) EOOS plant configuration considered in the plant safety analysis.

8.3 *Application for ATWS Analysis*

8.3.1 EM Applicability for Event Analysis

An ATWS scenario is an AOO followed by the failure of the reactor protection system to initiate a scram. After the initial dynamic phase of the event, natural circulation core flow is achieved with reactor power oscillating as the relief valves open and close to maintain pressure. Reactor shutdown is accomplished by initiation of the standby liquid control system (SLCS) which injects boron into the reactor coolant. Due to the delay in SLCS initiation and the time required for the boron to reach the core, peak core power and peak vessel pressure occur long before the boron reaches the core.

The AOOs for which the AURORA-B EM is applicable are identified in Section 3.1.2. The AURORA-B EM is applicable for analyzing these AOOs combined with failure of the reactor protection system. However, the AURORA-B EM described in this LTR does not model the SLCS or boron feedback to the neutronics models. Therefore, the EM calculation is overly conservative for predicting the reactor response past the time of SLCS initiation.

Application of the AURORA-B EM for ATWS analyses will be limited to the time period prior to the arrival of boron to the core region due to SLCS initiation. The scope of the intended use of AURORA-B for ATWS analyses is defined in the following section.

The limiting AOO for the ATWS analysis is generally the MSIV closure or the PRFO scenario. However, depending on plant specific configuration, performance characteristic, or licensing basis assumptions, other pressurization AOOs could potentially be limiting. The limiting event for the ATWS analysis is confirmed on a plant specific basis.

8.3.2 Use of Analysis Results

The probability of an AOO coincident with the multiple failures necessary to prevent scram initiation is much lower than that specified for an AOO or Accident; therefore, AOO or Accident acceptance criteria are not applicable for the ATWS event. Safety issues associated with the ATWS event have been evaluated since the early 1970s and the event was identified as an Unresolved Safety Issue (USI A-9). The USI A-9 was resolved by the publication of 10 CFR 50.62 in 1986. Although 10 CFR 50.62 does not require specific ATWS analyses, analysis of the event remains part of the licensing basis for BWRs. SRP 15.8 Revision 2 (March 2007) provides guidance for analysis requirements for the ATWS event. Application of the AURORA-B EM for ATWS analyses will be consistent with the assumptions and acceptance criteria for the current licensing basis of the supported plant.

The ATWS acceptance criteria generally include the following:

- Maintain reactor coolant pressure boundary integrity – The calculated reactor coolant system pressure should be less than ASME Service Level C Limits (120% of design pressure).
- Maintain coolable geometry – The core coolability requirements defined in 10 CFR 50.46 are applied and include: 1) peak cladding temperature less than 2200 ^{0}F, 2) maximum cladding oxidation less than 17% of cladding thickness, and 3) total core hydrogen generation less than 1% of maximum possible from all cladding.

- Maintain containment integrity – Containment pressure and temperature limits must not be exceeded during the event.

The AURORA-B EM is used to calculate the maximum reactor vessel pressure during the ATWS scenario. The calculated maximum reactor vessel pressure is compared to ASME Service Level C Limit (120% of design pressure) to demonstrate that the event acceptance criterion is met.

The AURORA-B EM is used to calculate the peak cladding temperature and oxidation during the ATWS scenario. The calculated peak cladding temperature and cladding oxidation are compared to 10 CFR 50.46 limits to demonstrate that the event acceptance criteria are met.

8.3.3 Calculation Uncertainty

The figures of merit used for the ATWS analysis are the maximum vessel pressure, the maximum cladding temperature, and the maximum cladding oxidation. Section 6.8.5 defines conservative measures to be applied with the AURORA-B EM that ensure biases and uncertainties in highly ranked PIRT phenomena are conservatively accounted for in the calculation of these figures of merit.

[

]

8.3.4 Plant Operating Conditions Envelope

The plant operating conditions envelope for the ATWS analysis is the same as described for AOO analyses. The approach used for selecting plant operating conditions for the ATWS analysis is the same as described for the AOO analyses in Section 8.1.4.

8.3.5 Plant Parameters

In general, the approach used for selecting plant input parameters for the ATWS analysis is the same as described for the AOO analyses in Section 8.1.5. However, the ATWS analysis has different regulatory requirements than the AOO analysis and a reduced level of conservatism in input selection is sometimes used in licensing calculations. The AURORA-B EM will be applied consistent with the assumptions for the ATWS analysis in the current licensing basis for the supported plant. Some key aspects of the input selection for the ATWS analysis are described below.

- All scram initiation signals during the event are disabled.
- The analysis is performed for the most limiting EOOS plant configuration considered in the plant safety analysis.

8.4 *Application for Accident Analysis*

8.4.1 EM Applicability for Event Analysis

The events for which AURORA-B EM is applicable are identified in Section 3.1.2. Some of the events identified in Section 3.1.2 are classified as Accidents in plant licensing bases. In addition, some of the events may be classified as Infrequent Events in some plants licensing bases. The scope of the intended use of AURORA-B for analysis of the Accidents and Infrequent Events identified in Section 3.1.2 is defined in the following section.

8.4.2 Use of Analysis Results

The purpose of plant accident analyses is to demonstrate that all regulatory acceptance criteria are not exceeded during the postulated event. As described in SRP 15.0, the regulatory acceptance criteria for accidents involve the following general safety concerns:

- **Maintain reactor coolant pressure boundary integrity:** The calculated maximum reactor coolant system pressure should be less than acceptable design limits.
- **Fuel cladding integrity:** Demonstrate that fuel cladding integrity is maintained or conservatively estimate the number of fuel rods that exceed fuel cladding integrity limits and are assumed to fail.
- **Maintain containment integrity:** The event should not cause the loss of any safety function required to mitigate the event, including the reactor containment system.
- **Release of radioactive material:** Offsite radiological dose resulting from predicted fuel failures should not exceed the limits specified in 10 CFR 100 or 10 CFR 50.67.

For each Accident or Infrequent Event, the SRP and the current plant licensing basis identifies specific event acceptance criteria and figures of merit related to the above general criteria. The event acceptance criteria considered in the AURORA-B EM application will be consistent with the acceptance criteria defined for the event in the current licensing basis for the supported plant.

The application of AURORA-B for Accident or Infrequent Event analyses will be limited to assessing the maximum reactor coolant system pressure and fuel cladding integrity for the events identified in Section 3.1.2. Depending on the event and the plant licensing basis, fuel cladding integrity is assessed in the following manner:

- Fuel cladding integrity is demonstrated (no fuel failure) if the transient MCPR remains above the safety limit MCPR.
- If the event MCPR for a fuel design is less than the safety limit MCPR, an approved safety limit MCPR methodology (e.g., Reference 18) is used to calculate the number of fuel rods that fail. The number of fuel rod failures is used to confirm or provide input for revised radiological consequence analyses.
- Fuel cladding integrity is demonstrated (no fuel failure) if the cladding strain and fuel centerline temperature remain below specified acceptable fuel design limits.
- Fuel cladding integrity is demonstrated (no fuel failure) if the maximum cladding temperature remains below the event acceptance criteria.

The AURORA-B EM is used to calculate the maximum reactor vessel pressure during the event. The calculated maximum reactor vessel pressure is compared to accident acceptance criteria (generally specified as ASME Service Level C Limit) to demonstrate that the event acceptance criterion is met.

The AURORA-B EM is used to calculate the ΔMCPR for each fuel design during the event. The ΔMCPR is used to demonstrate that no fuel failures occur or, with a USNRC approved safety limit MCPR methodology, to determine the number of failed fuel rods for use in radiological consequence assessments.

The AURORA-B EM is used to calculate the fuel rod transient power history during the event. The fuel rod transient power history is used as a boundary condition for fuel rod analyses performed with a USNRC approved fuel thermal-mechanical analysis methodology (e.g.,

Reference 7). The fuel thermal-mechanical analysis methodology is used to determine if fuel integrity limits (cladding strain and center line fuel temperature) are exceeded during the event.

The AURORA-B EM is used to calculate the maximum cladding temperature during the event. The maximum cladding temperature is used to demonstrate that no fuel failures occur or to determine the number of failed fuel rods for use in radiological consequence assessments.

8.4.3 Calculation Uncertainty

The figures of merit used for the accident analyses are the maximum vessel pressure, the ΔMCPR, the fuel rod transient power history, and the maximum cladding temperature. Section 6.8.5 defines conservative measures to be applied with the AURORA-B EM that ensure biases and uncertainties in highly ranked PIRT phenomena are conservatively accounted for in the calculation of these figures of merit.

[

]

8.4.4 Plant Operating Conditions Envelope

The plant operating conditions envelope for the accident analyses is the same as described for AOO analyses. The approach used for selecting plant operating conditions for the event analysis is the same as described for the AOO analyses in Section 8.1.4.

8.4.5 Plant Parameters

The approach used for selecting plant input parameters for the accident analyses is the same as described for the AOO analyses in Section 8.1.5.

9.0 Uses, Updates, and Modifications

The AURORA-B EM and the deterministic application methodology defined in this LTR are used for the following activities within the bounds of the conditions and limitations of the Safety Evaluation (SE) approving the LTR. The EM is applied to BWRs equipped with forced recirculation systems over the full domain of operating conditions, up to and including operation at extended power uprate conditions with expanded flow windows. Extended power uprate conditions are typically defined in the US licensing environment as 120% of original licensed thermal power. Expanded flow windows may go as low as 80% of rated core flow when operating at extended power uprate conditions.

1. This LTR can be referenced in the plant Technical Specifications as defining an acceptable methodology for establishing operating limits for MCPR in conjunction with an approved safety limit MCPR methodology.
2. This LTR can be referenced as defining an acceptable methodology for demonstrating the peak primary system pressure is maintained below 110 percent of design values in compliance with ASME limits as defined for AOOs.
3. This LTR can be referenced as defining an acceptable methodology for demonstrating the reactor coolant pressure boundary does not exceed specified requirements for BWRs during ATWS scenarios.
4. This LTR can be referenced as defining an acceptable methodology for evaluating the Fuel Integrity criteria for infrequent events and postulated accidents (other than LOCA) for which they may be evaluated.
5. This LTR can be referenced as defining an acceptable methodology for calculating "fast transient" boundary conditions to fuel thermal-mechanical codes within the bounds of approved fuel thermal-mechanical analysis methodologies.

9.1 *Updates and Changes to Components of the EM*

At the base of AURORA-B are several CCDs which have roles in other licensing activities such as cycle design and fuel rod thermal-mechanical analysis for which they have been approved outside of the AURORA-B EM. These are the "foundation methodology approvals" on which AURORA-B is built. In addition, approved CPR correlations are used within AURORA-B to determine the change in CPR in the analyzed scenarios. AREVA maintains processes to ensure the application of the approved CCDs and CPR correlations used within AURORA-B are done in a manner consistent with the approval and within the conditions and limitations identified in the SE of the respective approved document and/or as amended in subsequent SEs.

The following requirements are defined with respect to application and use of new foundation methodologies, new CPR correlations, new or revised fuel designs, and use of unapproved methodologies within the framework of AURORA-B:

1. Core simulator and cross section methodologies – Cycle depletions and cross sections input to the AURORA-B EM will be generated using an approved CCD. Applicability of a new CCD in this role within AURORA-B will be demonstrated in an approved document.
2. Fuel-mechanical models – Transient fuel-mechanical properties will be evaluated consistent with an approved fuel-mechanical CCD. Applicability of a new CCD in this role within AURORA-B will be demonstrated in an approved document.
3. Critical power correlations – Critical power will be evaluated using an approved critical power correlation or critical power correlation derived via an approved co-resident fuel methodology for each unique fuel design. The same correlation will be used in all steps of the reload licensing performed or supported by AREVA for each unique fuel design to ensure consistency: cycle design, transient analysis, safety limit analysis, and core monitoring. Applicability of the correlations to simulating transients will be demonstrated in an approved document. The approved range of applicability of critical power correlations will be assured when applying the correlations within AURORA-B through software and administrative means.
4. New or revised fuel designs – The licensing of new or revised fuel designs will address the impact of the new or revised design on transient behavior. The evaluation and/or disposition shall ensure that the AURORA-B EM and CCDs continue to be used within their conditions and limitations of approval, and within their verification, validation, and assessment bases.
5. Un-approved methodologies for Lead Assemblies – The use of un-approved CCDs or correlations supporting Lead Assemblies within the framework defined within this LTR will not occur without satisfying the requirements of 10 CFR 50.59, informing the USNRC of their use through a license amendment request (10 CFR 50.92), or other appropriate means as determined to be necessary by AREVA and the plant licensee. In such situations, application on a plant specific basis may be performed to support Lead Assemblies containing new features and materials. Use of CCDs or correlations which do not have approval will not occur within the framework defined within this LTR for reload quantities of fuel assemblies without approval as delineated above.

9.2 *Plant Modifications and Applications*

During the course of age management activities and programs to enhance operational flexibility, modifications may be made to the plants that introduce new features, hardware, and/or enhancements not presently incorporated into the BWR fleet. Examples of features, hardware, and/or enhancements already introduced into the operating fleet since the start of commercial

operation include: digital feedwater control systems, new steam dryers, more accurate thermal power measurement devices, variable speed recirculation pump drive motors, longer duration fuel cycles, power uprate strategies, and expanded flow domain strategies.

When incorporated in the analyses (i.e. the inputs, initial conditions, plant parameters, and boundary conditions accurately represent the plant configuration), most modifications and enhancements do not alter the relevant BWR event characteristics predicted by AURORA-B because they do not alter the performance of the underlying systems, components, geometries, or processes. AREVA maintains processes that ensure changes in the "as operating" state of the plant are communicated between the plant customer and fuel vendor on a cycle specific basis, and these changes are accounted for in the fuel reload licensing activities.

The following actions are taken with respect to accommodating new features, hardware, and/or enhancements not presently incorporated into the BWR fleet. These actions are in addition to any requirements associated with USNRC approved enhancements or modifications such as Extended Power Uprate or expanded flow windows (e.g. MELLLA+);

1. AREVA will review the impact of introducing new features, components, and/or enhancements into plants for which it performs licensing activities to ensure that the characteristics of said features, hardware, and/or enhancements are;
    a. adequately simulated by AURORA-B,
    b. do not adversely impact the bias, uncertainties, and sensitivities of highly ranked phenomena and processes delineated in this LTR,
    c. bounded by the analysis parameters (which can be determined through plant parameter sensitivity studies similar to the studies demonstrated in this LTR, as needed),
    d. within the conditions and limitations identified with AURORA-B and affiliated CCD approvals, and
    e. can be adequately addressed by making code modifications within the scope delineated in Section 9.4.

    AREVA will take action through an LTR submittal, plant specific application submittal, License Amendment Request, or other appropriate means if one of these items is not satisfied.
2. If the above stated review finds the change acceptable, AREVA will maintain input models, physical models, and correlations that adequately represent the "as operating" state of the plant.

As stated earlier, AURORA-B is applicable to all BWRs equipped with forced recirculation systems. AREVA has United States and international experience analyzing all types of forced recirculation BWRs. This experience is sufficient to ensure that AURORA-B is capable of analyzing all important features and components of these BWR types. Example applications are provided in this LTR to demonstrate the methodology for currently operating jet-pump equipped BWR plants and a generic BWR equipped with internal recirculation pumps.

Since no BWR equipped with internal recirculation pumps is operational in the US at this time, detailed design information is not available for the plant. Therefore, the following step will be made with respect to first-time application of AURORA-B to a BWR equipped with internal recirculation pumps operating in the US;

- AREVA (through the license holder) will provide a demonstration analysis of AURORA-B for the first-time application of the methodology to a BWR equipped with internal recirculation pumps that simulates the "as operating" state of the plant, including plant specific geometry, reactor protection system, etc. This demonstration will confirm the applicability of AURORA-B to the plant design. Measures to assure conservative results as described in the application methodology will be confirmed to be appropriate to the plant design, or new measures will be defined.

9.3 *Definitions of Significance*

The following definitions are used within this LTR to classify significance of change in the figures of merit described in Section 3.2 in sensitivity analyses and when determining the impact of a code change:

[ ]

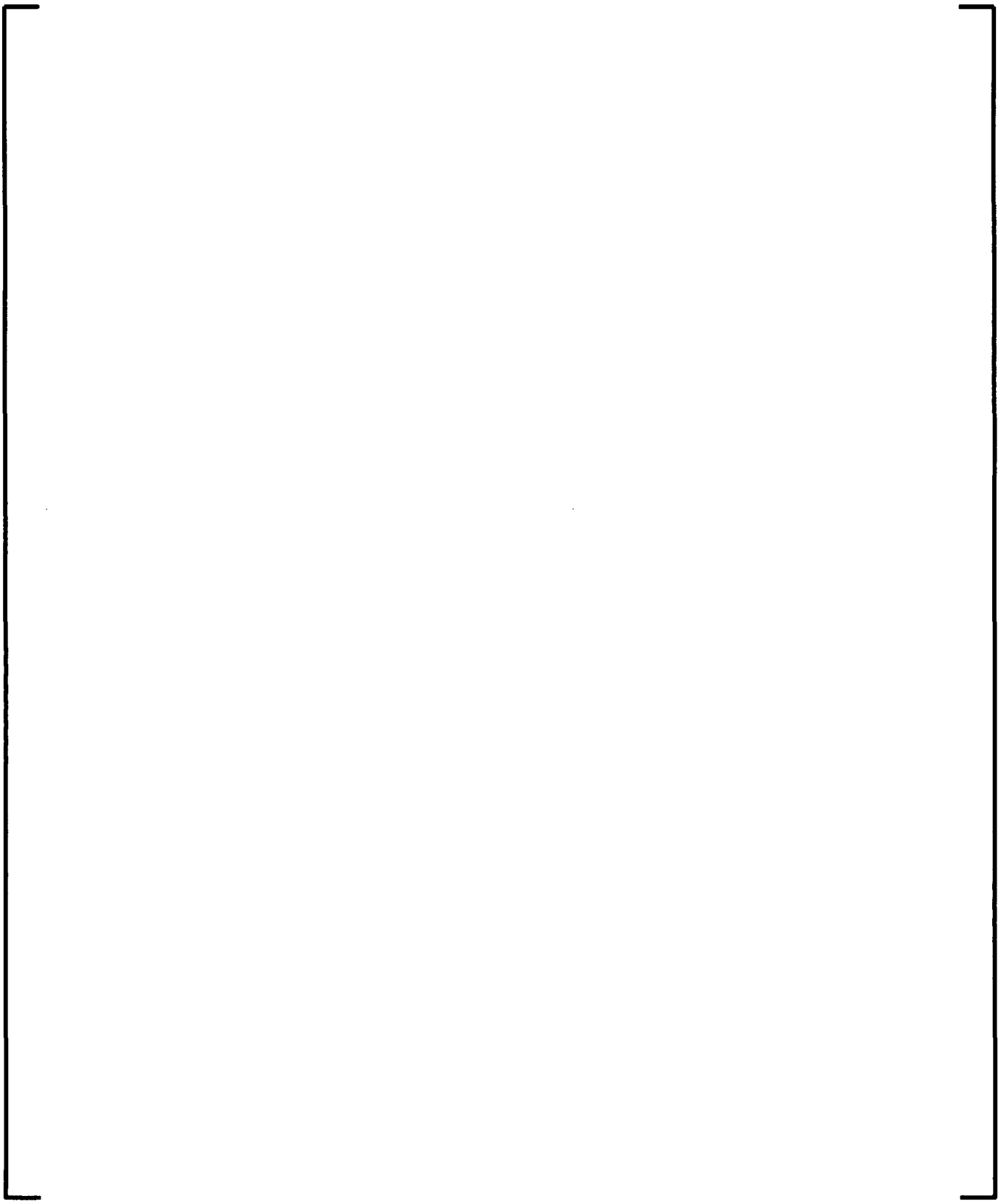

9.4 *Code Modifications*

Code modifications to improve the analysis models may be made to AURORA-B, the CCDs, and correlations during the course of the software and methodology lifecycle. AREVA maintains a quality program (including software quality) that is compliant with 10 CFR 50 Appendix B requirements. This quality program assures modifications are made within the bounds of USNRC licensing requirements and SE conditions and limitations.

10.0 References

1. United States Code of Federal Regulations, Part 10 (Energy) Section 50 Appendix A, *General Design Criteria for Nuclear Power Plants*.

2. U. S. Nuclear Regulatory Commission Regulatory Guide 1.203, *Transient and Accident Analysis Methods*, December 2005.

3. EMF-2103(P)(A) Revision 0, *Realistic Large Break LOCA Methodology for Pressurized Water Reactors*, Framatome ANP, April 2003.

4. EMF-2100(P), Revision 14, *S-RELAP5 Models and Correlations Manual*, AREVA NP Inc., December 2009.

5. EMF-2158(P)(A) Revision 0, *Siemens Power Corporation Methodology for Boiling Water Reactors: Evaluation and Validation of CASMO-4 / MICROBURN-B2*" Siemens Power Corporation, October 1999.

6. AREVA NP Inc. Document 2A4-MB2-K-0, *Advanced Neutron Kinetics Method for BWR Transient Analysis*, December 2009.

7. BAW-10247PA Revision 0, *Realistic Thermal Mechanical Fuel Rod Methodology for Boiling Water Reactors*, AREVA NP Inc., April 2008.

8. EMF-2994, Revision 0, *RODEX4: Thermal-Mechanical Fuel Rod Performance Code Theory Manual*, Framatome ANP, Inc., August 2004.

9. NUREG-0800, *Standard Review Plan for the Review of Safety Analysis Reports for Nuclear Power Plants*, LWR Edition, applicable revisions.

10. EMF-2328(P)(A), *PWR Small Break LOCA Evaluation Model, S-RELAP5 Based*, Framatome ANP, March 2001.

11. EMF-2310(P)(A) Revision 1, *SRP Chapter 15 Non-LOCA Methodology for Pressurized Water Reactors*, Framatome ANP, May 2004.

12. NUREG/CR-5249, *Quantifying Reactor Safety Margins*, Nuclear Regulatory Commission, December 1989.

13. ANP-2829P, *General BWR Design and Event Descriptions*, AREVA NP, December 2009.

14. ANP-2830P, *Control System and Reactor Protection System Requirements for Modeling BWR Events*, AREVA NP, December 2009.

15. ANP-2831P, *Identification of Code Capabilities and PIRT Development for BWR Transient Analyses*, December 2009.

16. XN-NF-80-19(P)(A) Volume 3 Revision 2, *Exxon Nuclear Methodology for Boiling Water Reactors, THERMEX: Thermal Limits Methodology Summary Description*, Exxon Nuclear Company, January 1987.

17. ANF-524(P)(A) Revision 2 and Supplements 1 and 2, *ANF Critical Power Methodology for Boiling Water Reactors*, Advanced Nuclear Fuels Corporation, November 1990.

18. ANP-10307P Revision 0, A*REVA MCPR Safety Limit Methodology for Boiling Water Reactors*, AREVA NP Inc., October 2009.

19. NUREG-1230, *Compendium of ECCS Research for Realistic LOCA Analysis*, US Nuclear Regulatory Commission, August 1988.

20. NEA/CSNI/R(96)16, *Evaluation of the Separate Effects Tests (SET) Validation Matrix*, Nuclear Energy Agency, Organization for Economic Co-Operation And Development, Paris, France, November 1996.

21. NEA/CSNI/R(96)17, *CSNI Integral Test Facility Validation Matrix for The Assessment of Thermal-Hydraulic Codes for LWR LOCA and Transients*, Nuclear Energy Agency, Organization for Economic Co-Operation And Development, Paris, France, July 1996.

22. NUREG/CR-6720, *TRAC-M Validation Test Matrix*, US Nuclear Regulatory Commission, July 2001.

23. Takashi Hara, et al., *Current Status of the Post Boiling Transition Research in Japan Integrity Evaluation of Nuclear Fuel Assemblies after Boiling Transition and Development of Rewetting Correlations*, Journal of Nuclear Science and Technology, Vol. 40 (2003) , No. 10 p.852-861.

24. O. Nylund et al., "Hydrodynamic and heat transfer measurements on a full-scale simulated 36-rod Marviken fuel element with uniform heat flux distribution," FRIGG-2, R-447/RTL-1007, May 1968.

25. EMF-2102(P), S-RELAP5: Code Verification and Validation, Framatome ANP, Inc., August 2001.

26. O. Nylund et al., *Hydrodynamic and Heat Transfer Measurements on A Full-Scale Simulated 36-Rod Marviken Fuel Element with Non-Uniform Radial Heat Flux Distribution*, FRIGG-3, R-494/RL-1154, November 1969.

27. J. Skaug et al., *FT-36b, Results of void Measurements*, FRIGG-PM-15, May 1968.

28. H. Christensen, *Power-to-Void Transfer Function, Doctorial Dissertation,* Massachusetts Institute of Technology, September 1961 (and ANL-6385, July 1961).

29. Allis-Chalmers Atomic Energy Division, J*oint US/EURATOM R&D Program AT (11-1)-1272; Investigation of Vapor Volume Fraction and Slip Velocity Under the Euratom Program; Final Report,* ACNP-64029, November, 1964.

30. Allis-Chalmers Atomic Energy Division, "*Joint US/EURATOM R&D Program AT (11-1)-1186; Steam Separation Technology Under the Euratom Program; Quarterly Progress Report; April 1, 1964-June 30, 1963*, ACNP-63021, July 10, 1963.

31. Allis-Chalmers Atomic Energy Division, *Joint US/EURATOM R&D Program AT (11-1)-1186; Steam Separation Technology Under the Euratom Program; Quarterly Progress Report; October 1, 1963-December 31, 1963*, ACNP-63035, January 10, 1964.

32. J.F. Wilson, R.J. Grenada, J.F. Patterson, *The Velocity of Rising Steam in a Bubbling Two-Phase Mixture*, ANS Transactions 5, 151, 1962.

33. I. Kataoka, M. Ishii, *Drift Flux Model for Large Diameter Pipe and New Correlation for Pool Void Fraction*, International Journal Heat Mass Transfer, 30, No. 9, pp. 1927-1939, 1987.

34. J. A. Findlay, *BWR Refill-Reflood Program Task 4.8 - Model Qualification Task Plan,* NUREG/CR-1899, EPRI NP-1527, GEAP-24898, August 1981.

35. L. A. Hageman and J. B. Yasinsky, *Comparison of Alternating-Direction Time-Differencing Methods with Other Implicit Methods for the Solution of the Neutron Group-Diffusion Equations*, Nuclear Science and Engineering, 38, 8-32 (1969).

36. S. Langenbuch, W. Maurer, and W. Werner (LMW), *Coarse-Mesh Flux-Expansion Method for the Analysis of Space-Time Effects in Large Light Water Reactor Cores*, Nuclear Science and Engineering, 63, 437-456 (1977).

37. *Argonne Code Center: Benchmark Problem Book*, ANL-7416, Supplement 2 (1977).

38. T. Sutton and B. Aviles, *Diffusion Theory Methods for Spatial Kinetics Calculations*, Progress in Nuclear Energy, Vol. 30, No.2, pp. 119-182, 1996.

39. M. Tamitani, T. Iwamoto and B. Moore, *Development of Kinetics Model for BWR Core Simulator AETNA*, Journal of Nuclear Science and Technology, Vol.40, No.4, p.201-212 (April 2003).

40. V. Zimin and H. Ninokata, *Nodal Neutron Kinetics Model Based on Nonlinear Iteration Procedure for LWR Analysis*, Annals of Nuclear Energy, Vol. 25, No. 8, pp. 507-528, 1998.

41. K. S. Smith, *An Analytic Nodal Method for Solving the Two Group Multidimensional Diffusion Equations*, Thesis, M.I.T. (1979).

42. E. Brega, F. Di Pasquantonio and E. Salina, *Computation Accuracy and Efficiency of A Coarse-Mesh Analytic Nodal Method for LWR Transient Problems, in Comparison with A Space-Time Synthesis Method*, Ann. Nucl. Energy, 8, 509-524, 1981.

43. S. Wolf, and R. H. Moen, *Advances in Steam-Water Separators for Boiling Water Reactors*, ASME 73-WA/PWR-4, November 1973.

44. EMF-2209(P)(A) Revision 3, *SPCB Critical Power Correlation*, AREVA NP Inc., September 2009.

45. ANP-10249PA Revision 1, *ACE/ATRIUM-10 Critical Power Correlation*, AREVA NP Inc., September 2009.

46. ANP-10298(P) Revision 0, *ACE/ATRIUM 10XM Critical Power Correlation*, AREVA NP Inc., December 2008.

47. Nuclear Energy Agency, *Boiling Water Reactor Turbine Trip (TT) Benchmark,* Volume I: Final Specifications. Technical Report NEA/NSC/DOC(2001)1, Nuclear Energy Agency, October 2001. Revision 1.

48. Electric Power Research Institute, *Transient and Stability Tests at Peach Bottom Atomic Power Station Unit 2 at End of Cycle 2.* Technical Report NP-564, EPRI, June 1978.

49. NUREG/CR-2576, *BWR Full Integral Simulation Test (FIST) Program Facility Description Report*, U.S. Nuclear Regulatory Commission, December 1982 (Also issued as EPRI NP-2314 and GEAP-22054).

50. NUREG/CR-3711. *BWR Full Integral Simulation Test (FIST) Phase I Test Results*, U.S. Nuclear Regulatory Commission, November 1983 (Also issued as EPRI NP-3602 and GEAP-30496).

51. NUREG/CR-4128, *BWR Full Integral Simulation Test: Phase 2 Test Results and TRAC-BWR Model Qualification*, U.S. Nuclear Regulatory Commission, June 1985. (Also issued as EPRI NP-3988 and GEAP-30876).

52. Electric Power Research Institute, *Core Design and Operating Data for Cycles 1 and 2 of Peach Bottom 2*, Technical Report EPRI NP-563, EPRI, June 1978.

53. ANF-913(P)(A) Volume 1 Revision 1 and Volume 1 Supplements 2, 3 and 4, *COTRANSA2: A Computer Program for Boiling Water Reactor Transient Analyses*, Advanced Nuclear Fuels Corporation, August 1990.